AD

USAAVLABS TECHNICAL REPORT 66-83

GENERALIZED ROTOR PERFORMANCE

By

E. Kisielowski

R. Bumstead

P. Fissel

I. Chinsky

February 1967

U. S. ARMY AVIATION MATERIEL LABORATORIES
FORT EUSTIS, VIRGINIA

CONTRACT DA 44-177-AMC-142(T)
VERTOL DIVISION
THE BOEING COMPANY
MORTON, PENNSYLVANIA

Disclaimers

The findings in this report are not to be construed as an official Department of the Army position unless so designated by other authorized documents.

When Government drawings, specifications, or other data are used for any purpose other than in connection with a definitely related Government procurement operation, the United States Government thereby incurs no responsibility nor any obligation whatsoever; and the fact that the Government may have formulated, furnished, or in any way supplied the said drawings, specifications, or other data is not to be regarded by implication or otherwise as in any manner licensing the holder or any other person or corporation, or conveying any rights or permission, to manufacture, use, or sell any patented invention that may in any way be related thereto.

Disposition Instructions

Destroy this report when no longer needed. Do not return it to originator.

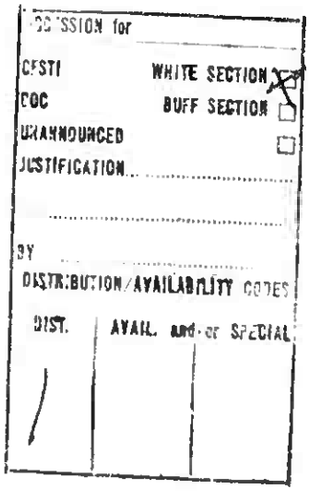

DEPARTMENT OF THE ARMY
U. S. ARMY AVIATION MATERIEL LABORATORIES
FORT EUSTIS, VIRGINIA 23604

This report has been reviewed by the U. S. Army Aviation Materiel Laboratories and is judged to be technically sound. The work was undertaken to present rotor power required over a wide range of lift and propulsion requirements, in generalized nondimensional form, suitable for use in rotary-wing preliminary design studies.

The performance obtained with these charts may be optimistic in the high-tip-speed-ratio (above 0.5) regime of operation because of the assumptions retained in the analysis. A more rigorous treatment which includes the combined effects of nonuniform downwash, radial flow, and blade elasticity would be required to provide greater accuracy of the data at the high-tip-speed ratios.

Task 1P121401A14309
Contract DA 44-177-AMC-142(T)
USAAVLABS Technical Report 66-83
February 1967

GENERALIZED ROTOR PERFORMANCE

R-390

by

E. Kisielowski
R. Bumstead
P. Fissel
I. Chinsky

Prepared by

VERTOL DIVISION
THE BOEING COMPANY
Morton, Pennsylvania

for

U. S. ARMY AVIATION MATERIEL LABORATORIES
Fort Eustis, Virginia

SUMMARY

This report presents theoretical rotor performance data in graphical format especially suitable for preliminary design studies in the rotary-wing field. Generality is achieved by nondimensional presentation of power requirements over the complete range of rotor lift and propulsive requirements for a wide spectrum of speed conditions. Lines of constant power are shown on a lift-drag coordinate system for each speed condition, providing a useful tool in the development of rotored aircraft configurations. Techniques are presented for employing the charts in a variety of design problems, including the compound helicopter, where the optimum combination of rotors, wings, and auxiliary propulsion devices is desired.

The charts are based upon calculations for a rotor of conventional geometry using the NACA 0012 airfoil section characteristics. Refinements of this analysis over older simplified rotor analyses include:

1. Elimination of small angle assumptions
2. Use of actual airfoil section characteristics over the entire range of angle of attack and Mach number
3. Accounting for stall effects
4. Accounting for compressibility effects
5. Accounting for effects of reversed flow

Simplifying assumptions retained in this effort are:

1. Uniform downwash over the rotor disc
2. Radial flow not considered in the computation of blade forces
4. Constant rotational speed about the shaft axis
5. Steady-state, two-dimensional airfoil section characteristics

The operating conditions encompass forward speeds from 50 knots to 300 knots, and tip speeds from 310 feet per second to 800 feet per second, with advance ratios ($V/\Omega R$) ranging from 0.13 to 1.5. Twist values presented are -4 degrees, -8 degrees, and -12 degrees.

For most conditions, data are presented to cover the full range of shaft angles from 20 degrees aft through the normal helicopter range to full 90 degrees forward (propeller state).

The data are nondimensionalized by rotor diameter and solidity. The resulting generality is approximate, but will give useful results over a limited range of solidities. Techniques are presented for correcting for solidities beyond this range.

FOREWORD

The purpose of this report is to present a summary of generalized rotor performance charts suitable for preliminary design studies in the rotary wing field.

The project was originated by the United States Army Aviation Materiel Laboratories (USAAVLABS) at Fort Eustis, Virginia, and the work was performed by the Vertol Division of The Boeing Company under contract DA 44-177-AMC-142(T).

Mr. F. A. Raitch and Mr. J. P. Whitman were the USAAVLABS project engineers, and Mr. E. Kisielewski was the Vertol project engineer, with Mr. R. Bumstead, Mr. P. Fissel, and Mr. I. Chinsky contributing.

CONTENTS

ILLUSTRATIONS

SYMBOLS

Symbol		Unit
a	Slope of lift curve or Speed of sound	per radian fps
a_1	Blade first harmonic longitudinal flapping angle	deg
b	Number of blades per rotor	
c	Chord of rotor blade	ft
d	Rotor diameter	ft
D_E	Rotor effective drag (P/V-X)	lb
e	Flapping hinge offset	ft
f_e	Parasite flat-plate area	lb
g	Acceleration due to gravity	ft/sec^2
H	Rotor shaft normal force	lb
I_f	Blade mass moment of inertia about flap hinge	$slug\text{-}ft^2$
L	Rotor lift	lb
$L/qd^2\sigma$	Nondimensional rotor lift	
M_T	Advancing blade tip Mach number $\left(\frac{V + \Omega R}{a}\right)$	
M_W	Weight moment of rotor blade about flap hinge	ft-lb
P	Rotor power required	ft-lb/sec
$P/qd^2V\sigma$	Nondimensional rotor power required	
q	Dynamic pressure	psf
R	Rotor blade radius	ft
V	Forward speed	knots or fps
X	Rotor propulsive force	lb
$X/qd^2\sigma$	Nondimensional rotor propulsive force	

Symbol		Unit
α_s	Shaft angle	deg
$\alpha_{(1)(270)}$	Retreating blade tip angle of attack	deg
β	Rotor blade flap angle	deg
β_0	Rotor coning angle	deg
γ	Lock number $\left(\frac{\rho a c R^4}{I_f}\right)$	
θ_1	Blade twist, $\not{\text{c}}$ of rotation to tip	deg
$\theta_{.75}$	Collective pitch at .75R	deg
λ	Rotor inflow ratio	
μ'	Advance ratio (V/ΩR)	
ρ	Density of air	slugs/ft^3
σ	Rotor solidity (bc/πR)	
ΩR	Blade tip speed	pfs

INTRODUCTION

In the high-speed regime of flight, the classical rotor performance methods break down because of the various simplifying assumptions used, such as linear lift curve slope, small angle assumptions, neglect of stall effects and compressibility effects, etc. The study of advanced rotary-wing aircraft with projected speeds of up to 300 knots requires more accurate knowledge of the rotor characteristics. Accurate knowledge is impossible to obtain without a rigorous rotor analysis which has no such simplifying assumptions. Analytical methods to provide greater accuracy are continually being developed and improved. Preliminary design efforts, however, will not wait for the ultimate rigorous analysis, and it is therefore necessary, at appropriate intervals, to present useful data based on the current analytical state of the art. This effort is based upon such a concept, and further refinements may be expected in the future as more and more of the simplifying assumptions are eliminated.

The complexity of this type of analysis usually prohibits its use directly in any given aircraft performance problem. However, the analysis may be used to map graphically the pertinent parameters over the full range of conditions anticipated to be of interest. The charts presented in this report result from an analysis of a rotor with constant chord and airfoil section (NACA 0012) which uses several different linear blade twists. The data are generalized by the use of nondimensional coefficients so that they are applicable to a rotor of any size. The charts encompass the full range of available rotor lift and propulsive force or rotor drag.

ANALYSIS

DESCRIPTION OF COMPUTING ANALYSIS

The data presented in the performance charts are the results of an iterative, numerical-integration, strip analysis which solves the second-order, nonlinear differential blade-flapping equation. The individual force contributions (both aerodynamic and inertial) are integrated radially at each azimuth station to determine the blade flapping motion. The aerodynamic forces are then integrated radially and averaged azimuthally to establish the average rotor thrust, lift, power, drag, and other pertinent parameters. Figure 1 is a block diagram showing the basic operational steps of the Rotor Analysis Program schematically.

Airfoil section properties of c_ℓ and c_d as a function of both angle of attack (α = 0 to α = 360 degrees) and Mach number (M = 0 to M = 1.0) comprise the aerodynamic input to this method.

Using final computed values of thrust, power, and drag for a given flight condition, performance variables of rotor lift, propulsive force, and power are determined as follows:

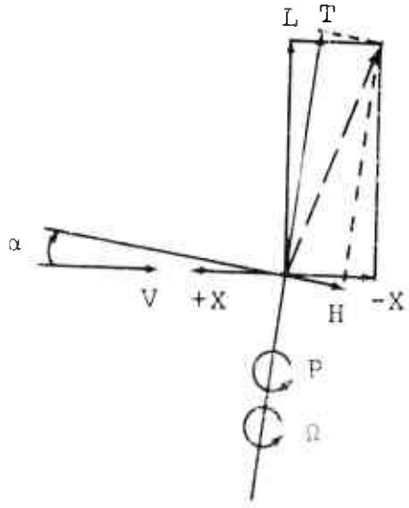

where

$L = T \cos \alpha - H \sin \alpha$

$X = -T \sin \alpha - H \cos \alpha$

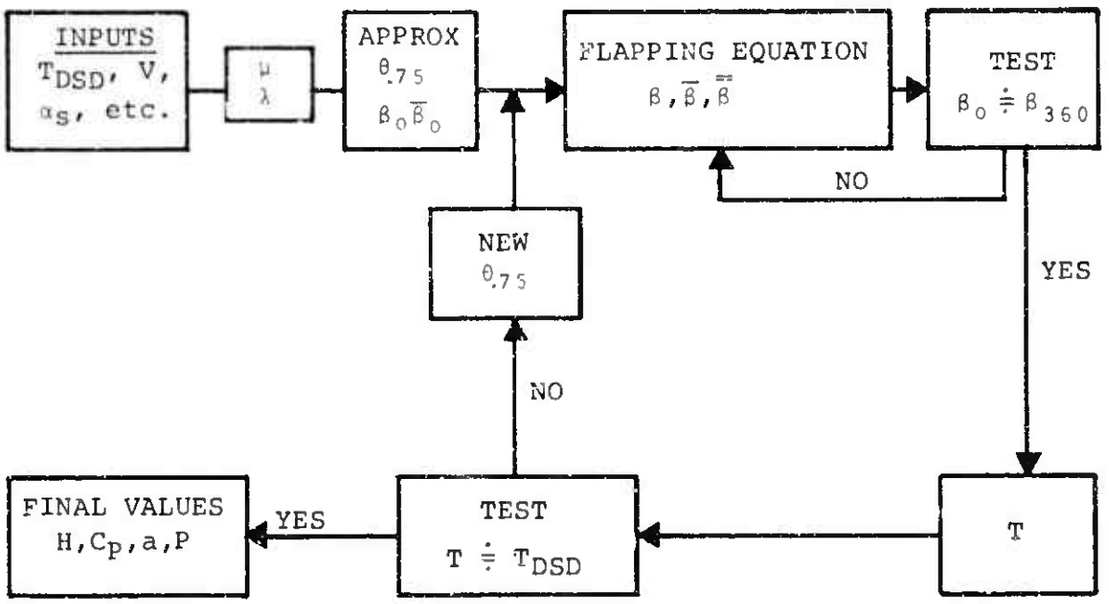

Figure 1. Rotor Analysis Flow Chart

Nondimensional lift and propulsive force are obtained by dividing by dynamic pressure ($q = \frac{1}{2}\rho V^2$), rotor diameter squared (d^2), and rotor solidity ($\sigma = bc/\pi R$). Nondimensional power is further divided by forward speed. Thus, with advance ratio defined as $\mu' = V/\Omega R$,

$$\frac{L}{qd^2\sigma} = \frac{\pi}{2(\mu')^2}\left(\frac{L}{\rho\pi R^2\Omega R^2\sigma}\right) = \frac{\pi}{2(\mu')^2}\, C_T'/\sigma$$

$$\frac{X}{qd^2\sigma} = \frac{\pi}{2(\mu')^2}\left(\frac{X}{\rho\pi R^2\Omega^2 R^2\sigma}\right) = \frac{\pi}{2(\mu')^2}\, C_X'/\sigma$$

$$\frac{P}{qd^2V\sigma} = \frac{\pi}{2(\mu')^2}\left(\frac{P}{\rho\pi R^2\Omega^3 R^3\sigma}\right) = \frac{\pi}{2(\mu')^2}\, C_p'/\sigma$$

Refinements of this analysis compared with older classical rotor theory include:

1. Elimination of small angle assumptions
2. Use of actual airfoil section characteristics over the entire range of angle of attack and Mach number
3. Accounting for stall effects
4. Accounting for compressibility effects
5. Accounting for effects of reversed flow

However, the following assumptions are retained in this analysis:

1. Uniform downwash over the rotor disc
2. Radial flow not considered in the computation of blade forces
3. Inelastic blades
4. Constant rotational speed about the shaft axis (neglect of lead-lag motion)

5. Steady-state, two-dimensional airfoil section characteristics

DATA VALIDITY

The retained assumptions have a significance with regard to data validity which should be considered. Preliminary estimates of the combined effects of nonuniform downwash, radial flow, and blade elasticity indicate that as the tip speed ratio increases from about $\mu' = V/\Omega R = .5$, the actual rotor power required may be increasingly greater than indicated by the use of these charts.

However, the maximum limiting values of lift and propulsion, as determined from these charts, are approximately correct as shown and, therefore, the charts may be used to design vehicles with a reasonable level of confidence, although the resulting performance may be optimistic in the high-tip-speed-ratio regime of operation.

GENERALITY OF DATA

Each chart is presented for a specific combination of advance ratio ($\mu' = V/\Omega R$) and advancing tip Mach number $\left(M_T = \frac{V + \Omega R}{a} \right)$. This completely generalizes the data for any combination of temperature and altitude desired. The temperature and pressure together with the μ' and M_T combination will then define the forward speed, tip speed, and dynamic pressure. (The speed values shown on the charts are only reference values for standard sea level conditions.) The data are nondimensionalized by the coefficients $L/qd^2\sigma$, $X/qd^2\sigma$, and $P/qd^2V\sigma$; thus, for a given solidity, the data are completely generalized for any rotor diameter. In order to allow for variations in solidity (σ), the coefficients include the solidity term. For small changes in solidity from the value used in the calculations ($\sigma = .062$), this will provide approximate generalization of the solidity effects. However, it does neglect the effect of solidity on induced drag, due to a change in total lift for a change in solidity when d and $L/qd^2\sigma$ remain fixed. For greater accuracy, corrections are therefore required to the propulsion (or drag) coefficient ($X/qd^2\sigma$) and the rotor angle of attack (α_s). These are described more fully under "SOLIDITY CORRECTION DERIVATION" (see page 9).

The charts presented herein were calculated for a rotor blade with the following characteristics:

Airfoil Section	NACA 0012
Planform	Rectangular
Solidity	0.062
Lock Number $\left(\gamma = \frac{\rho a c R^4}{I_f}\right)$	7.6
Blade Root Cutout (x_c)	0.20R
Nondimensional Mass Moment of Inertia ($I_f/\rho R^5$)	0.03953
Nondimensional Weight Moment ($M_W/g\rho R^4$)	0.06384
Flapping Hinge Offset (e)	0.0226R
Tip Loss Factor (B)	0.97
Blade Twist (θ_1), degrees	-4, -8, -12
Longitudinal Cyclic Pitch Angle (B_1), degrees	0

The influence of most of the above parameters, within broad tolerances, is negligible with respect to the final performance results. However, the use of the charts should be restricted to the use of rectangular blades of a constant NACA 0012 airfoil section, with linear twists as indicated on the charts.

AIRFOIL DATA

Figures 2 and 3 show the section characteristics of the NACA 0012 airfoil used in these analyses. The characteristics are based upon synthesized data derived from helicopter rotor hovering performance presented in NACA TN 4357. The data were extended to cover all angles of attack from 0 to 180 degrees on the basis of two-dimensional tests* of an NACA 0015

*Alan Pope, The Forces and Pressures Over An NACA-0015 Airfoil Through 180 Degrees Angle of Attack, Report No. E-102, Georgia School of Technology, February, 1947.

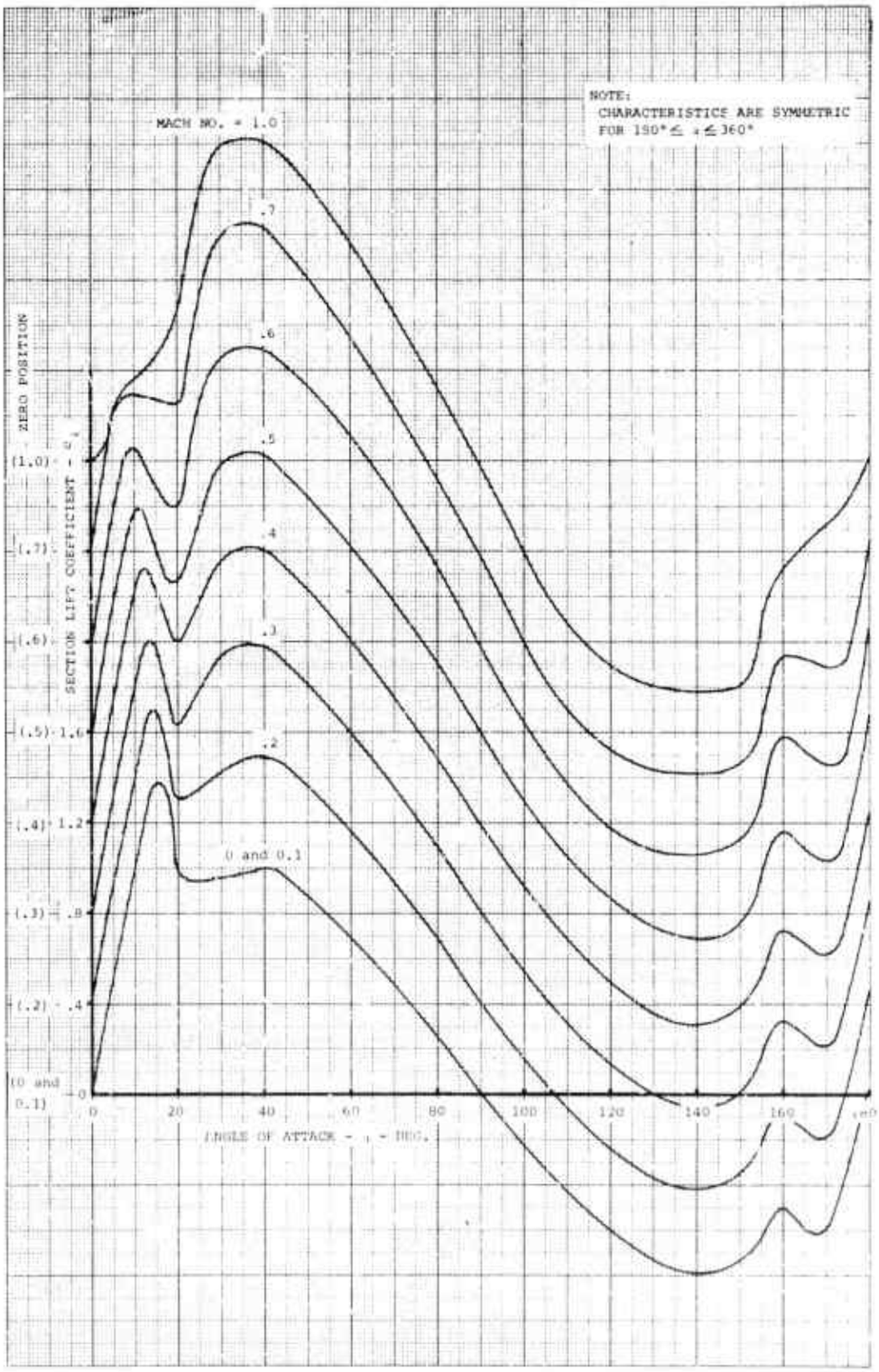

Figure 2. Section Lift Coefficient vs Angle of Attack - NACA 0012

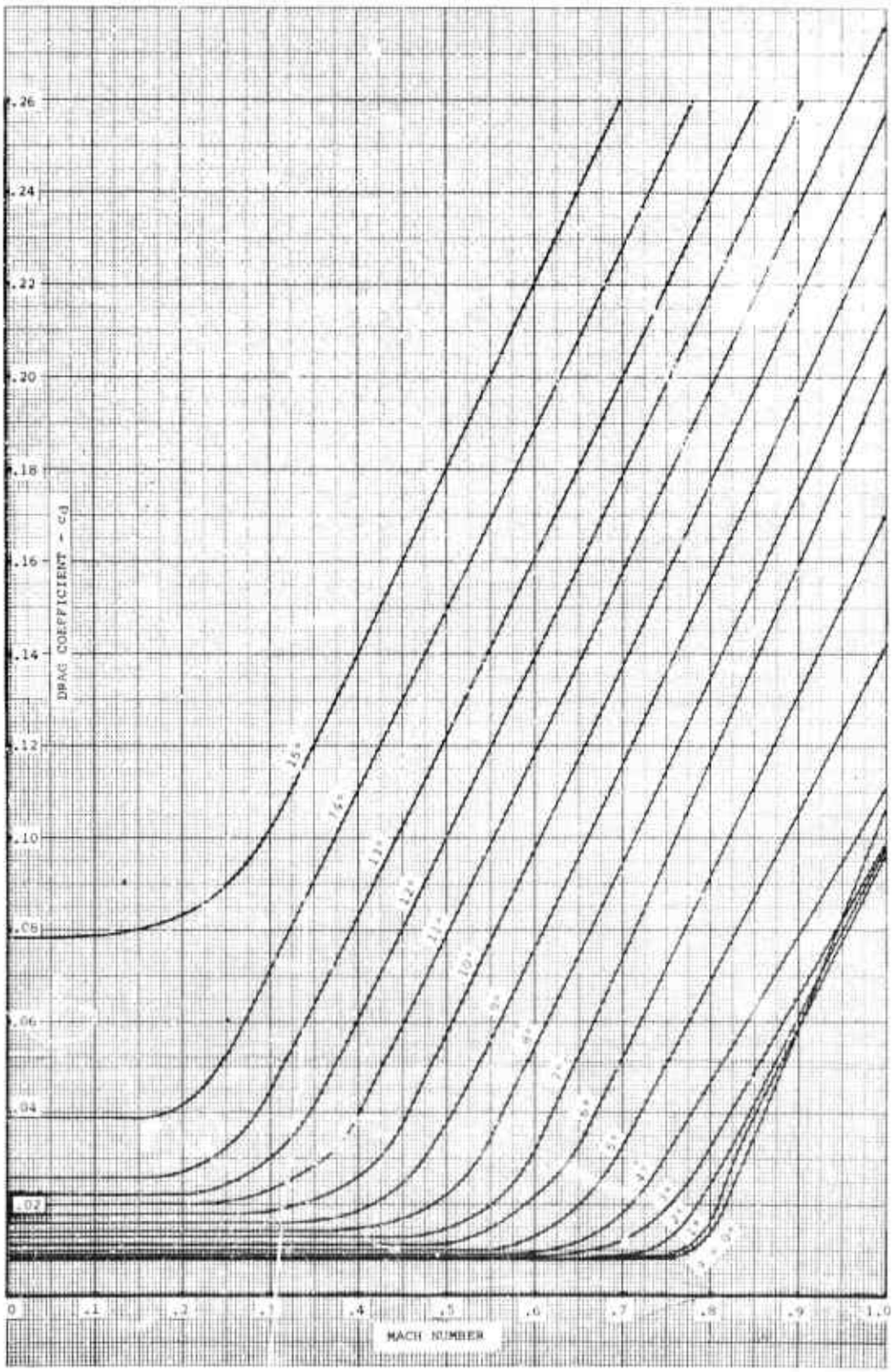

Figure 3. Section Drag Coefficient versus Mach Number - NACA 0012

airfoil through 180 degrees angle of attack. A further refinement of data was introduced in the reversed-flow angle-of-attack range (170 to 180 degrees) based on two-dimensional tests of an NACA 0012 airfoil conducted by the contractor.

OPERATIONAL LIMITATIONS

As an aid in defining the range of usable data at low to moderate advance ratios ($\mu' = 0.13$ to $\mu' = 0.7$), the conventional stall criteria, i.e., the angle of attack at the tip of the retreating blade, $\alpha_{(1)(270)}$, has been used. Experience has shown that at $\alpha_{(1)(270)} = 12$ degrees the effects of stall may become apparent, while operation above an upper limit of $\alpha_{(1)(270)} = 14$ degrees is considered to be undesirable. At values of advance ratio approaching $\mu' = 1.0$ and higher, the angle-of-attack limits are not shown, as the angle of attack of the retreating blade tip has lost its significance because of the low (or negative, at greater than 1.0) dynamic pressure.

The flapping angle, $a_1 = 10$ degrees, has been superimposed on the charts for the higher values of advance ratios ($\mu' = .75$ and higher). This is intended to indicate an order of magnitude for the cyclic trim requirements for the rotor in order to minimize shaft bending moments. Since $a_1 = 10$ degrees is measured with respect to the plane-of-no-feathering, 10 degrees of longitudinal cyclic pitch ($B_1 = 10$ degrees) would be required to obtain zero flapping with respect to the shaft. Calculations have also indicated that 10 degrees of flapping is often associated with the onset of flapping divergence and, for this reason, little data are obtainable beyond this value.

SOLIDITY CORRECTION DERIVATION

The coefficients used in this presentation are based on blade area ($d^2\sigma$), rather than disc area, by the use of the solidity ratio in the denominator. This is proper, since the blade angles of attack, and therefore the section lift-drag characteristics, are based upon blade area rather than disc area. However, when considering a solidity other than the one used in the preparation of these charts ($\sigma = .062$), a small error is introduced with respect to the induced velocities, since these are predominately dependent upon disc area alone. This, in turn, results in a small error in the rotor shaft angle of attack and in the rotor induced drag, which is one component of the available propulsive force. A simple correction may be

applied, however, to the rotor shaft angle of attack and the available propulsive force as follows:

$$\Delta\alpha_S = (L/qd^2\sigma)\ \frac{\Delta\sigma}{\pi}$$

$$\Delta X/qd^2\sigma = -(L/qd^2\sigma)^2\ \frac{\Delta\sigma}{\pi}$$

These corrections are derived as follows:

From momentum considerations of a rotor in forward flight, the mean induced velocity (v) is defined

$$L = 2\pi R^2 \rho V v = \pi d^2 \tfrac{1}{2}\rho V v = \pi d^2 q\ \frac{v}{V} \tag{1}$$

Solving for the mean induced angle, $\frac{v}{V}$,

$$\frac{v}{V} = \frac{L}{\pi q d^2} = \frac{1}{\pi}\ (L/qd^2) \tag{2}$$

Since the inflow ratio, λ, is defined

$$\lambda = \frac{V \sin\alpha - v}{\Omega R}, \tag{3}$$

$$\text{then } \sin\alpha = \frac{\lambda \Omega R}{V} + \frac{v}{V} = \frac{\lambda}{\mu'} + \frac{v}{V} \tag{4}$$

From (2) and (4),

$$\sin\alpha = \frac{\lambda}{\mu'} + \frac{1}{\pi}\ (L/qd^2) = \frac{\lambda}{\mu'} + \frac{\sigma}{\pi}(L/qd^2\sigma) \tag{5}$$

Using the subscript "1" to indicate the uncorrected solidity (σ_1 = .062 for the charts presented in this report) and the subscript "2" to indicate the desired value of solidity, then, from equation (5),

$$\sin\alpha_2 - \sin\alpha_1 = \frac{(\sigma_2 - \sigma_1)}{\pi}\ (L/qd^2\sigma) \tag{6}$$

For the small angular corrections involved, it is acceptable to approximate

$$\sin\alpha_2 - \sin\alpha_1 = \alpha_2 - \alpha_1 = \Delta\alpha \tag{7}$$

and therefore,

$$\Delta\alpha = (L/qd^2\sigma)\ \frac{\Delta\sigma}{\pi} = (L/qd^2\sigma)\ \frac{(\sigma - .062)}{\pi} \qquad (8)$$

The induced angle-of-attack change, $\Delta\alpha$, will cause an increment of rotor drag, or negative increment of propulsive force, $-\Delta X$, which is equal to the rotor lift times the angular increment:

$$-\Delta X = L\Delta\alpha \qquad (9)$$

Changing to coefficient form,

$$-\Delta X/qd^2\sigma = (L/qd^2\sigma)\Delta\alpha, \qquad (10)$$

and combining equations (8) and (10),

$$\Delta X/qd^2\sigma = -(L/qd^2\sigma)^2\ \frac{\Delta\sigma}{\pi} = -(L/qd^2\sigma)^2\ \frac{(\sigma - .062)}{\pi} \qquad (11)$$

The desired corrections are equations (8) and (11). See page 19 for an explanation of the use of these solidity corrections.

SCOPE OF THE DATA

Performance charts are presented for a range of forward speeds and tip speeds corresponding to advance ratios of from 0.13 to 1.5 and advancing blade tip Mach numbers from 0.64 to 0.98. Tables I, II, and III specify the combinations presented. The use of the advance ratio and advancing tip Mach number permits the data to be used for any altitude and temperature combination, whereas the sea level tip speeds and forward speeds are presented as a reference which will aid in visualizing the actual magnitudes involved. Figure 4 indicates graphically the operating conditions for which the charts are presented. Each operating condition presents data covering a range of shaft angles (α_s).

A shaft angle range of α_s = +20 degrees (usually windmill brake state with negative values of power) to -90 degrees (propeller state) is presented for all advance ratios up to 0.75. At higher advance ratios, however, the usable shaft angle is limited, because of mathematical indications of large flapping angles.

In the majority of the chart presentations, it has been possible to maintain the intended $L/qd^2\sigma$ versus $X/qd^2\sigma$ format. At values of advance ratio above μ' = .75, however, the power lines begin to fold back on one another to such an extent that the chart becomes unreadable in this format. In such cases, it has become necessary to plot $P/qd^2V\sigma$ and $X/qd^2\sigma$ versus shaft angle, α_s, for lines of constant $L/qd^2\sigma$ (e.g., Figure 18).

Data for advance ratios in excess of μ' = 1.5 were attempted; however, the range of usable conditions was so limited within the operating boundaries (flapping boundary of 10 degrees, positive $L/qd^2\sigma$, and stable flapping values) that the study was discontinued at this point.

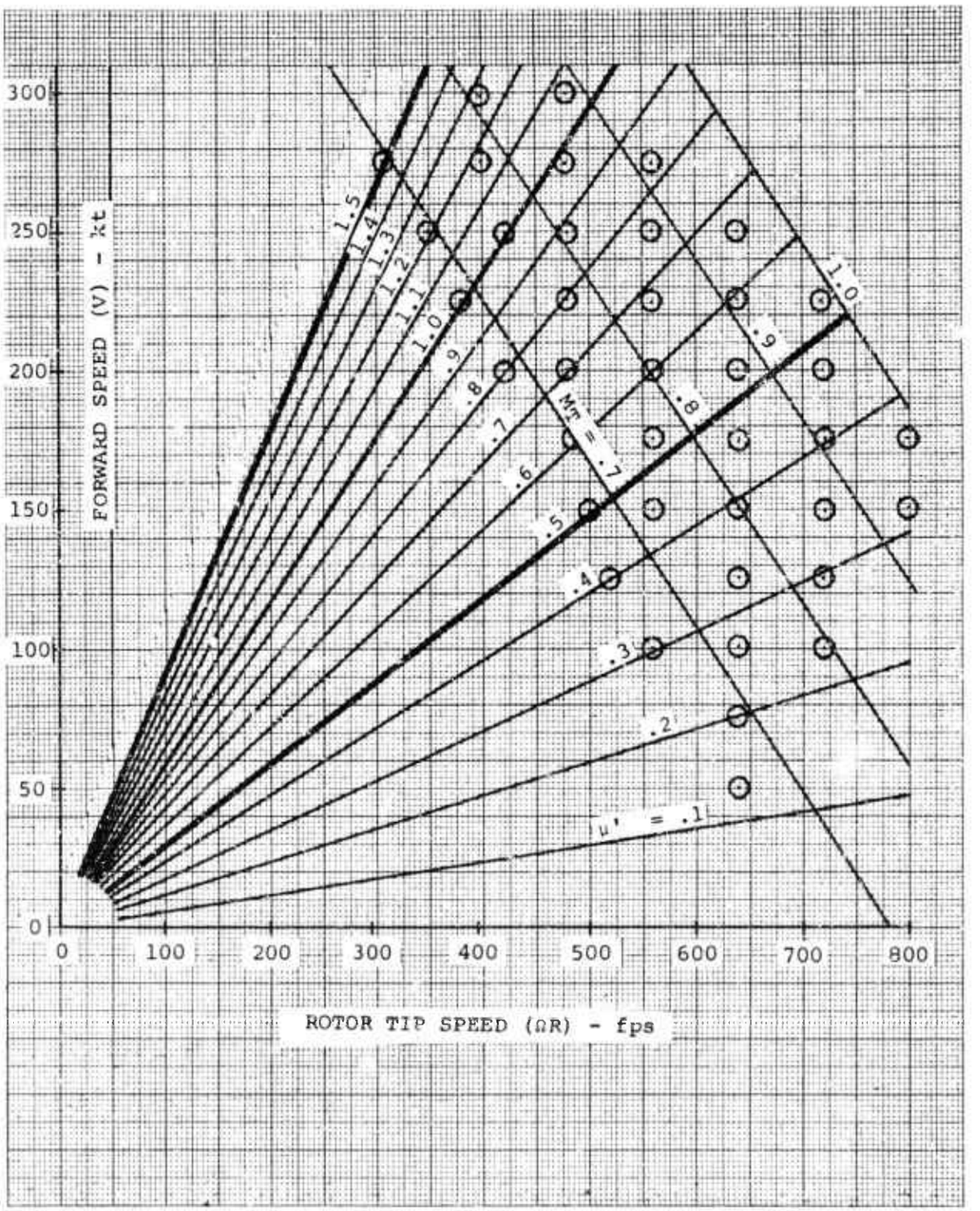

Figure 4. Operating Conditions

TABLE I. OPERATING CONDITIONS FOR θ_1 = -4°

V (kt @ SL)	50	150	200	250	300
V (fps @ SL)	84.4	253.3	337.8	422.2	506.7
q (psf @ SL)	8.5	76.3	135.7	212.0	305.2
ΩR (fps @ SL)	640	500	420	350	400
M_T	.648	.674	.678	.691	.811
μ'	.132	.507	.804	1.206	1.267
ΩR (fps @ SL)	-	560	480	420	480
M_T	-	.728	.732	.754	.883
μ'	-	.452	.704	1.005	1.056
ΩR (fps @ SL)	-	640	560	480	-
M_T	-	.799	.803	.807	-
μ'	-	.396	.603	.880	-
ΩR (fps @ SL)	-	720	640	560	-
M_T	-	.871	.875	879	-
μ'	-	.352	.528	.754	-
ΩR (fps @ SL)	-	800	720	640	-
M	-	.943	.947	.951	-
μ'	-	.317	.469	.660	-

TABLE II. OPERATING CONDITIONS

V(kt @ SL)	50	75	100	125	150	17
V(fps @ SL)	84.4	126.7	168.9	211.1	253.3	29
q(psf @ SL)	8.5	19.1	33.9	53.0	76.3	10
ΩR(fps @ SL)	640	640	560	520	500	
M_T	.648	.686	.652	.654	.674	.
μ'	.132	.198	.302	.406	.507	.
ΩR(fps @ SL)	-	-	640	640	560	
M_T	-	-	.724	.762	.728	.
μ'	-	-	.264	.330	.452	.
ΩR(fps @ SL)	-	-	720	780	640	
M_T	-	-	.795	.833	.799	.
μ'	-	-	.235	.293	.396	.
ΩR(fps @ SL)	-	-	-	-	720	
M_T	-	-	-	-	.871	.
μ'	-	-	-	-	.352	.
ΩR(fps @ SL)	-	-	-	-	800	
M_T	-	-	-	-	.943	.
μ'	-	-	-	-	.317	.

CONDITIONS FOR $\theta_1 = -8°$

	175	200	225	250	275	300
	295.6	337.8	380.0	422.2	464.4	506.7
	103.9	135.7	171.7	212.0	256.5	305.2
	485	420	380	350	310	400
	.698	.678	.680	.691	.693	.811
	.609	.804	1.000	1.206	1.498	1.267
	560	480	480	420	400	480
	.766	.732	.770	.754	.774	.883
	.528	.704	.792	1.005	1.161	1.056
	640	560	560	480	480	-
	.837	.803	.841	.807	.845	-
	.462	.603	.679	.880	.968	-
	720	640	640	560	560	-
	.909	.875	.913	.879	.917	-
	.411	.528	.594	.754	.829	-
	800	720	720	640	-	-
	.980	.947	.984	.951	-	-
	.369	.469	.528	.660	-	-

TABLE III. OPERATING CONDITIONS FOR $\theta_1 = -12°$					
V (kt @ SL)	50	150	200	250	300
V (fps @ SL)	84.4	253.3	337.8	422.2	506.7
q (psf @ SL)	8.5	76.3	135.7	212.0	305.2
ΩR (fps @ SL)	640	500	420	350	400
M_T	.648	.674	.678	.691	.811
μ'	.132	.507	.804	1.206	1.267
ΩR (fps @ SL)	-	560	480	420	480
M_T	-	.728	.732	.754	.883
μ'	-	.452	.704	1.005	1.056
ΩR (fps @ SL)	-	640	560	480	-
M_T	-	.799	.803	.807	-
μ'	-	.396	.603	.880	-
ΩR (fps @ SL)	-	720	640	560	-
M_T	-	.871	.875	.879	-
μ'	-	.352	.528	.754	-
ΩR (fps @ SL)	-	800	720	640	-
M_T	-	.943	.947	.951	-
μ'	-	.317	.469	.660	-

USE OF THE CHARTS

GENERAL

The graphical method of presentation used herein nondimensionalizes lift, propulsive force, and power by free-stream velocity, rather than by tip speed (as is usually done in rotary-wing work). The results can be directly compared to the lift-drag polar of a wing, which is the cornerstone of the performance problem and a common ground for all aerodynamicists. This is especially important when considering compound helicopters, as it permits direct solutions in designing for optimum performance with any amount of rotor lift unloading or auxiliary propulsion.

Figure 5 illustrates this type of presentation. The typical drag polar of lift (on the ordinate), drag to the right and propulsive force to the left (on the abscissa) is standard. By varying the shaft angle from -90 degrees (propeller state) to +20 degrees (autogyro or windmill brake state), at several values of power, a complete evaluation of the rotor's ability to produce lift and/or propulsive force is readily apparent. The case of zero power (autorotation) produces the drag polar of the lifting rotor. By increasing the level of power input, the rotor will produce increasing levels of propulsive force ($X/qd^2\sigma$) varying from 0.00 to 0.02, 0.04, 0.06, etc.

A measure of the rotor's ability to convert additional power into increased propulsive force can be seen by reviewing, for example, the increment in propulsive force associated with a change in power level from 0.06 to 0.08.

At $L/\sigma d^2\sigma = 0.32$,

$$\frac{\Delta X}{qd^2\sigma} = 0.016 - (-0.0008) = .0168$$

Noting that for 100-percent efficiency $\frac{\Delta X}{qd^2\sigma} = \frac{\Delta XV}{qd^2V\sigma} = \frac{\Delta P}{qd^2V\sigma}$, we might have hoped that the increment in nondimensional propulsive force would have equalled the increment in nondimensional power, $\frac{\Delta P}{qd^2V\sigma} = .08 - .06 = .02$, instead of the value of .0168 obtained above. One definition of incremental propulsive efficiency might therefore be

$$\eta_p = \frac{\Delta X/qd^2\sigma}{\Delta P/qd^2V\sigma} = \frac{0.0168}{0.02} = 0.84$$

NOTE: Since the propulsion efficiency is of the same order of magnitude as the efficiency of a propeller, consideration should be given to using auxiliary propulsion for further increases in propulsive requirements.

The effects of blade stall can be seen as rotor lift is increased at constant power. At the higher values of rotor lift there is a significant reduction in the propulsive capability of the rotor, gradually developed as the retreating blade tip angle of attack exceeds a nominal 14 degrees.

USE OF SOLIDITY CORRECTIONS

The following corrections were derived on pages 9, 10, and 11.

Holding $L/qd^2\sigma$ and $P/qd^2V\sigma$ constant,

$$\Delta\alpha_s = (L/qd^2\sigma)\ \frac{\Delta\sigma}{\pi} = (L/qd^2\sigma)\left(\frac{\sigma - .062}{\pi}\right)$$

$$\Delta X/qd^2\sigma = -(L/qd^2\sigma)^2\ \frac{\Delta\sigma}{\pi} = -(L/qd^2\sigma)^2\left(\frac{\sigma - .062}{\pi}\right)$$

In order to keep the signs of the corrections straight, it may be helpful to consider the following:

1. An increase in solidity (above .062) will increase the disc loading at a given value of $L/qd^2\sigma$

2. An increased disc loading will cause an increased induced drag (at a given value of P/qd^2V)

3. An increased induced drag will decrease the propulsive force

4. An increased induced velocity will increase the free-stream shaft angle of attack for a given local shaft angle of attack

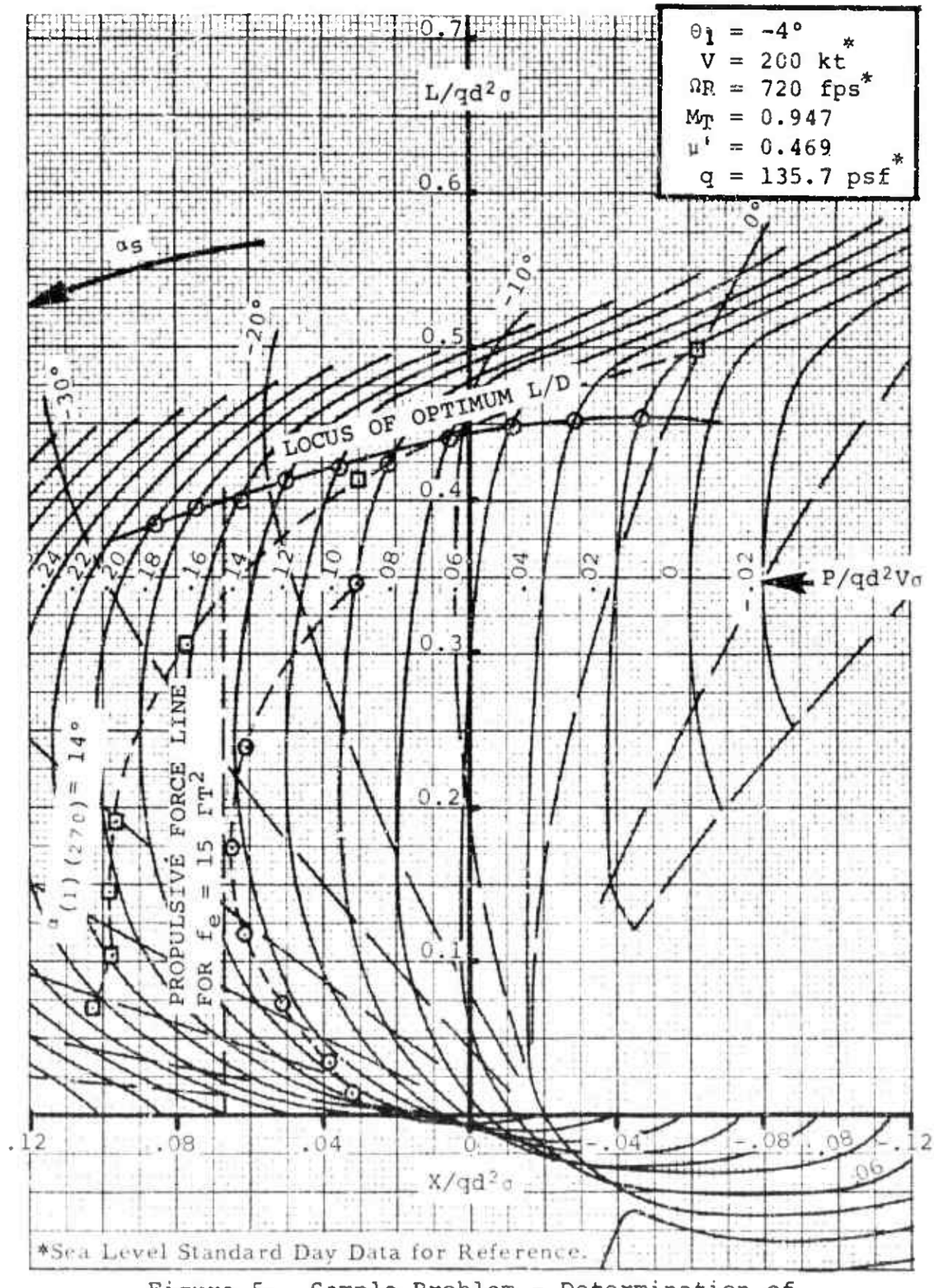

Figure 5. Sample Problem - Determination of Maximum L/D

An alternate way of visualizing item (2) is to consider that an increased disc loading will cause an increased induced power (at a given value of $X/qd^2\sigma$). The magnitude of the generalized power increase, $P/qd^2V\sigma$, will approximately equal the magnitude of the alternate generalized drag increase (or propulsive force decrease).

$$\Delta P/qd^2V\sigma \cong -\Delta X/qd^2\sigma$$

SAMPLE PROBLEM FOR DETERMINING MAXIMUM L/D

For a rotor operating at V = 200 knots (q = 135.7 psf) with a tip speed of 720 fps, determine the lift for maximum L/D of the rotor for 15 square feet of drag and a rotor diameter of 60 feet. The solidity is 0.062 and the blade twist (θ_1) is -4 degrees. What is the L/D_E of the rotor and the L/D of the configuration at this point?

Step 1. Determine the best lift-to-drag ratio point for each constant power line by constructing a line through $X/qd^2\sigma = P/qd^2V\sigma$ at $L/qd^2 = 0$ and tangent to the particular constant power line. These points of tangency are the best L/D points for these values of power. Construct the locus of the best L/D points. (Refer to Figure 5.)

Step 2. Calculate the rotor propulsive force for a flat-plate area of 15 square feet.

$$X/qd^2\sigma = \frac{f_e}{d^2\sigma} = \frac{15}{(60)^2\ (0.062)} = 0.0673$$

Construct the constant $X/qd^2\sigma = 0.0673$ line and extend it to the locus of best L/D points.

Step 3. The intersection of the above lines determines maximum L/D for the specified rotor configuration.

A. Lift for maximum L/D is

$$\frac{L}{qd^2\sigma} = 0.4$$

$$L = 0.4\ (135.659)(3600)(0.062)$$

$$L = 12{,}100 \text{ pounds}$$

B. L/D_E of rotor at intersection point is

$$\frac{L}{D_E} = \frac{L}{P/V - X} = \frac{L/qd^2\sigma}{P/qd^2V\sigma - X/qd^2\sigma}$$

$$= \frac{0.4}{0.169 - 0.0673}$$

$$\frac{L}{D_E} = 3.94$$

C. L/D of the configuration is

$$\frac{L}{D} = \frac{L}{P/V} = \frac{L/qd^2\sigma}{P/qd^2V\sigma} = \frac{0.4}{0.169}$$

$$\frac{L}{D} = 2.365$$

This intersection occurs above $\alpha(1)(270)$ = 14 degrees and therefore should be reduced to the 14-degree stall limit in order to calculate the operational value of lift, L/D_E, of the rotor, and L/D of the configuration.

$$L/qd^2\sigma = 0.337$$

$$L = 0.337\ (135.659)(3600)(0.062)$$

$$= 10,200 \text{ pounds}$$

$$L/D_E = \frac{L}{P - X} = \frac{0.337}{0.151 - 0.0673} = 4.03$$

$$L/D = \frac{L}{P} = \frac{0.337}{0.151} = 2.23$$

It should be noted that in a case like this, it would be appropriate to investigate a rotor with more twist (θ_1 = -8 degrees or -12 degrees) to see if the best L/D point might not occur within the 14-degree stall boundary.

SAMPLE PROBLEM FOR A PURE HELICOPTER

What is the variation of main rotor horsepower with main rotor solidity for a single rotor helicopter weighing 20,000 pounds, having an equivalent parasite drag area (f_e) of 15 square feet and a main rotor diameter of 60 feet? The operating condition is 200 knots at sea level (q = 135.7 psf) with a tip speed of 720 fps. The blade twist (θ_1) is equal to -4.0 degrees.

The charts are based on a solidity of 0.062. Solidity corrections must, therefore, be applied to the propulsive force as outlined in the previous section. In this case, rather than subtract from the available propulsive forces the drag increment due to a solidity increase, it is more convenient to add the drag increment to the required propulsive force, as shown in the following calculation. (It should be noted that the resulting propulsive force coefficient is fictitious and is only used as a convenience to obtain intersections with the power lines at the proper values of lift coefficients.)

$$\Delta\left(\frac{X}{qd^2\sigma}\right) = -\left(\frac{L}{qd^2\sigma}\right)^2 \frac{\Delta\sigma}{\pi}$$

Assume Rotor Lift = Gross Weight = 20,000 pounds

Propulsive Force, $X = f_e q = 15 \times 135.7 = 2030$ pounds

Use Figures 6 and 7 to determine the power required for each of the various solidities shown below.

① σ	② $L/qd^2\sigma$ $\frac{20000}{qd^2\sigma}$	③ $X/qd^2\sigma$ $\frac{2030}{qd^2\sigma}$	④ $\Delta\sigma$ (① - .062)	⑤ $\Delta X/qd^2\sigma$ ②^2 x ④/π	⑥ $(X/qd^2\sigma)$ Corr for Solidity ③ + ⑤	⑦ $P/qd^2V\sigma$ Using ②, ⑥ Inter-polate fr.Chart	⑧ RHP ⑦ ① $\frac{qd^2V}{550}$ ⑦ x ① x 2.99×10^5
0.06	0.683	0.0693	-0.002	-0.000296	0.06900	---	---
0.08	0.512	0.0520	0.018	0.0015	0.0535	0.271	6500
0.10	0.410	0.0416	0.038	0.002035	0.04364	0.129	3860
0.12	0.3415	0.0346	0.058	0.00215	0.03675	0.108	3890
0.14	0.2925	0.0297	0.078	0.00212	0.03182	0.097	4050
0.16	0.256	0.0259	0.098	0.00204	0.02794	0.092	4400

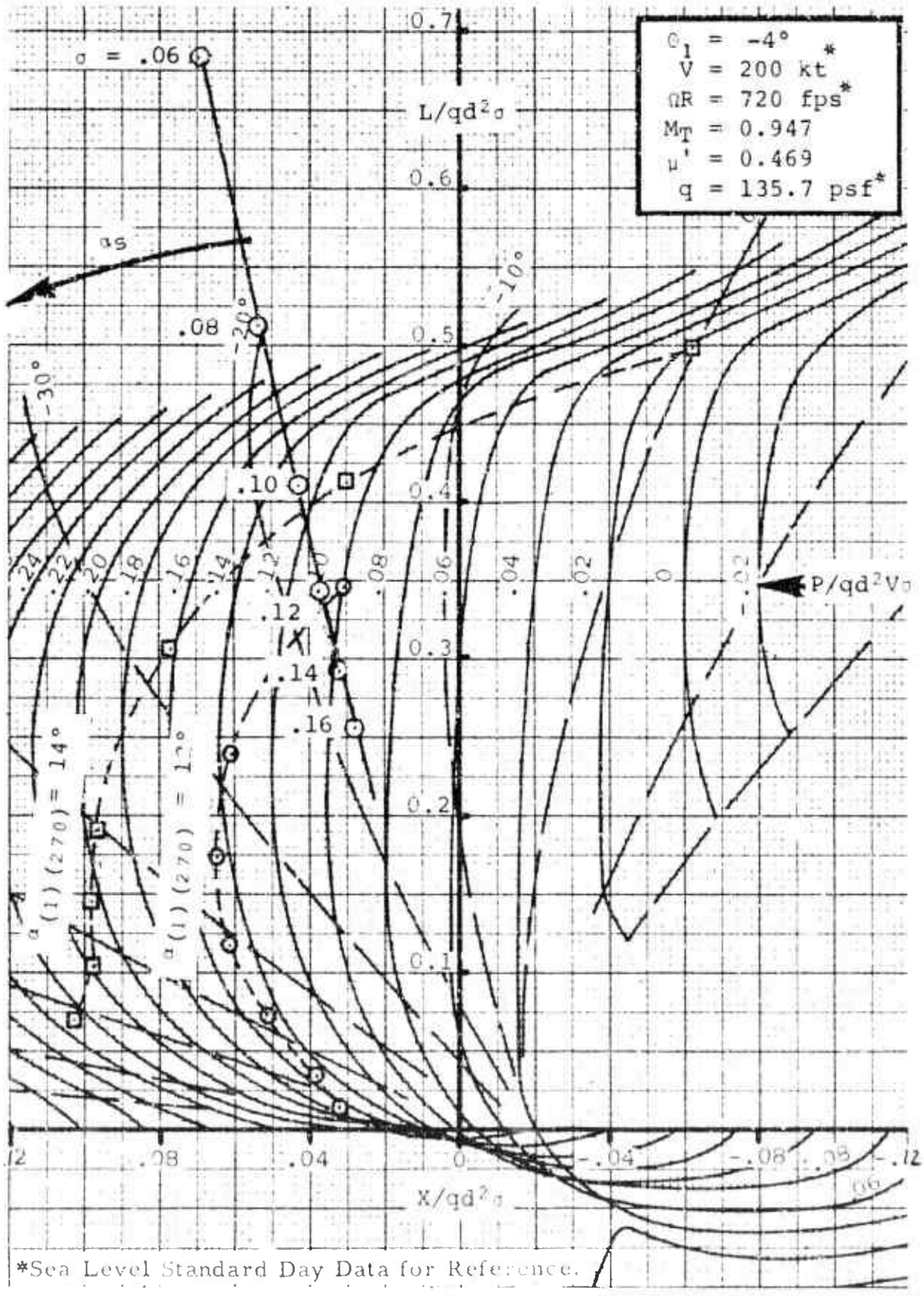

Figure 6. Sample Problem - Effect of Solidity

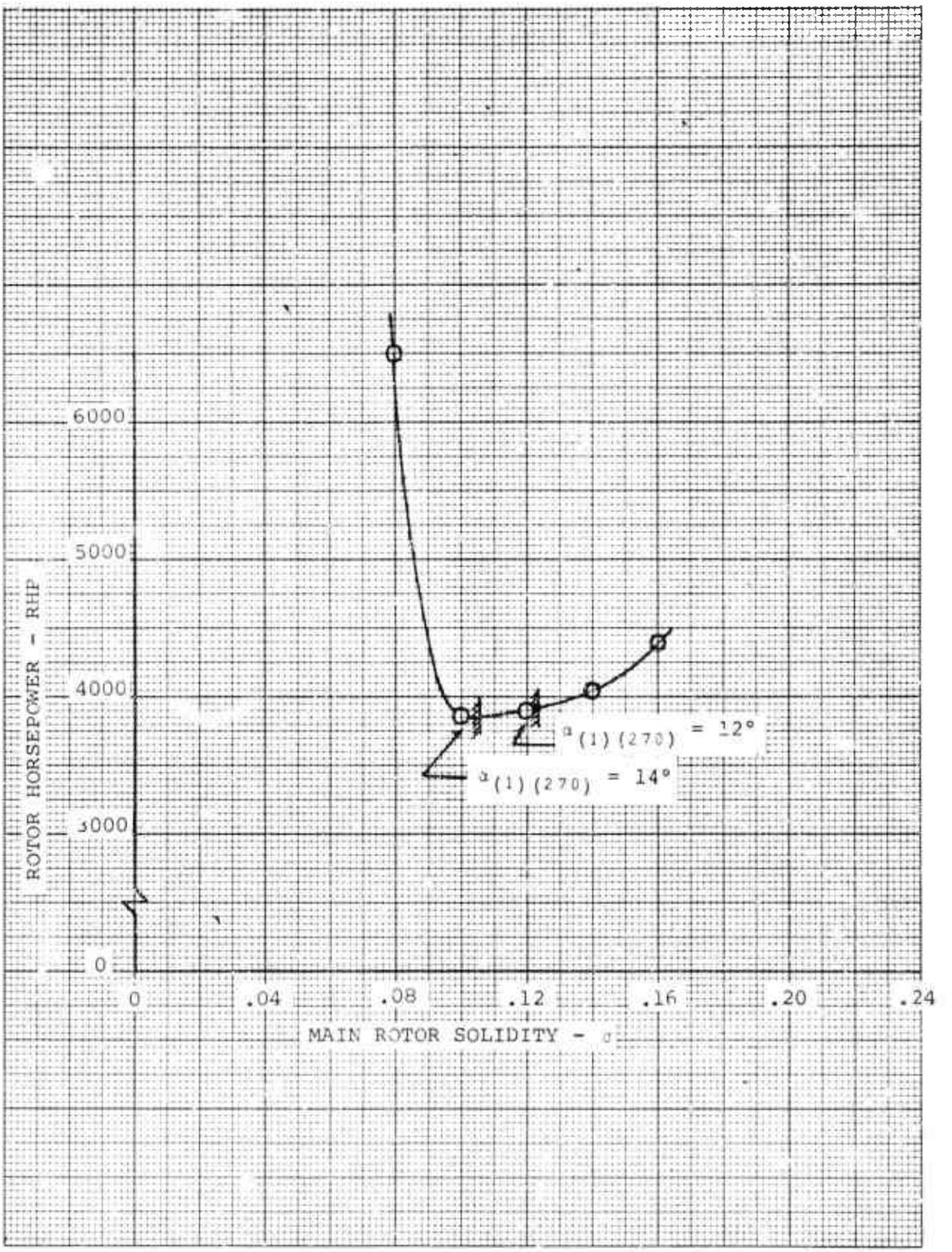

Figure 7. Variation of Rotor Horsepower with Main Rotor Solidity

SAMPLE PROBLEM FOR A WINGED HELICOPTER

What is the variation of rotor horsepower with wing area for a single rotor helicopter weighing 20,000 pounds having an equivalent parasite drag area (f_e) of 15 square feet (excluding wing drag), a rotor diameter of 60 feet, and a solidity of 0.10? The operating condition is 200 knots at sea level (q = 135.659 psf) with a blade tip speed of 720 fps. Assume the wing has a resultant wing L/D of 15 and that the wing operates at a C_L = 0.5.

Step 1. Determine the basic operating point with no wing

$$\frac{L}{qd^2\sigma} = \frac{GW}{qd^2\sigma} = \frac{20000}{135.659(60)^2(0.1)} = 0.41$$

$$\frac{X}{qd^2\sigma} = \frac{f_e}{d^2\sigma} = \frac{15}{(60)^2(0.1)} = 0.0417$$

Step 2. Construct the rotor unloading line through the operating point by adding one unit of propulsive force requirement for every 15 units of rotor lift unloading. Refer to Figure 8.

Step 3. Apply the solidity correction, $\Delta X/qd^2\sigma = (L/qd^2\sigma)^2 \frac{\Delta\sigma}{\pi}$, to the rotor unloading line and establish a new rotor unloading line by adding ΔX to the original required values of X.

$(L/qd^2\sigma)$	$(L/qd^2\sigma)^2$	$(L/qd^2\sigma)^2\frac{\Delta\sigma}{\pi}$	$(X/qd^2\sigma)$	$(X/qd^2\sigma)_{corr}$
0.1	0.01	0.000121	0.0615	0.06162
0.2	0.04	0.000484	0.0550	0.05548
0.3	0.09	0.001090	0.0485	0.04959
0.4	0.16	0.001935	0.0425	0.04444
0.5	0.25	0.003025	0.0355	0.03852
0.6	0.36	0.004350	0.0290	0.03335

Step 4. With the new rotor unloading line established, reduce the rotor lift by approximately 50 percent in 2000-pound increments along the rotor unloading line, and tabulate $P/qd^2V\sigma$.

L_{rotor} (lb)	$L/qd^2\sigma$	$P/qd^2V\sigma$
20000	0.410	0.130
18000	0.369	0.124
16000	0.329	0.122
14000	0.287	0.122
12000	0.247	0.124
10000	0.205	0.127

Step 5. Compute rotor horsepower (RHP) at each value of total rotor lift.

$$RHP = \left(\frac{P}{qd^2V\sigma} \right) \left(\frac{qd^2V\sigma}{550} \right) = 2.99\ (10)^4 \left(\frac{P}{qd^2V\sigma} \right)$$

$P/qd^2V\sigma$	RHP
0.130	3885
0.124	3710
0.122	3645
0.122	3645
0.124	3695
0.127	3800

Step 6. Determine wing area (S_w) using a wing design lift coefficient of $C_L = 0.5$.

$$L_{wing} = L_{total} - L_{rotor}$$

$$L_{wing} = C_L q S_w = 0.5\ (135.659)\ S_w$$

L_{rotor} (lb)	L_{wing} (lb)	S_w (ft^2)
20000	0	0
18000	2000	29.5
16000	4000	59.0
14000	6000	88.5
12000	8000	118.0
10000	10000	147.5

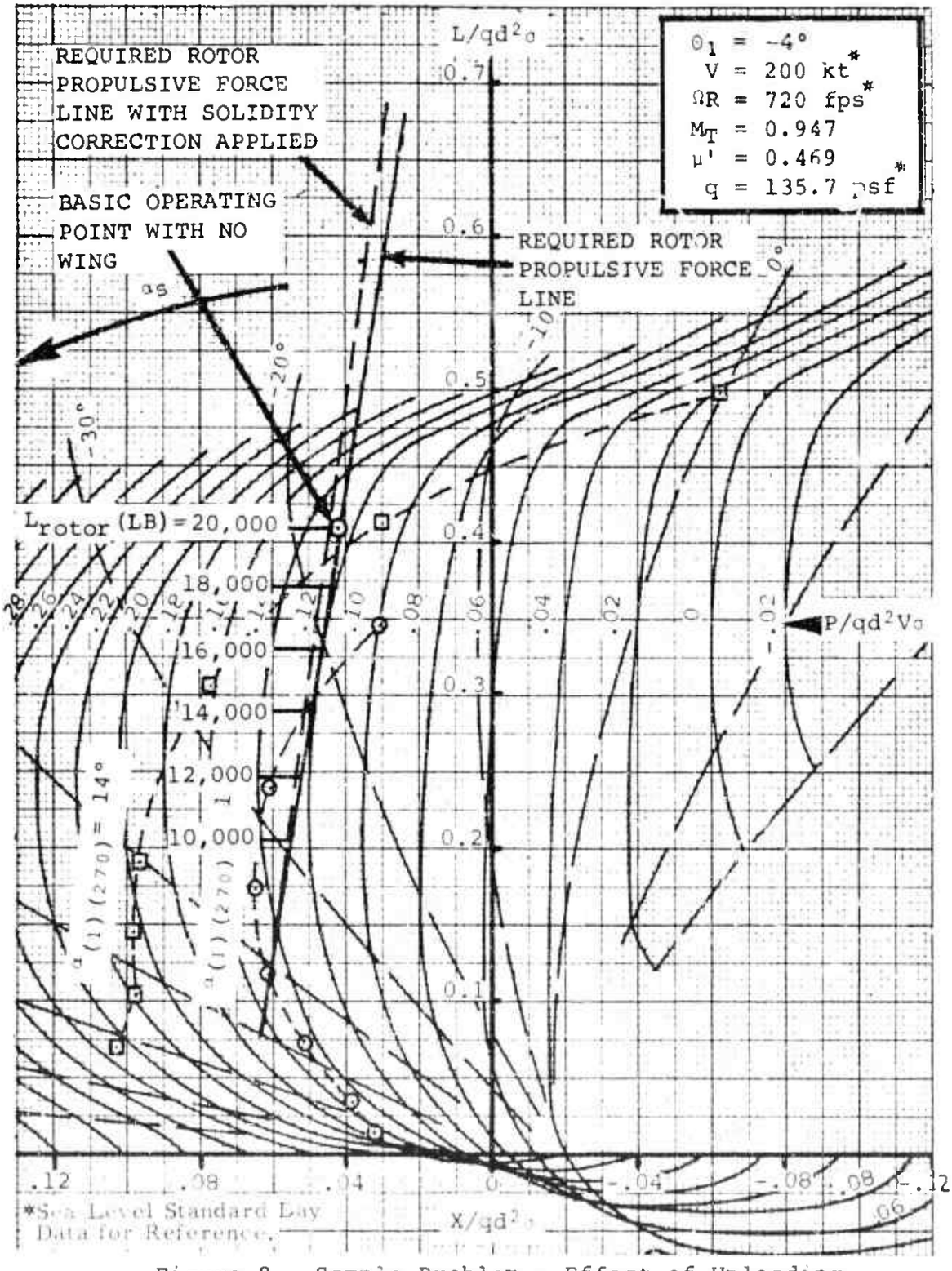

Figure 8. Sample Problem - Effect of Unloading Rotor with Wing

Step 7. Summary Table (Refer to Figure 9.)

L_{rotor}	L_{wing}	S_w	RHP
20000	0	0	3885
18000	2000	29.5	3710
16000	4000	59.0	3645
14000	6000	88.5	3645
12000	8000	118.0	3695
10000	10000	147.5	3800

SAMPLE PROBLEM FOR COMPOUND HELICOPTER WITH AUXILIARY PROPULSION

What is the variation of total aircraft power with increasing auxiliary propulsive force achieved by means of a propeller (assume a propulsive efficiency $\eta_p = 0.85$) for a single-rotor helicopter weighing 20,000 pounds, with an equivalent parasite drag area (excluding wing drag) of 15 square feet, a wing which provides 2000 pounds of lift at a resultant L/D = 15, and a rotor diameter of 60 feet? The rotor solidity is 0.10 and the operating condition is 200 knots at sea level ($q = 135.7$ psf) with a tip speed of 720 fps.

Step 1. Determine the basic operating point with no wing

$$\frac{L}{qd^2\sigma} = \frac{GW}{qd^2\sigma} = \frac{20000}{135.659(60)^2(0.1)} = 0.41$$

$$\frac{X}{qd^2\sigma} = \frac{f_e}{d^2\sigma} = \frac{15}{(60)^2(0.1)} = 0.041$$

Step 2. Construct the rotor unloading line through the Operating point by adding one unit of propulsive force requirement for every 15 units of rotor lift unloading. (Refer to Figure 10.)

Step 3. Caluclate the value of $L/qd^2\sigma$ which corresponds to a constant wing loading line of 2000 pounds, and use the intersection of this line and the rotor unloading line as the starting point for rotor propulsive unloading (i.e., increasing auxiliary propulsive force).

$$(L/qd^2\sigma) \text{ at } L_W = 2000 = \frac{\text{Gross Weight} - L_{wing}}{qd^2\sigma}$$

$$= \frac{20000 - 2000}{(135.659)(60)^2(0.1)}$$

$$L/qd^2\sigma = 0.369$$

Step 4. Apply the solidity correction $\frac{\Delta X}{qd^2\sigma} = -\left(\frac{L}{qd^2\sigma}\right)^2 \frac{\Delta\sigma}{\pi}$ to values of $X/qd^2\sigma$ where constant lines of $P/qd^2V\sigma$ cross the constant wing loading line of 2000 pounds.

$$\frac{\Delta X}{qd^2\sigma} = -(0.369)^2\left(\frac{.038}{\pi}\right) = -0.001645$$

$P/qd^2V\sigma$	$X/qd^2\sigma$	$(X/qd^2\sigma)_{corr}$
0.14	0.0565	0.05485
0.12	0.0428	0.04115
0.10	0.029	0.02735
0.08	0.0128	0.01115
0.06	-0.0035	-0.00515
0.04	-0.0212	-0.02284
0.02	-0.0405	-0.04214
0.0	-0.0605	-0.06215

Step 5. Using the intersection in Step 3 as the starting point, tabulate $(P/qd^2V\sigma)_{rotor}$, $(X/qd^2\sigma)_{rotor}$, and $(X/qd^2\sigma)_{prop}$:

$$(X/qd^2\sigma)_{prop} = (X/qd^2\sigma)_{total} - (X/qd^2\sigma)_{rotor}$$

$$= 0.044 - (Xqd^2\sigma)_{rotor}$$

$(P/qd^2V\sigma)_{rotor}$	$(X/qd^2\sigma)_{rotor}$	$(X/qd^2\sigma)_{prop}$
0.124	0.044	0.0
0.10	0.02735	0.01665
0.08	0.01135	0.03265
0.06	-0.00515	0.04915
0.04	-0.02365	0.06765
0.02	-0.04165	0.08565
0.0	-0.06215	0.10615

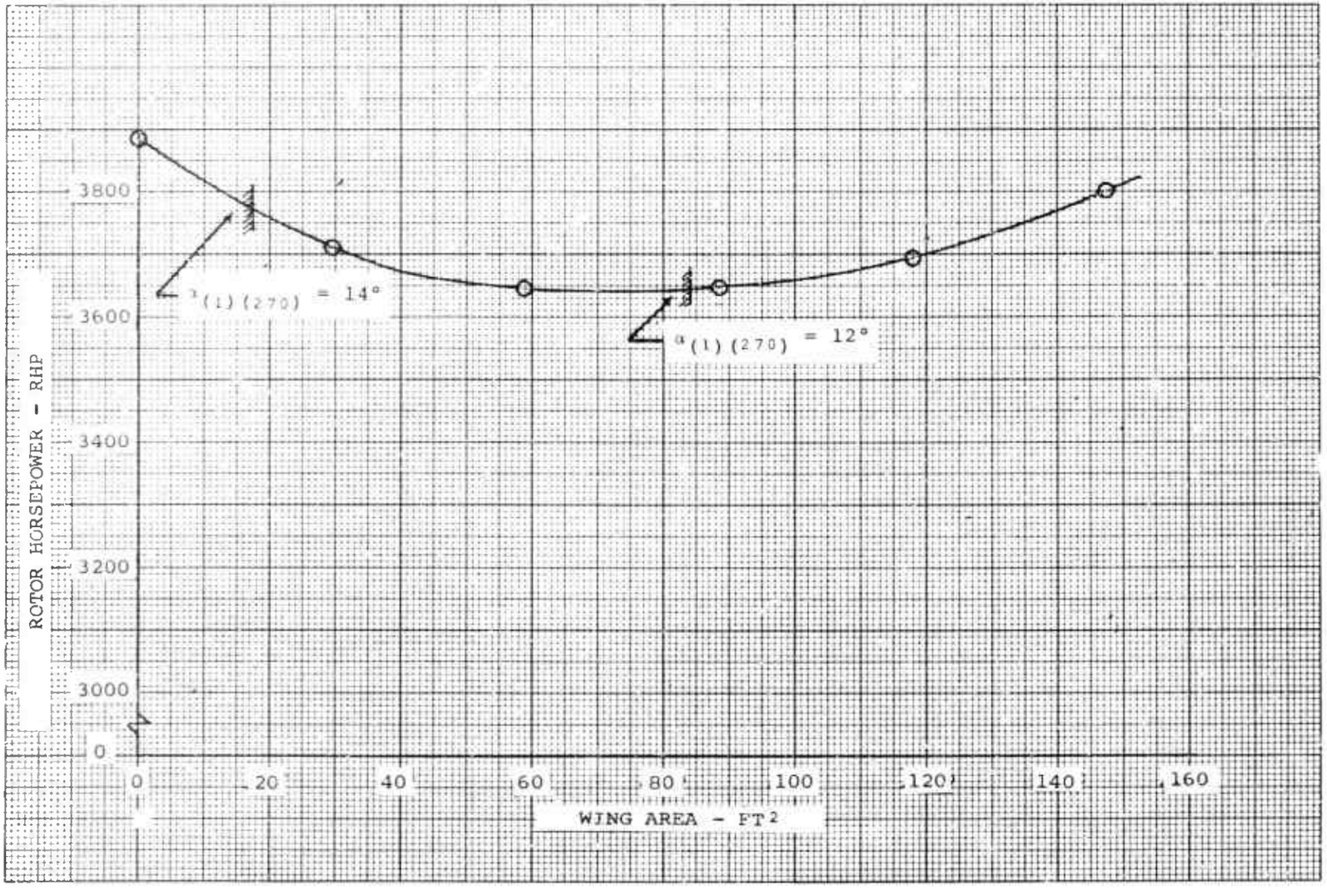

Figure 9. Variation of Rotor Horsepower with Auxiliary Wing Area

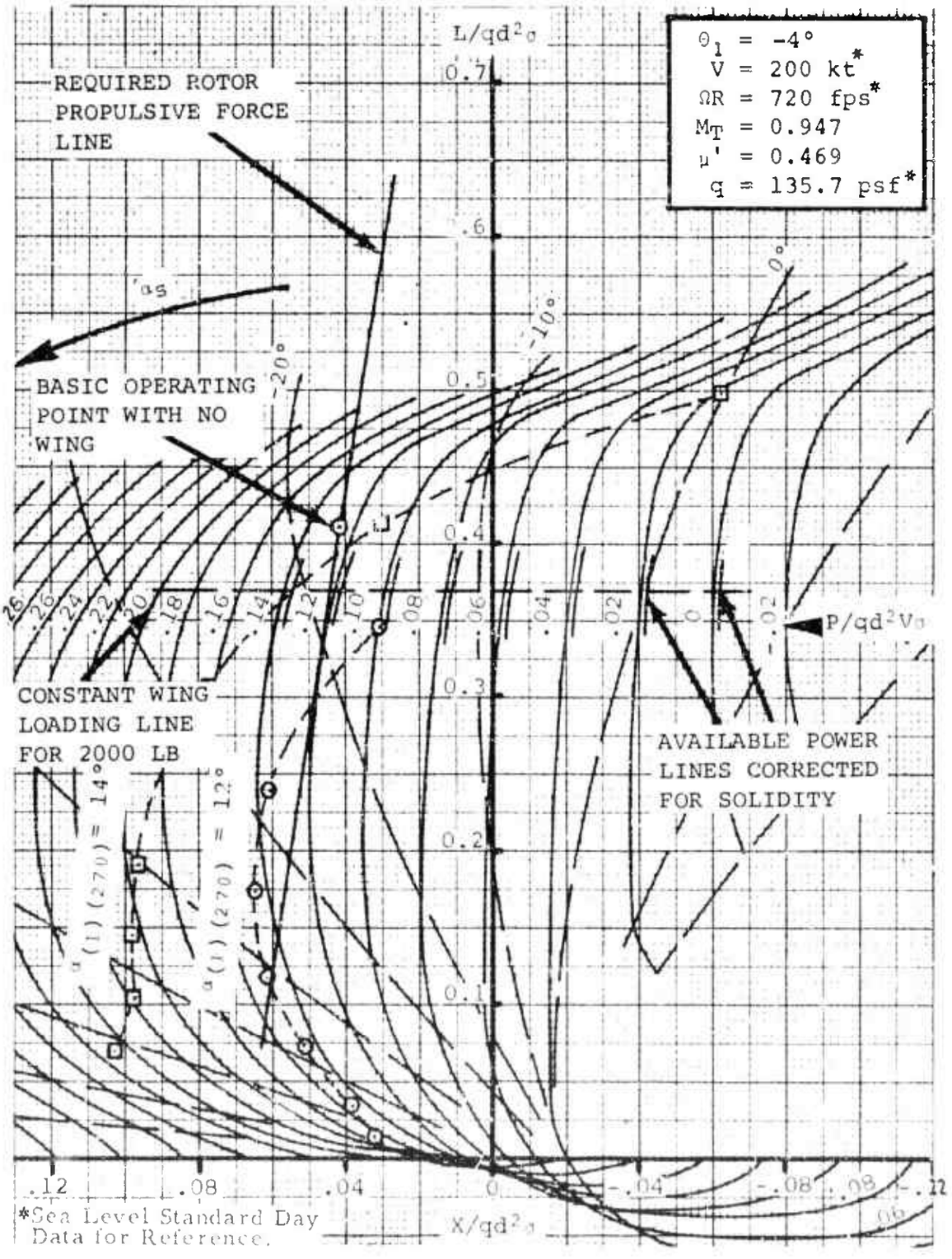

Figure 10. Effect of Auxiliary Propulsive Force

Step 6. Calculate auxiliary propulsive force and propeller horsepower.

$$X_{prop} = \left[\left(\frac{X}{qd^2\sigma}\right)_{prop}\right] qd^2\sigma = 48700\left(\frac{X}{qd^2\sigma}\right)_{prop}$$

$$HP_{prop} = \left[\left(\frac{X}{qd^2\sigma}\right)_{prop}\right] qd^2\sigma \frac{V}{550\eta_p}$$

$$= 35290 \left(\frac{X}{qd^2\sigma}\right)_{prop}$$

$(X/qd^2\sigma)_{prop}$	X_{prop}	HP_{prop}
0.0	0	0
0.01665	810	588
0.03265	1590	1152
0.04915	2390	1735
0.06765	3300	2385
0.08565	4170	3020
0.10615	5180	3740

Step 7. Calculate rotor horsepower required.

$$RHP = \left(\frac{P}{qd^2V\sigma}\right)\left(\frac{qd^2V\sigma}{550}\right) = 2.99\ (10)^4\ (P/qd^2V\sigma)$$

$(P/qd^2V\sigma)_{rotor}$	RHP
0.124	3710
0.10	2990
0.08	2390
0.06	1795
0.04	1195
0.02	598
0.0	0

Step 8. Determine total aircraft power and include in summary table. Refer to Figure 11.

$$HP_{total} = HP_{rotor} + HP_{prop}$$

X_{prop} (lb)	HP_{rotor}	HP_{prop}	HP_{total}
0	3710	0	3710
810	2990	588	3578
1590	2390	1152	3542
2390	1795	1735	3530
3300	1195	2385	3580
4170	598	3020	3618
5180	0	3740	3740

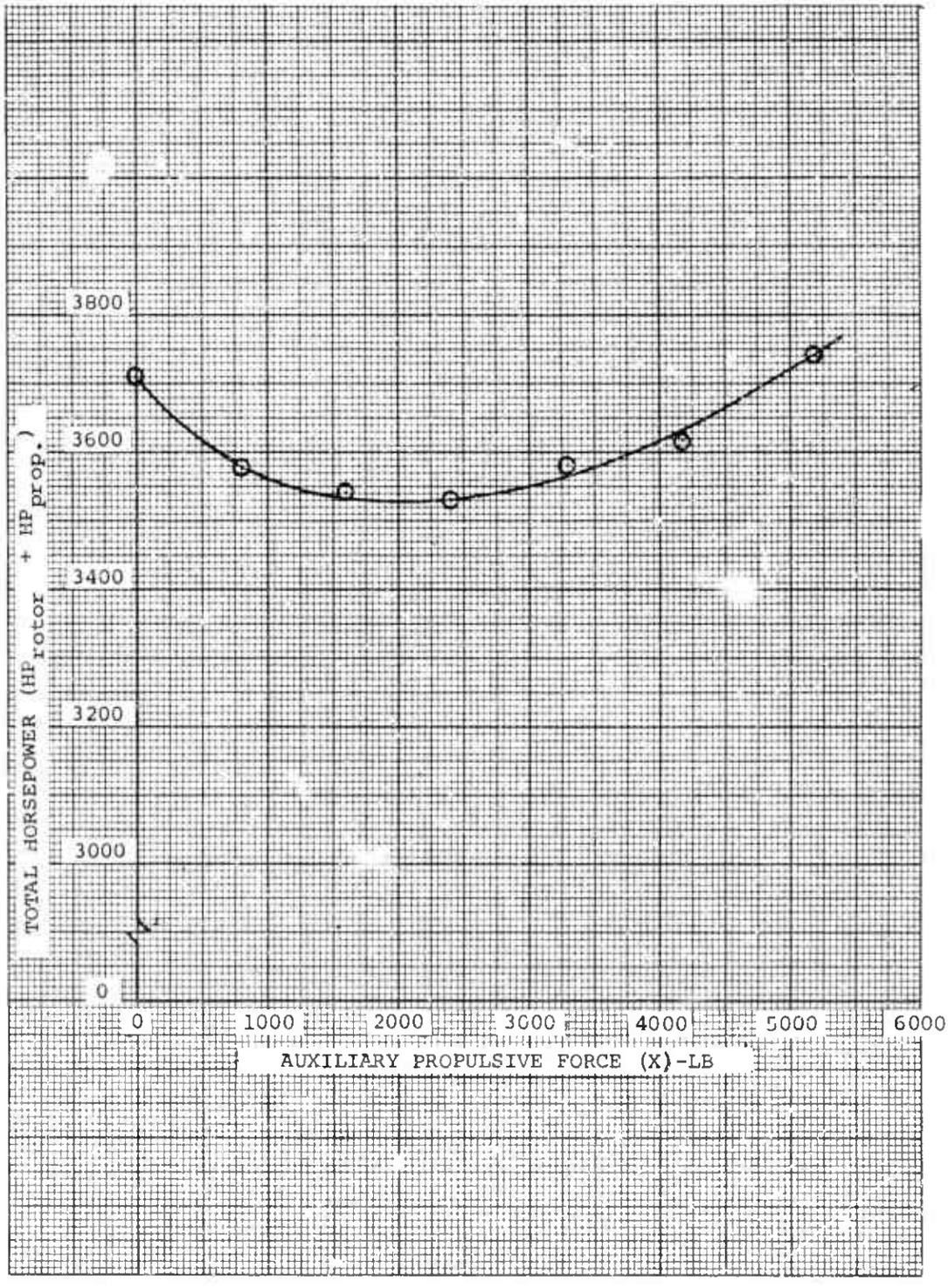

Figure 11. Variation of Total Aircraft Horsepower with Auxiliary Propulsive Force

NUMERICAL INDEX TO PERFORMANCE CHARTS

θ_1 = - 4 DEGREES					
Figure No.	V (kt @ SL)	ΩR (fps @ SL)	M_T	μ	Page
12	50	640	0.648	0.132	41
13	150	500	0.674	0.507	42
14	150	560	0.728	0.452	43
15	150	640	0.799	0.396	44
16	150	720	0.871	0.352	45
17	150	800	0.943	0.317	46
18	200	420	0.678	0.804	47
19	200	480	0.732	0.704	48
20	200	560	0.803	0.603	49
21	200	640	0.875	0.528	50
22	200	720	0.947	0.469	51
23	250	350	0.691	1.206	52
24	250	420	0.754	1.005	53
25	250	480	0.807	0.880	54
26	250	560	0.879	0.754	55
27	250	640	0.951	0.660	56
28	300	400	0.811	1.267	57
29	300	480	0.883	1.056	58

θ_1 = -8 DEGREES					
Figure No.	V (kt @ SL)	ΩR (fps @ SL)	M_T	μ'	Page
30	50	640	0.648	0.132	59
31	75	640	0.686	0.198	60
32	100	560	0.652	0.302	61
33	100	640	0.724	0.264	62
34	100	720	0.795	0.235	63
35	125	520	0.654	0.406	64
36	125	640	0.762	0.330	65
37	125	720	0.833	0.293	66
38	150	500	0.674	0.507	67
39	150	560	0.728	0.452	68
40	150	640	0.799	0.396	69
41	150	720	0.871	0.352	70
42	150	800	0.943	0.317	71
43	175	485	0.699	0.609	72
44	175	560	0.766	0.528	73
45	175	640	0.837	0.462	74
46	175	720	0.909	0.411	75
47	175	800	0.980	0.369	76
48	200	420	0.678	0.804	77
49	200	480	0.732	0.704	78

θ_1 = -8 DEGREES (CONT'D)					
Figure No.	V (kt @ SL)	ΩR (fps @ SL)	M_T	μ'	Page
50	200	560	0.803	0.603	79
51	200	640	0.875	0.528	80
52	200	720	0.947	0.469	81
53	225	380	0.680	1.000	82
54	225	480	0.770	0.792	83
55	225	560	0.841	0.679	84
56	225	640	0.913	0.594	85
57	225	720	0 984	0.528	86
58	250	350	0.691	1.206	87
59	250	420	0.754	1.005	88
60	250	480	0.807	0.880	89
61	250	560	0.879	0.754	90
62	250	640	0.951	0.660	91
63	275	310	0.693	1.498	92
64	275	400	0.774	1.161	93
65	275	480	0.845	0.968	94
66	275	560	0.917	0.829	95
67	300	400	0.811	1.267	96
68	300	480	0.883	1.056	97

θ = -12 DEGREES					
Figure No.	V (kt @ SL)	Ω R (fps @ SL)	M_T	μ'	Page
69	50	640	0.648	0.132	98
70	150	500	0.674	0.507	99
71	150	560	0.728	0.452	100
72	150	640	0.799	0.396	101
73	150	720	0.871	0.352	102
74	150	800	0.943	0.317	103
75	200	420	0.678	0.804	104
76	200	480	0.732	0.704	105
77	200	560	0.803	0.603	106
78	200	640	0.875	0.528	107
79	200	720	0.947	0.469	108
80	250	350	0.691	1.206	109
81	250	420	0.754	1.005	110
82	250	480	0.807	0.880	111
83	250	560	0.879	0.754	112
84	250	640	0.951	0.660	113
85	300	400	0.811	1.267	114
86	300	480	0.883	1.056	115

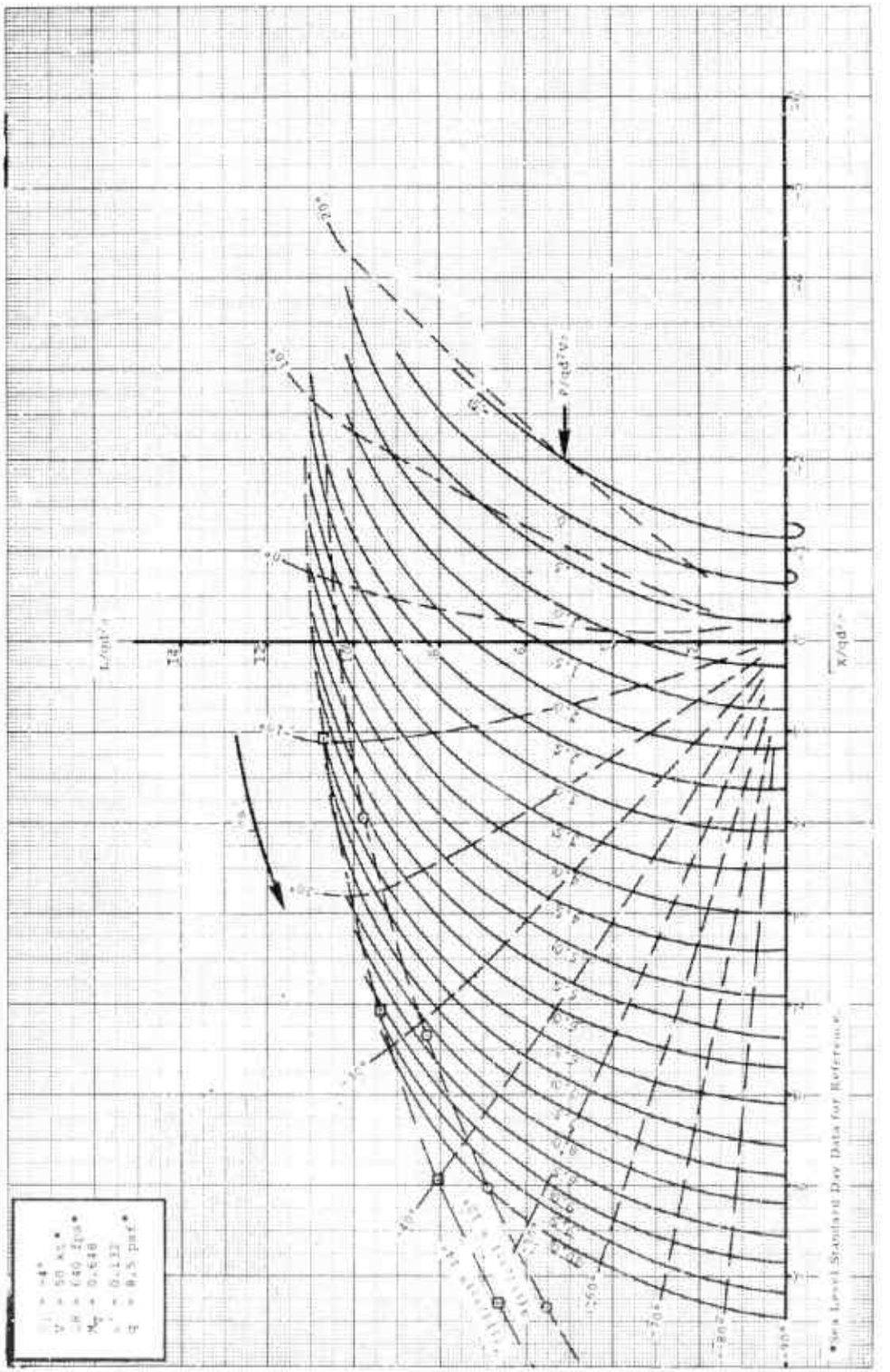

Figure 12.

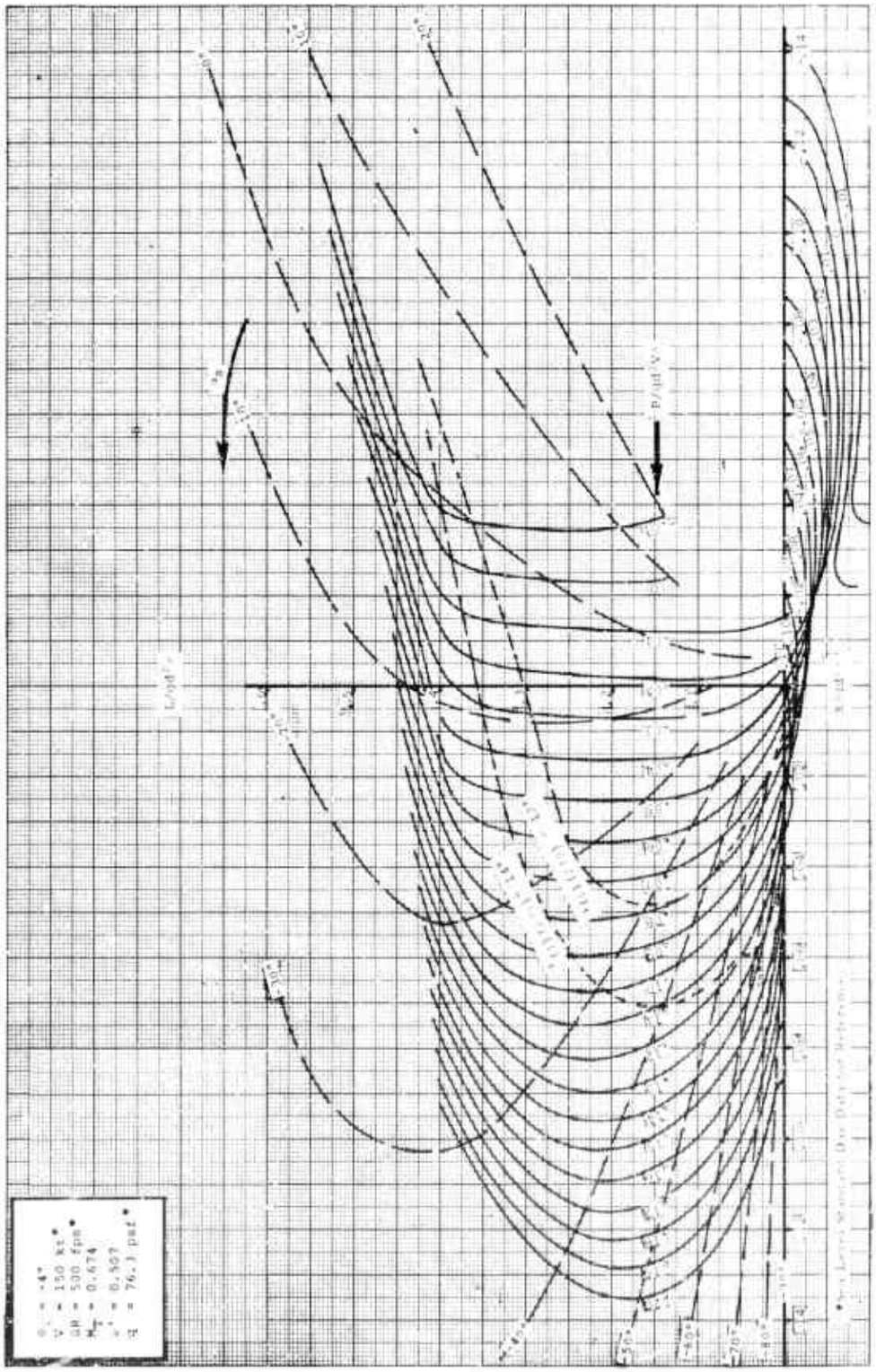

Figure 13.

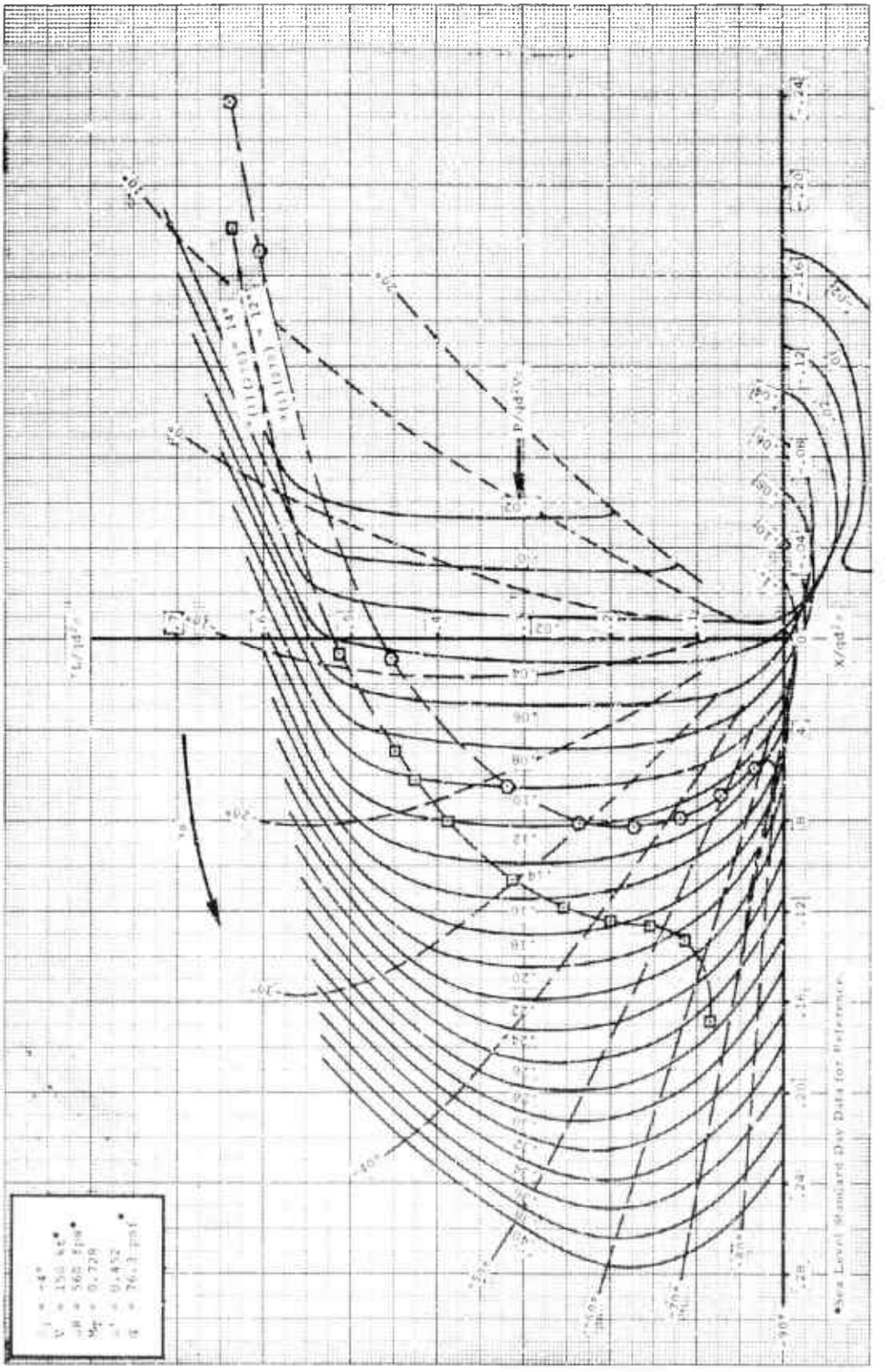

Figure 14.

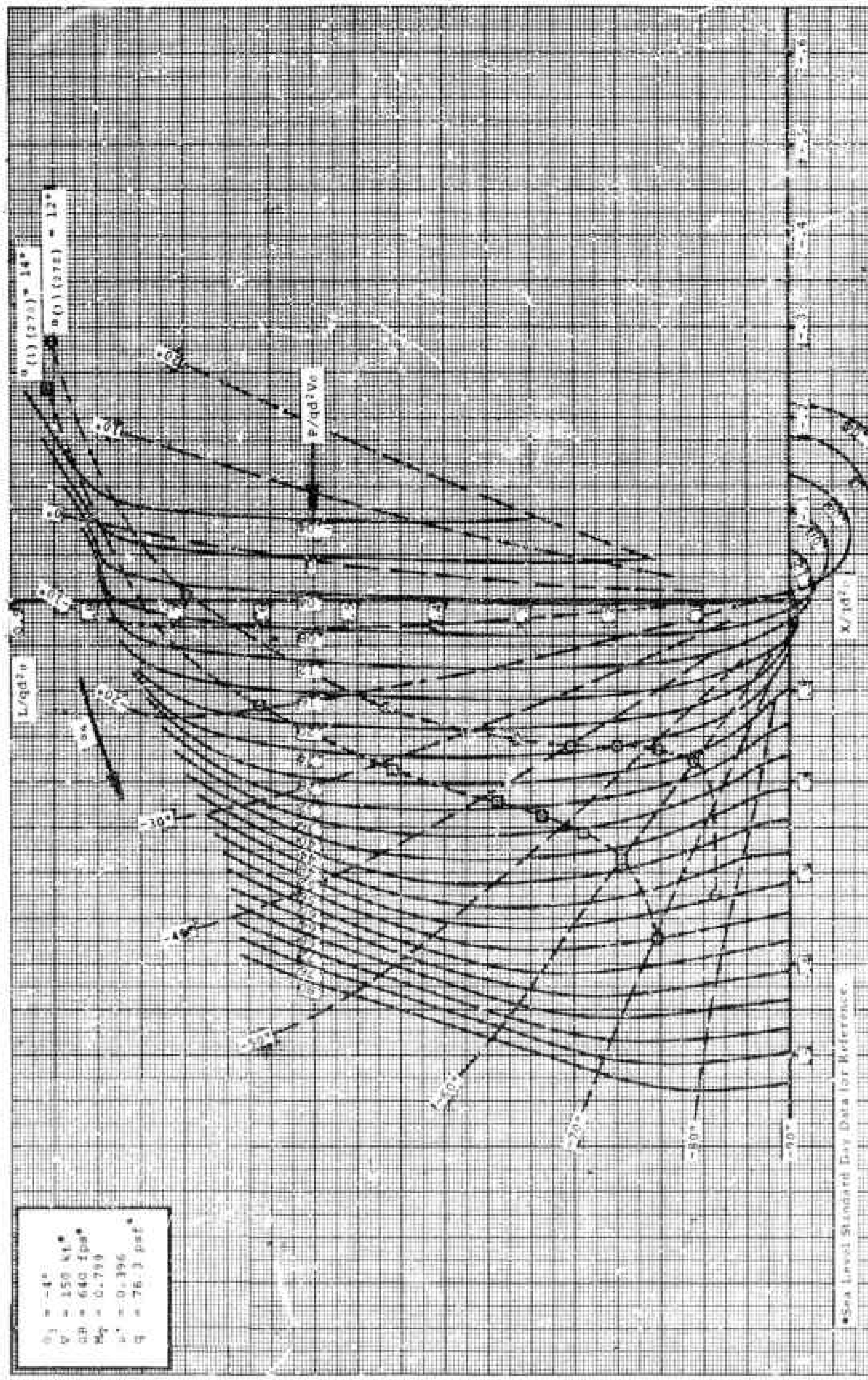

Figure 15.

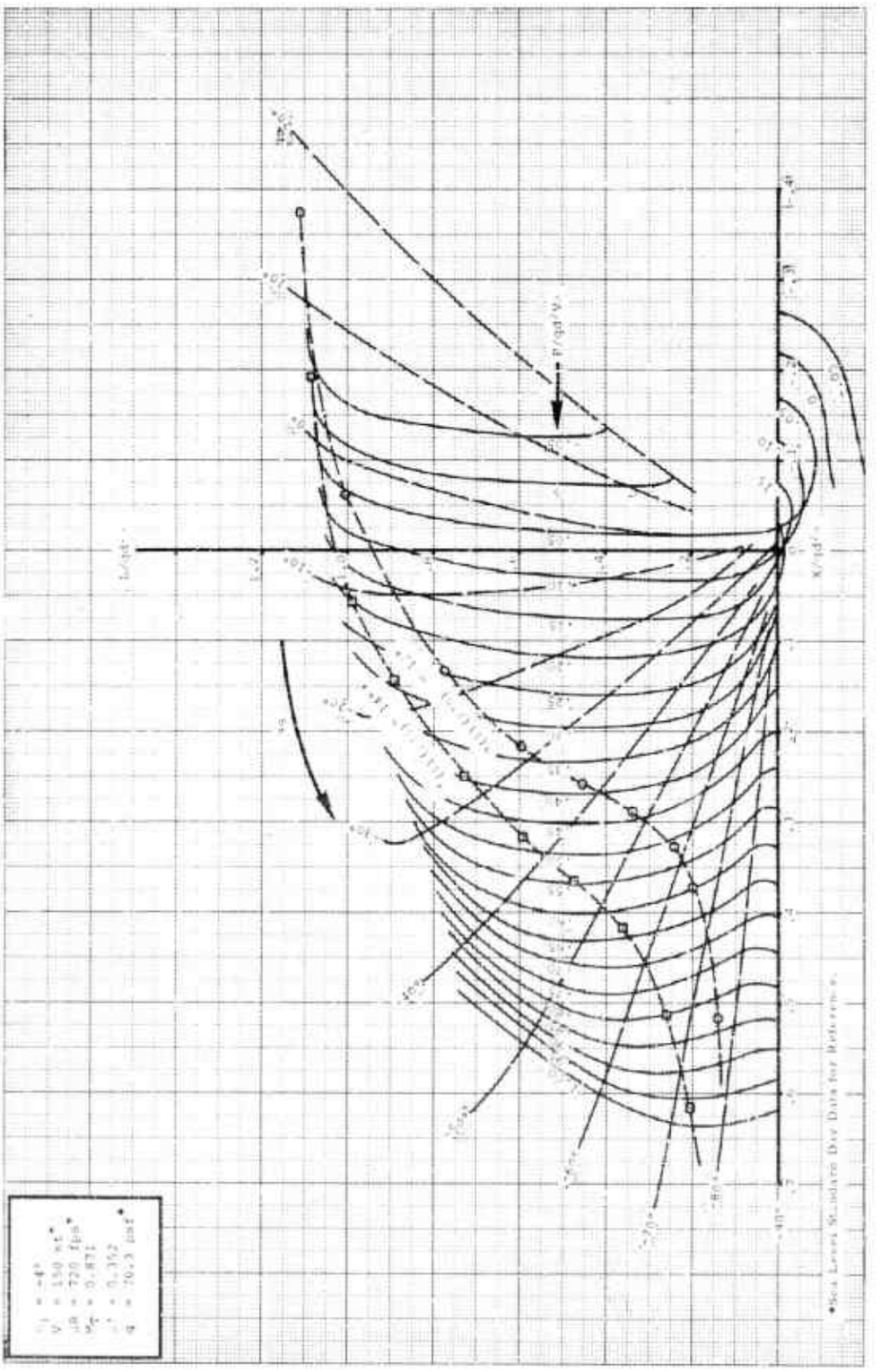

Figure 16.

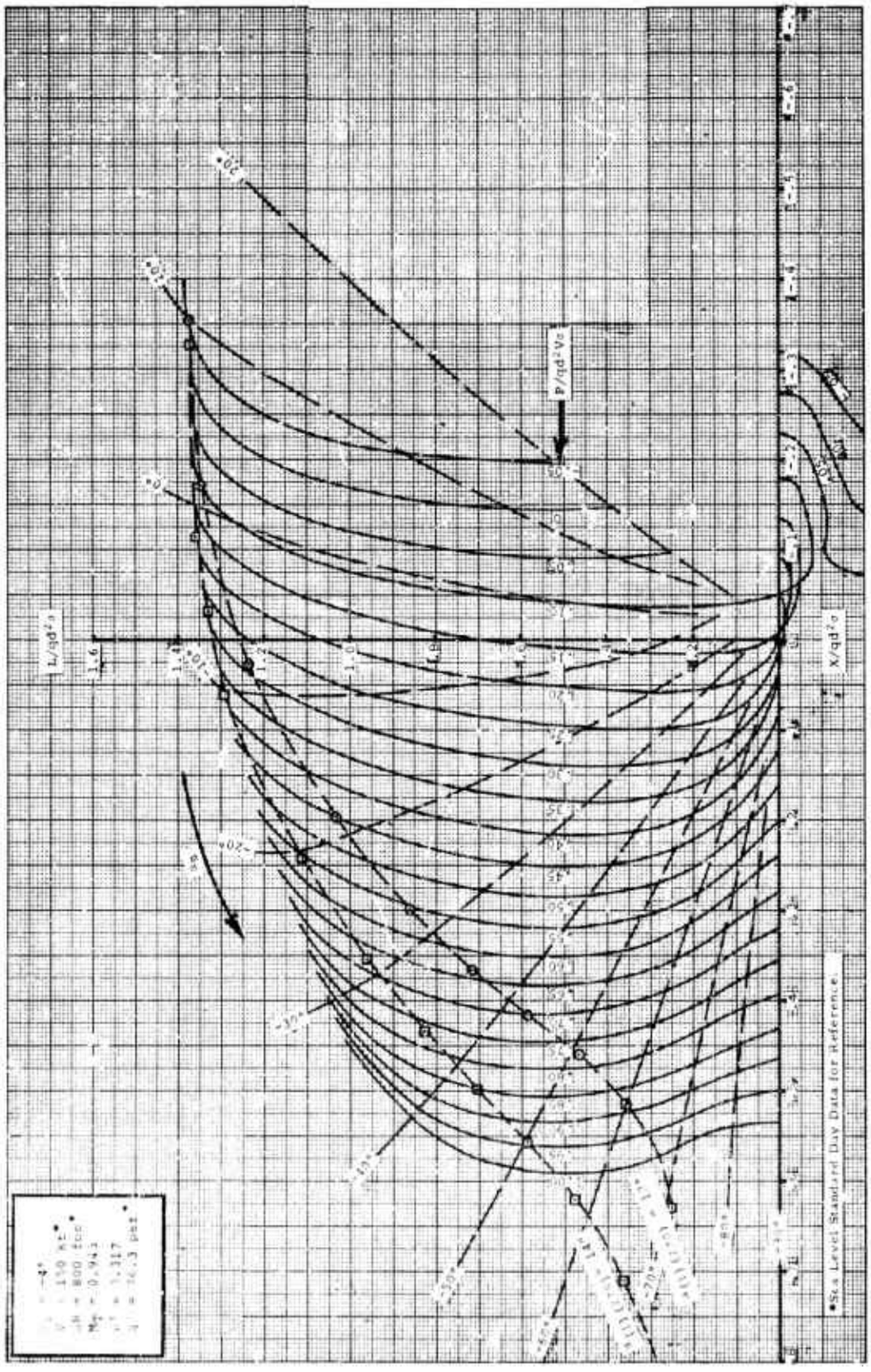
L/qd²a
X/qd²a
Δp/qd²a
*Sea Level Standard Day Data for Reference.

Figure 17.

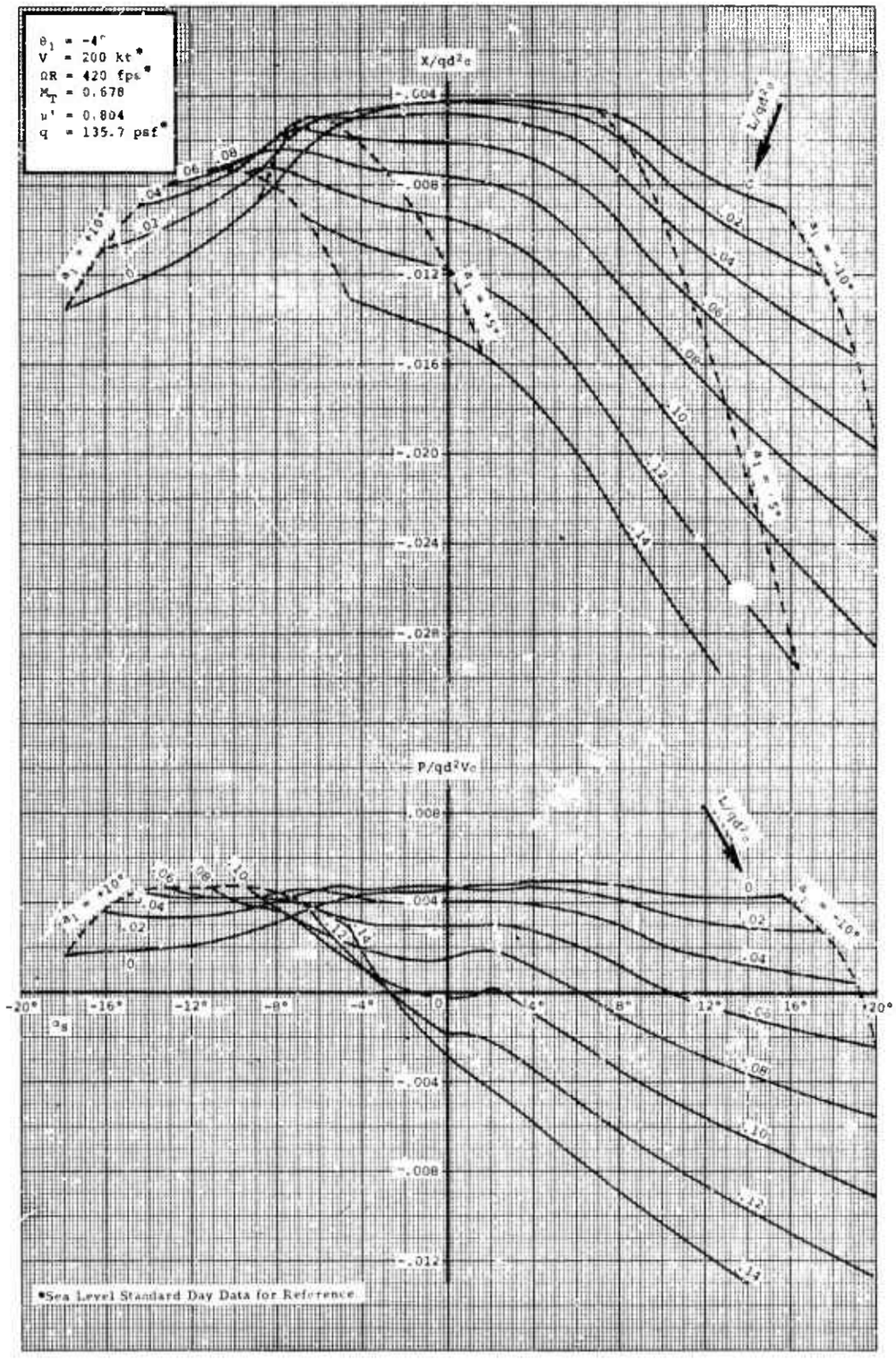
θ_1 = -4°
V = 200 kt*
ΩR = 420 fps*
M_T = 0.678
μ' = 0.804
q = 135.7 psf*
X/qd²σ
P/qd²Vσ
L/qd²σ
a_1 = +10°
a_1 = -5°
a_s
-20°
-16°
-12°
-8°
-4°
0
4°
8°
12°
16°
+20°
*Sea Level Standard Day Data for Reference

Figure 18.

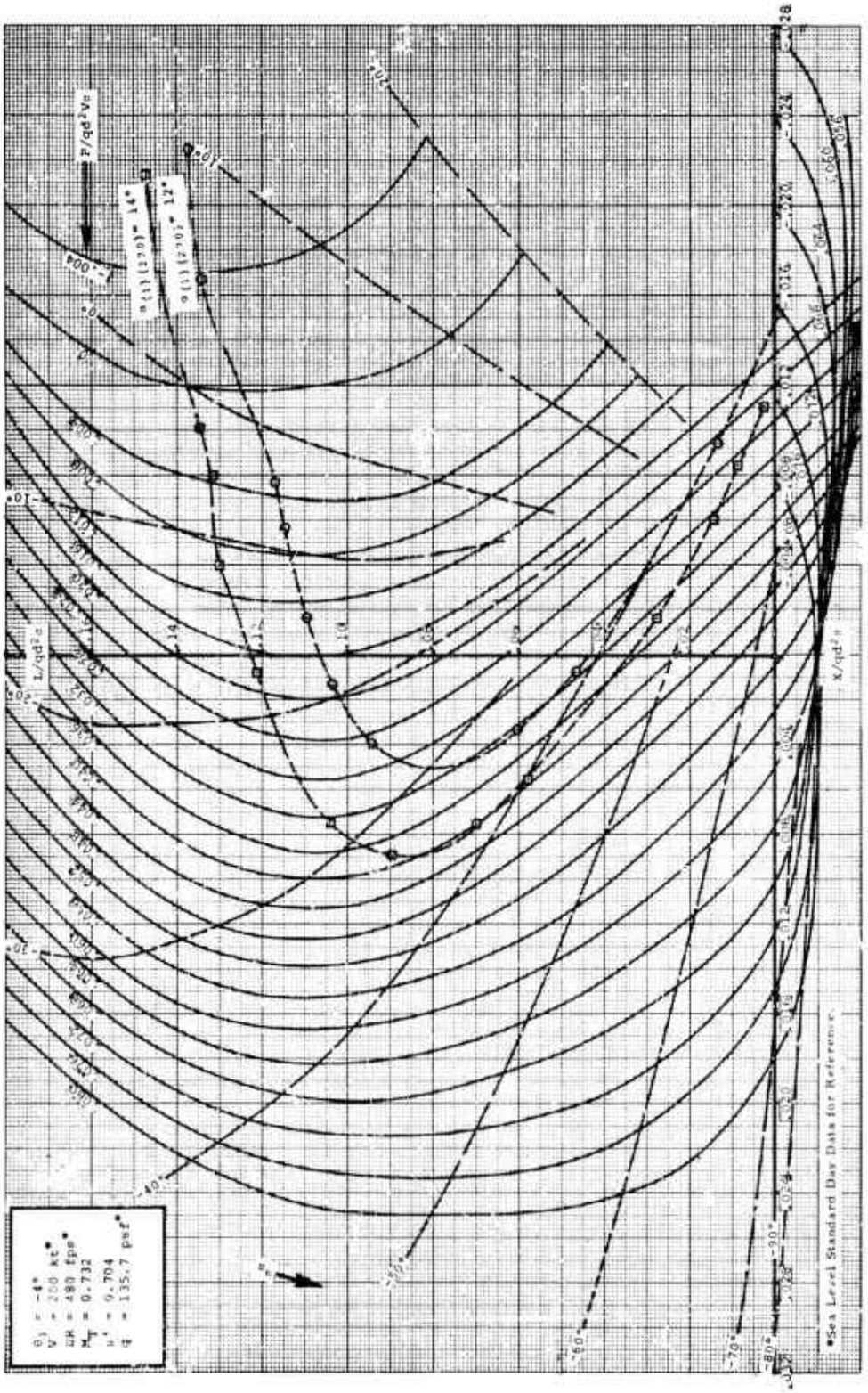
P/qd²Vs
L/qd²s
X/qd²s
*Sea Level Standard Day Data for Reference.

Figure 19.

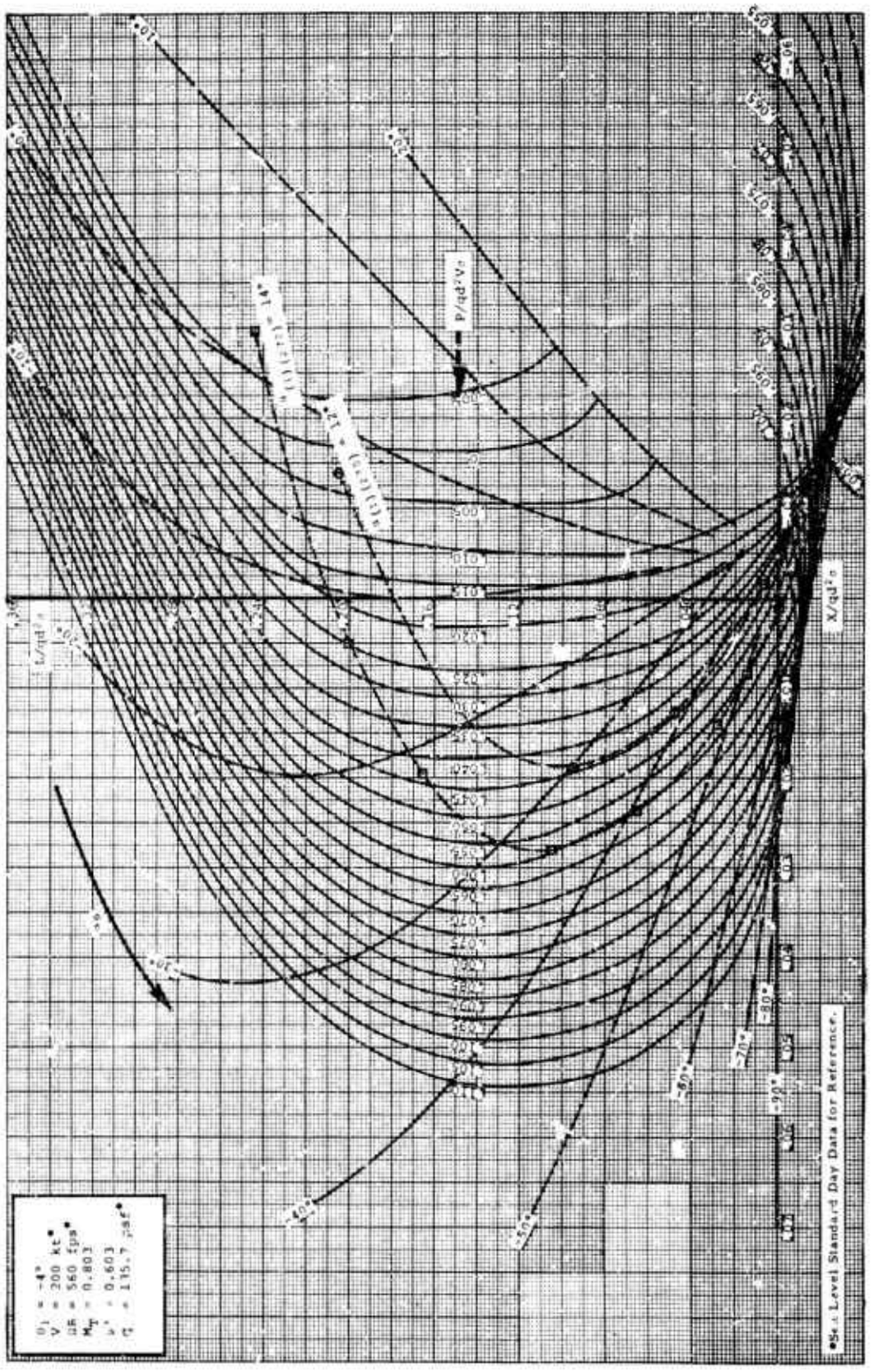
θ1 = -4°
V = 200 kt*
ΩR = 560 fps*
MT = 0.803
λ' = 0.603
Cf = 135.7 psf*
*Sea Level Standard Day Data for Reference.

Figure 20.

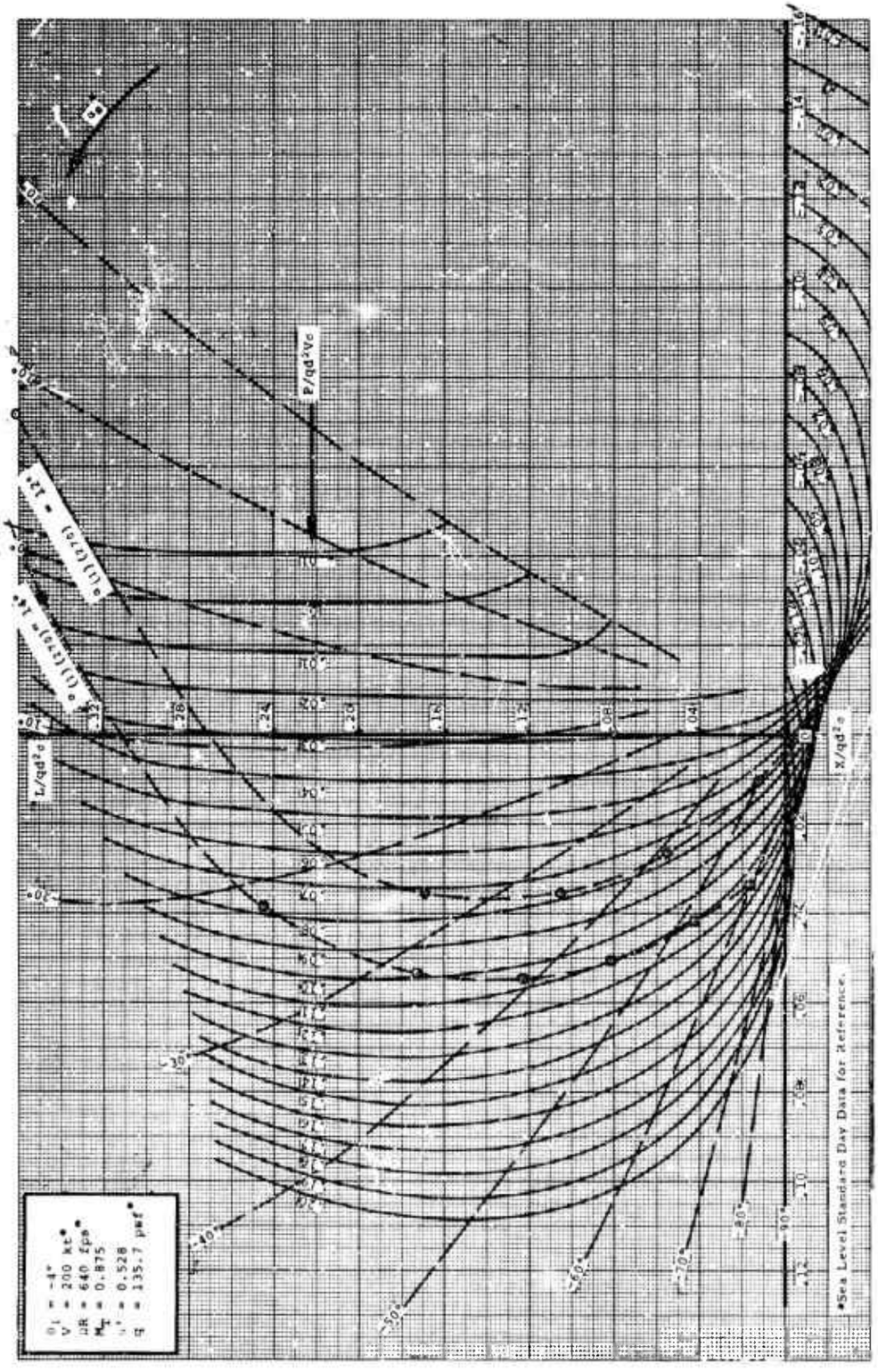
P/qd²Ve
L/qd²e
X/qd²e
*Sea Level Standard Day Data for Reference.

Figure 21.

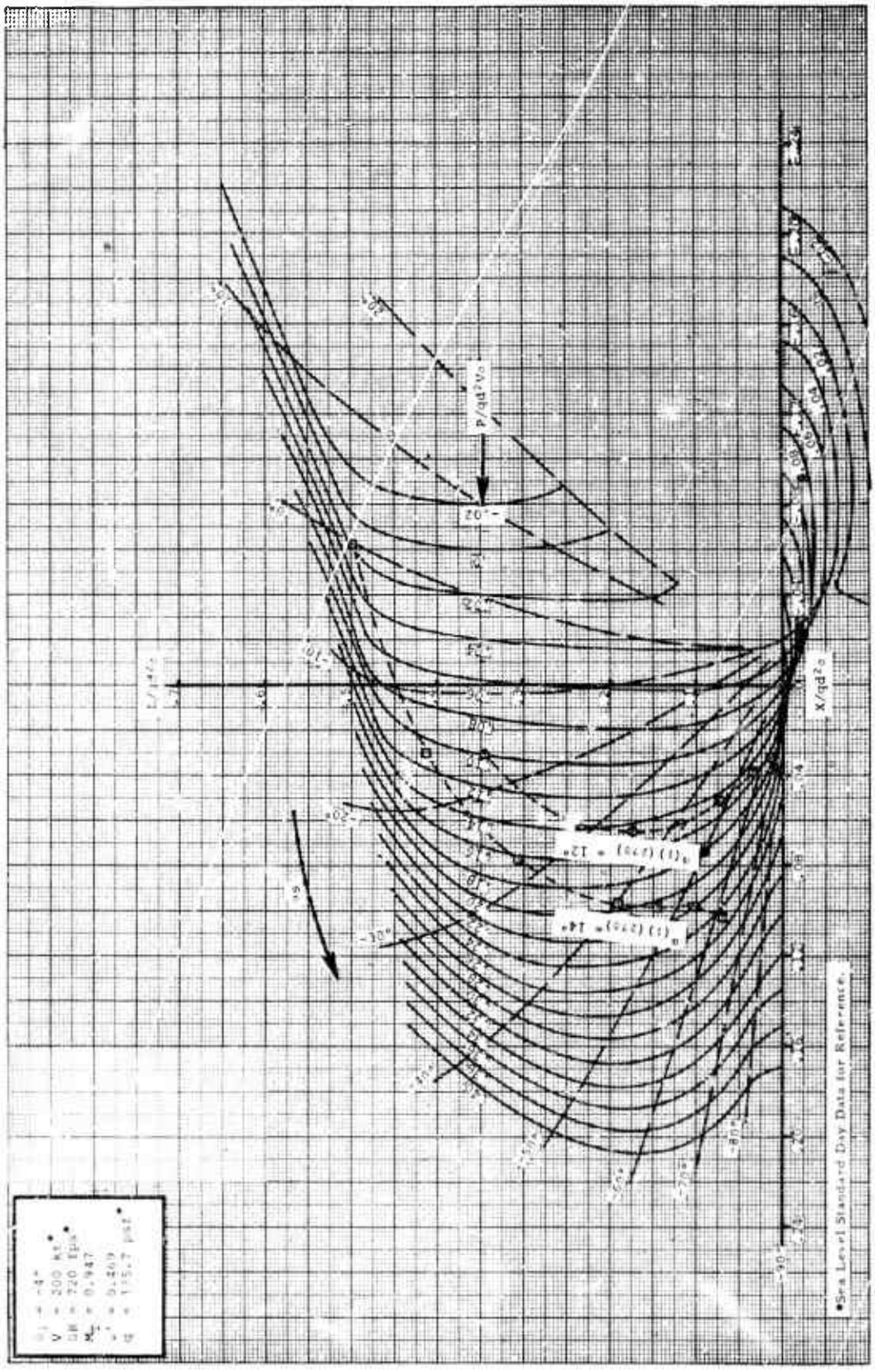
P/qd²Vo
X/qd²o
E/qd²o
•Sea Level Standard Day Data for Reference.

Figure 22.

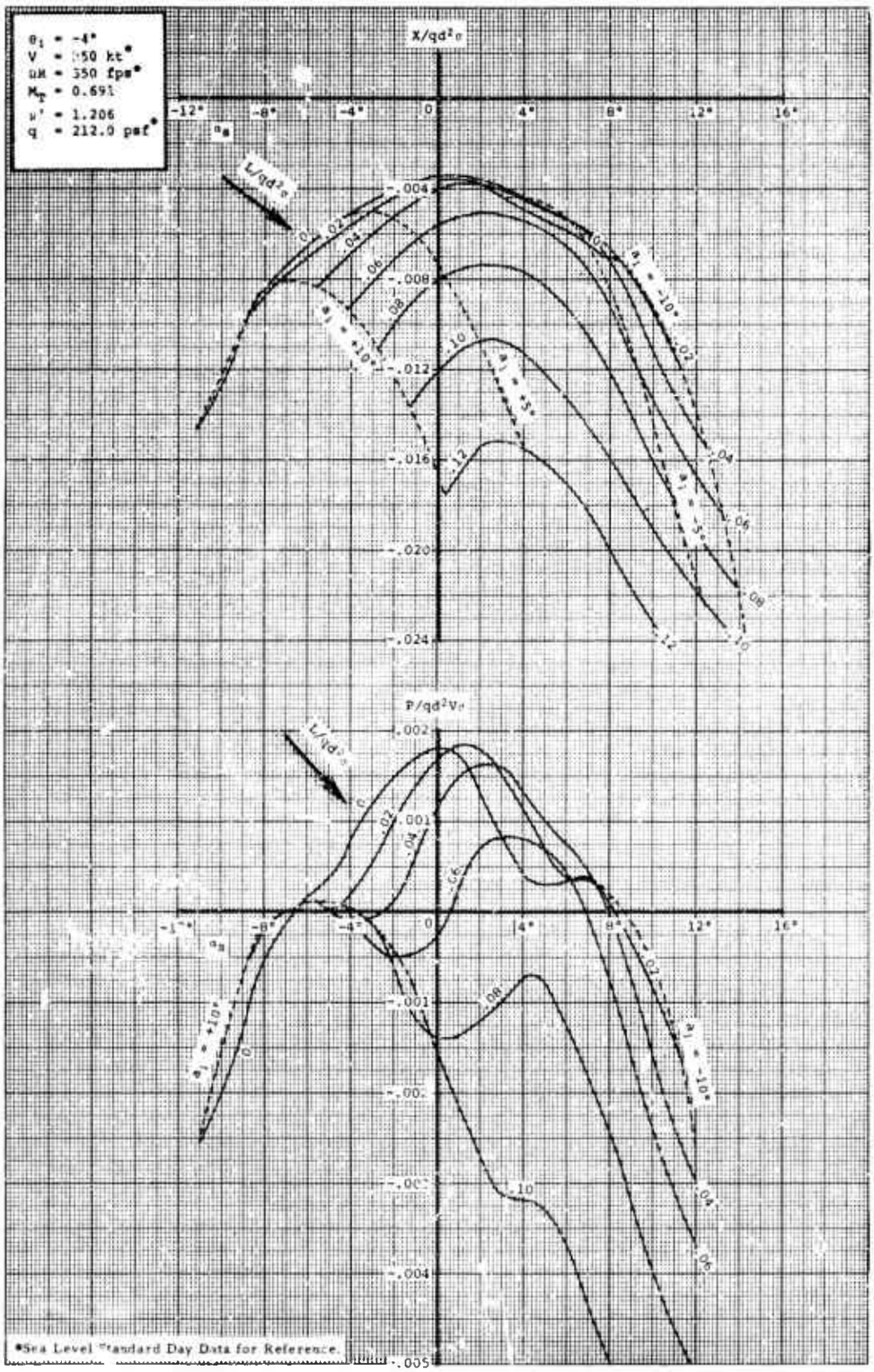
θ_i = -4°
V = 350 kt*
aR = 350 fps*
M_T = 0.691
μ' = 1.206
q = 212.0 psf*
X/qd²σ
P/qd²Vσ
α_s
α_i = +10°
α_i = +5°
α_i = -5°
α_i = -10°
*Sea Level Standard Day Data for Reference.

Figure 23.

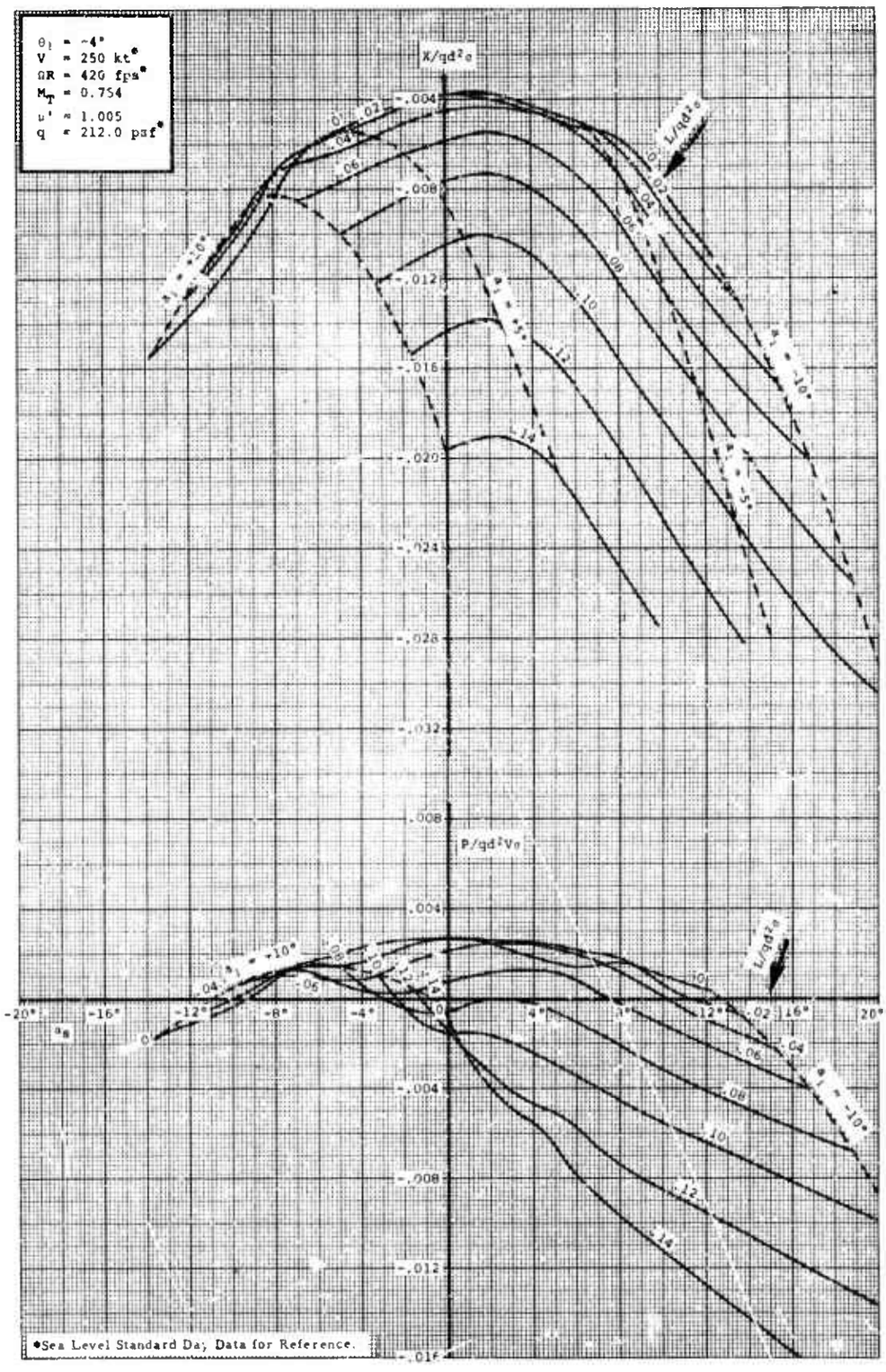
θ_1 = -4°
V = 250 kt*
ΩR = 420 fps*
M_T = 0.754
μ = 1.005
q = 212.0 psf*
X/qd²σ
L/qd²σ
P/qd²Vσ
α_s
*Sea Level Standard Day, Data for Reference.

Figure 24.

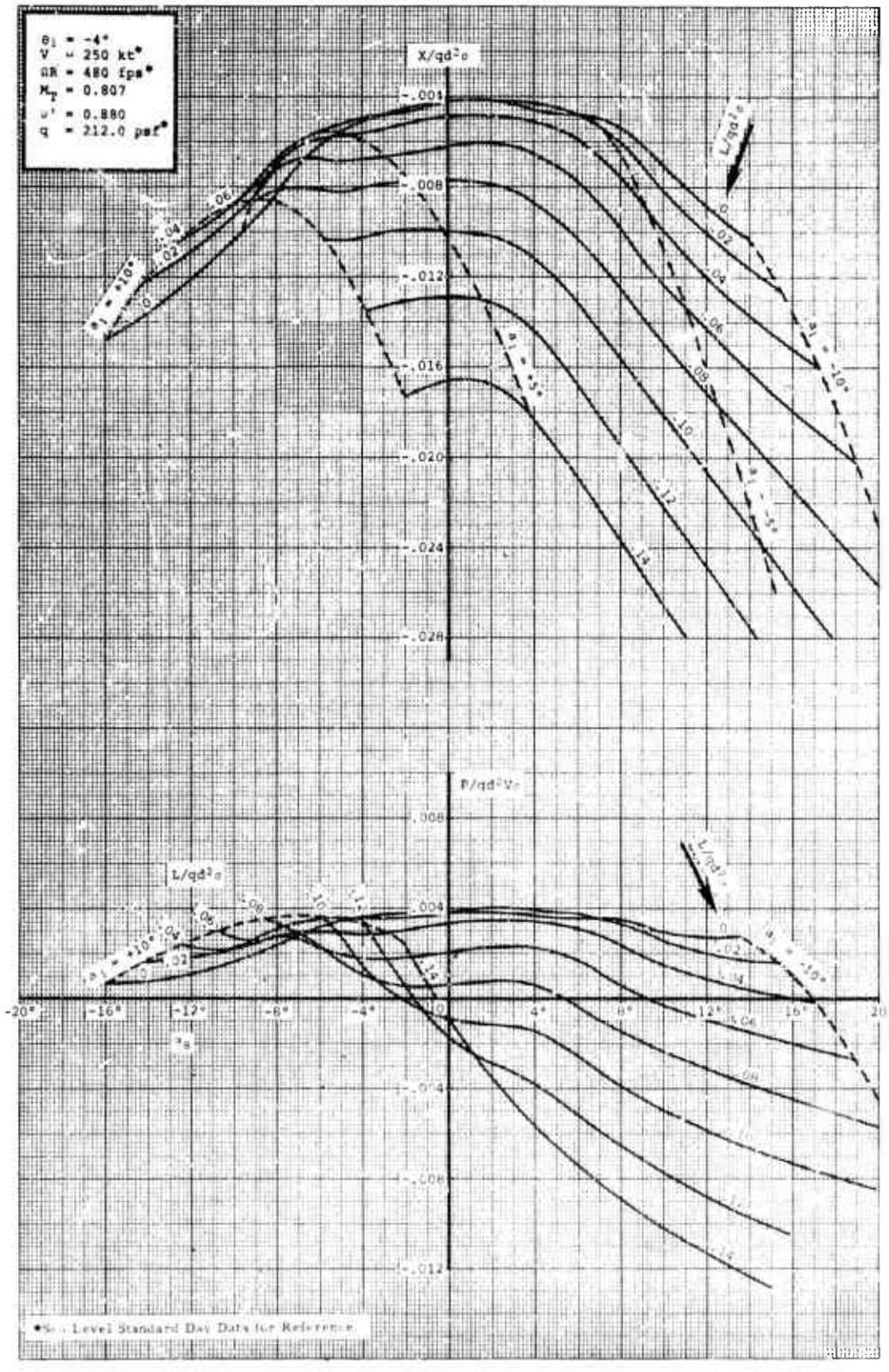
θ_1 = -4°
V = 250 kt*
ΩR = 480 fps*
M_T = 0.807
μ' = 0.880
q = 212.0 psf*
X/qd²σ
-.001
-.008
-.012
-.016
-.020
-.024
-.028
L/qd²σ
P/qd²V
.008
.004
-.004
-.008
-.012
-20°
-16°
-12°
-8°
-4°
0
4°
8°
12°
16°
20°
α_s
*Sea Level Standard Day Data for Reference

Figure 25.

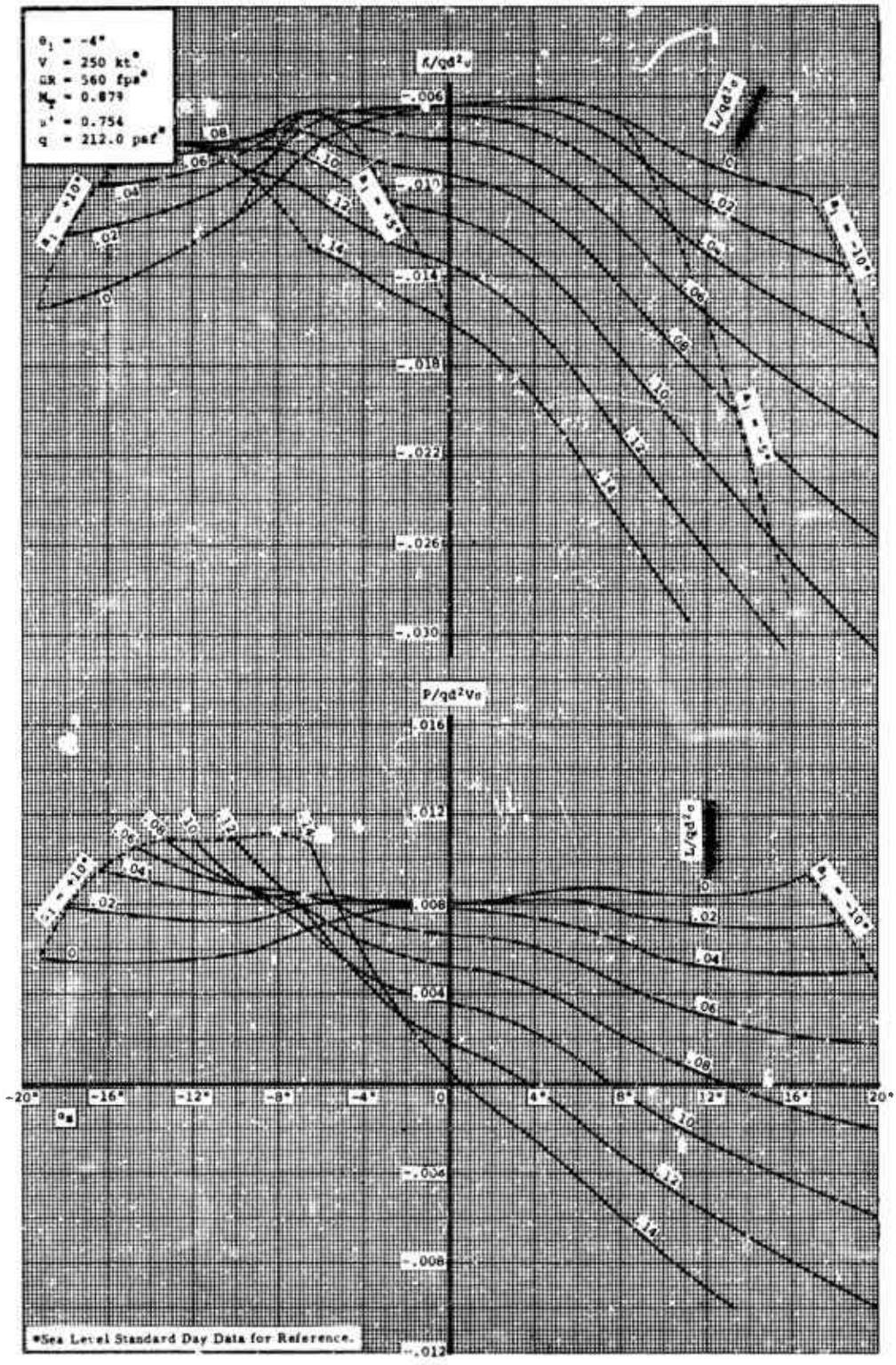
θ_1 = -4°
V = 250 kt*
GR = 560 fps*
M_∞ = 0.879
ρ' = 0.754
q = 212.0 psf*
L/qd²
D/qd²
P/qd²
C_L
C_m
i_t = +10°
i_t = +5°
i_t = -5°
i_t = -10°
-.006
-.010
-.014
-.018
-.022
-.026
-.030
.016
.012
.008
.004
-.004
-.008
-.012
-20°
-16°
-12°
-8°
-4°
0
4°
8°
12°
16°
20°
α_B
*Sea Level Standard Day Data for Reference.

Figure 26.

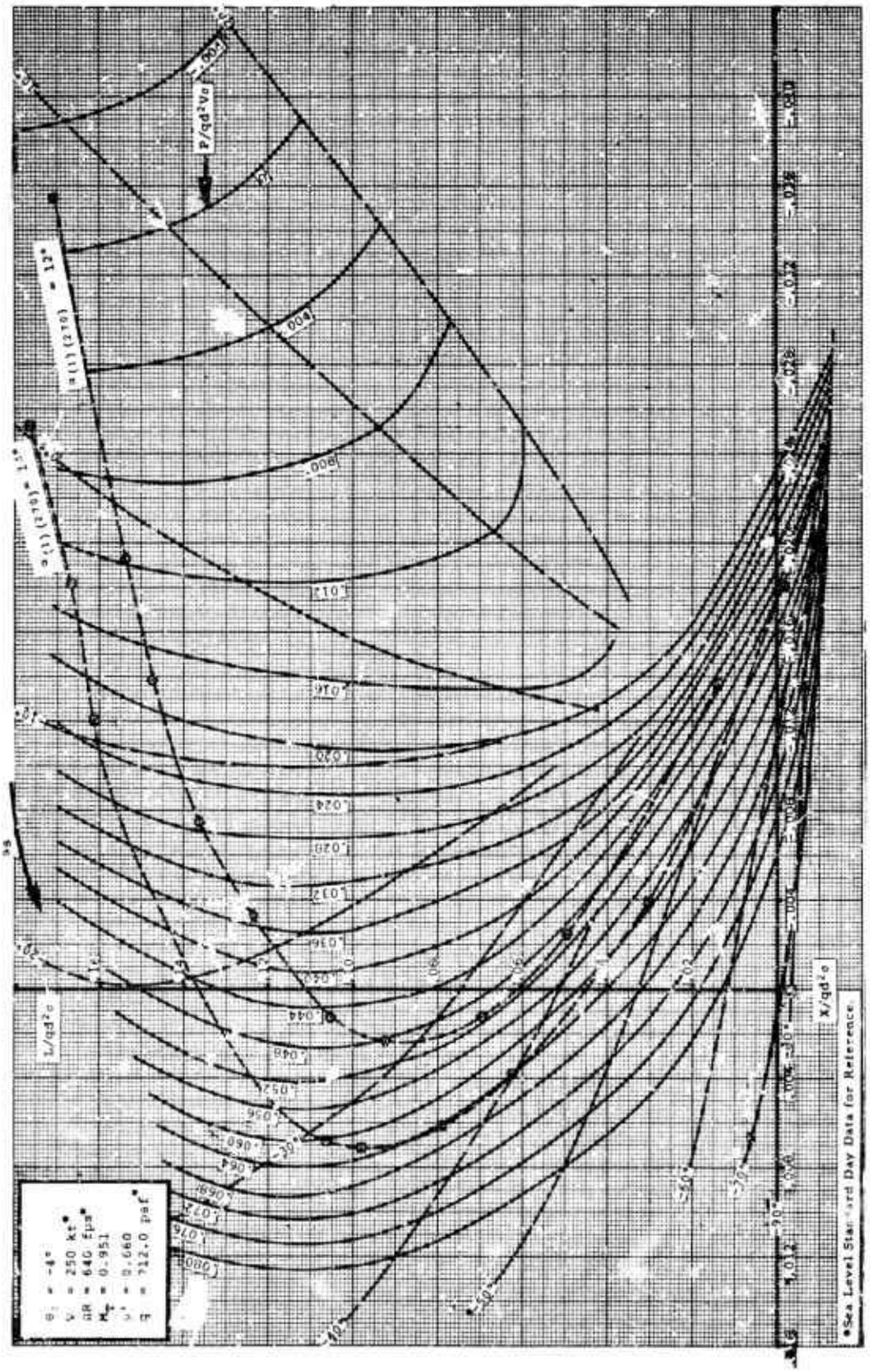
P/qd²Va = .001
.004
.008
.012
.016
.020
.024
.028
.032
.036
.040
.044
.048
.052
.056
.060
.064
.068
.072
.076
.080
L/qd²a
X/qd²a
*Sea Level Standard Day Data for Reference

Figure 27.

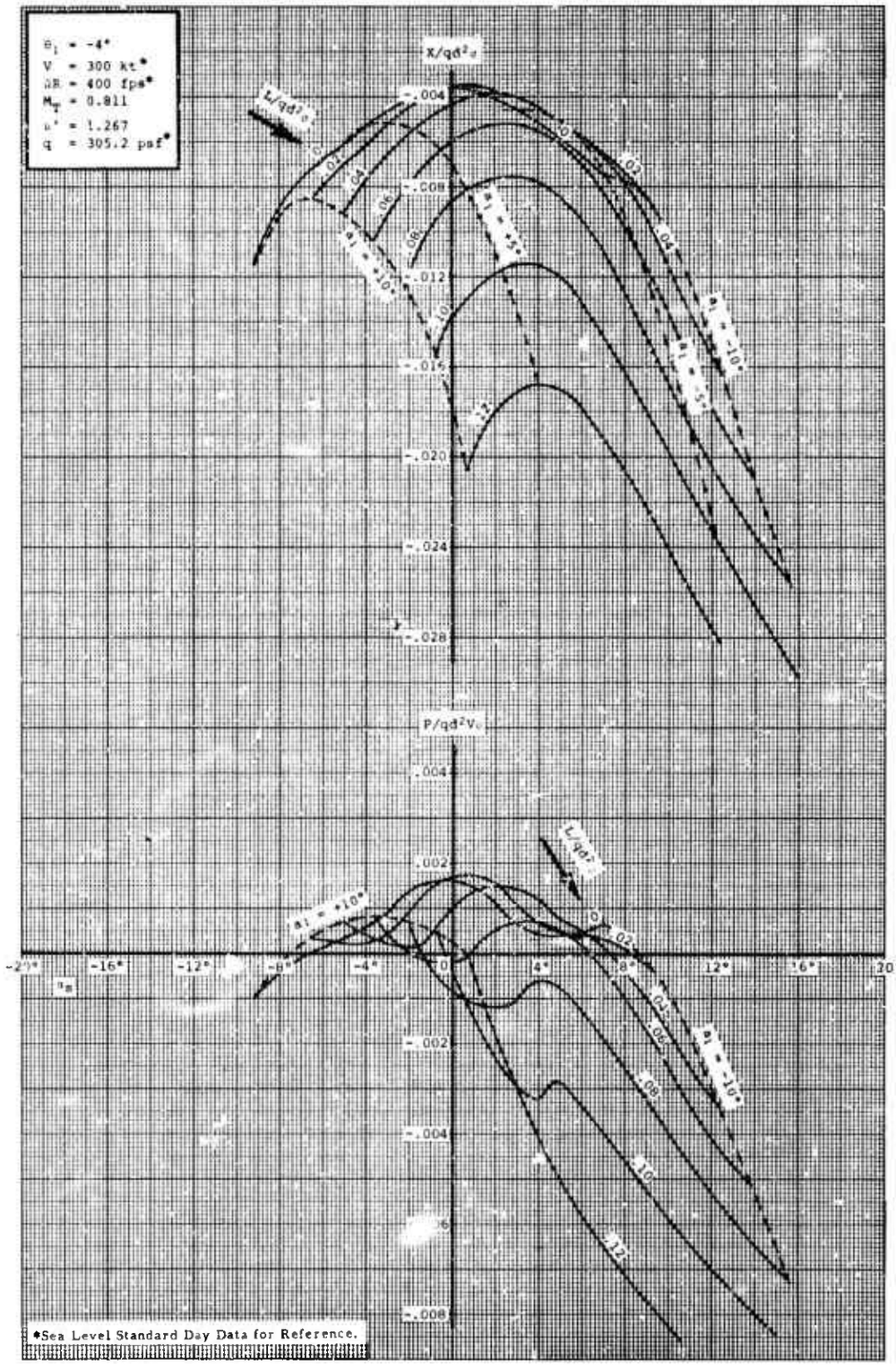
i_t = -4°
V = 300 kt*
AR = 400 fps*
M_T = 0.811
μ' = 1.267
q = 305.2 psf*
X/qd²
L/qd²
P/qd²V
-.004
-.008
-.012
-.016
-.020
-.024
-.028
.004
.002
-.002
-.004
-.008
-.10
-.08
-.06
-.04
-.02
0
.02
.04
.06
.08
.10
.12
α_i = +10°
α_i = +5°
α_i = -5°
α_i = -10°
-20°
-16°
-12°
-8°
-4°
0
4°
8°
12°
16°
20°
α_m
*Sea Level Standard Day Data for Reference.

Figure 28.

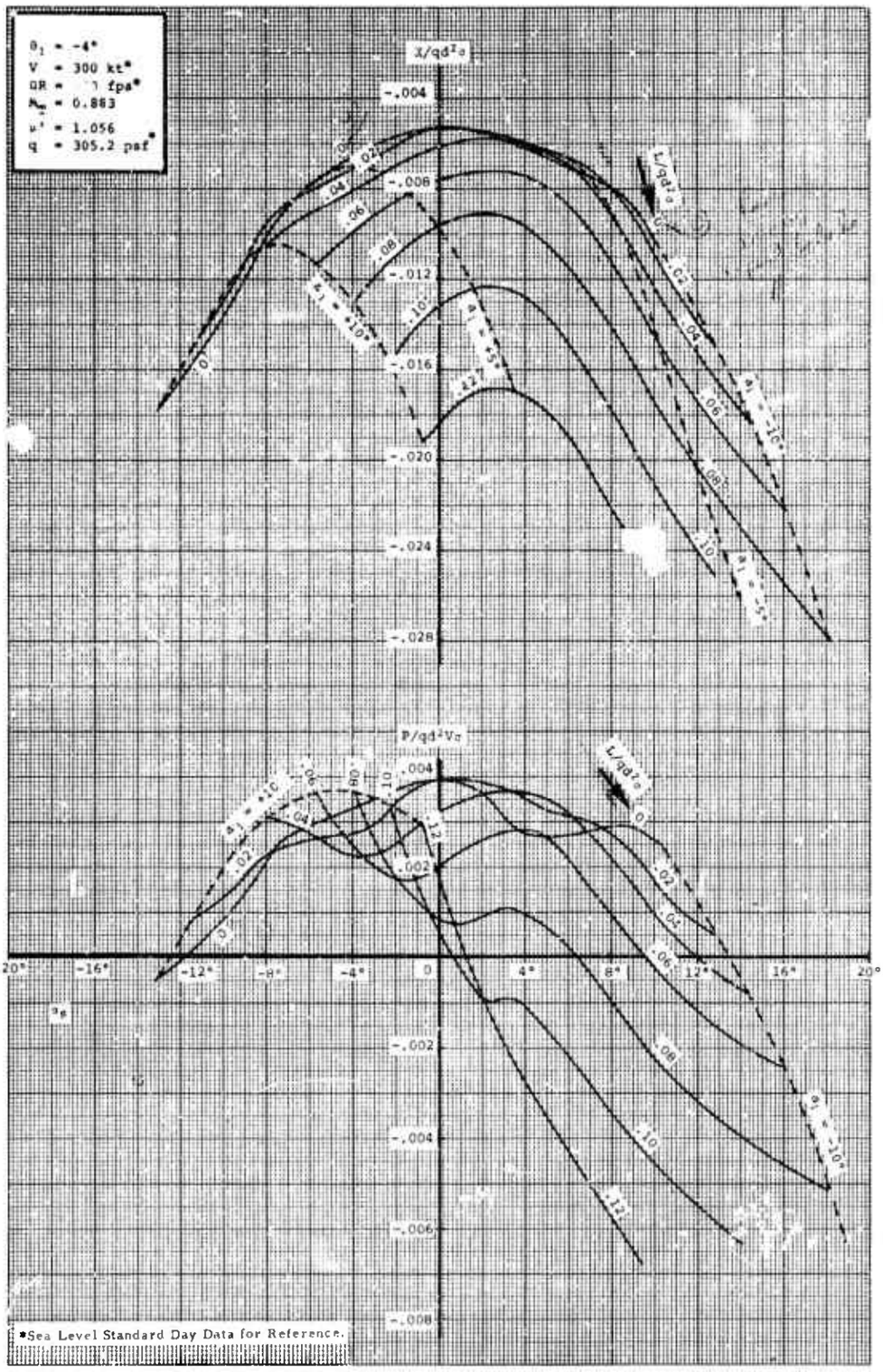
θ_1 = -4°
V = 300 kt*
QR = 1 fps*
M_∞ = 0.863
μ' = 1.056
q = 305.2 psf*
X/qd²σ
-.004
-.008
-.012
-.016
-.020
-.024
-.028
L/qd²σ
i1 = +10°
i1 = +5°
i1 = -5°
i1 = -10°
P/qd²Vσ
.004
.002
-.002
-.004
-.006
-.008
-20°
-16°
-12°
-8°
-4°
0
4°
8°
12°
16°
20°
α_s
*Sea Level Standard Day Data for Reference.

Figure 29.

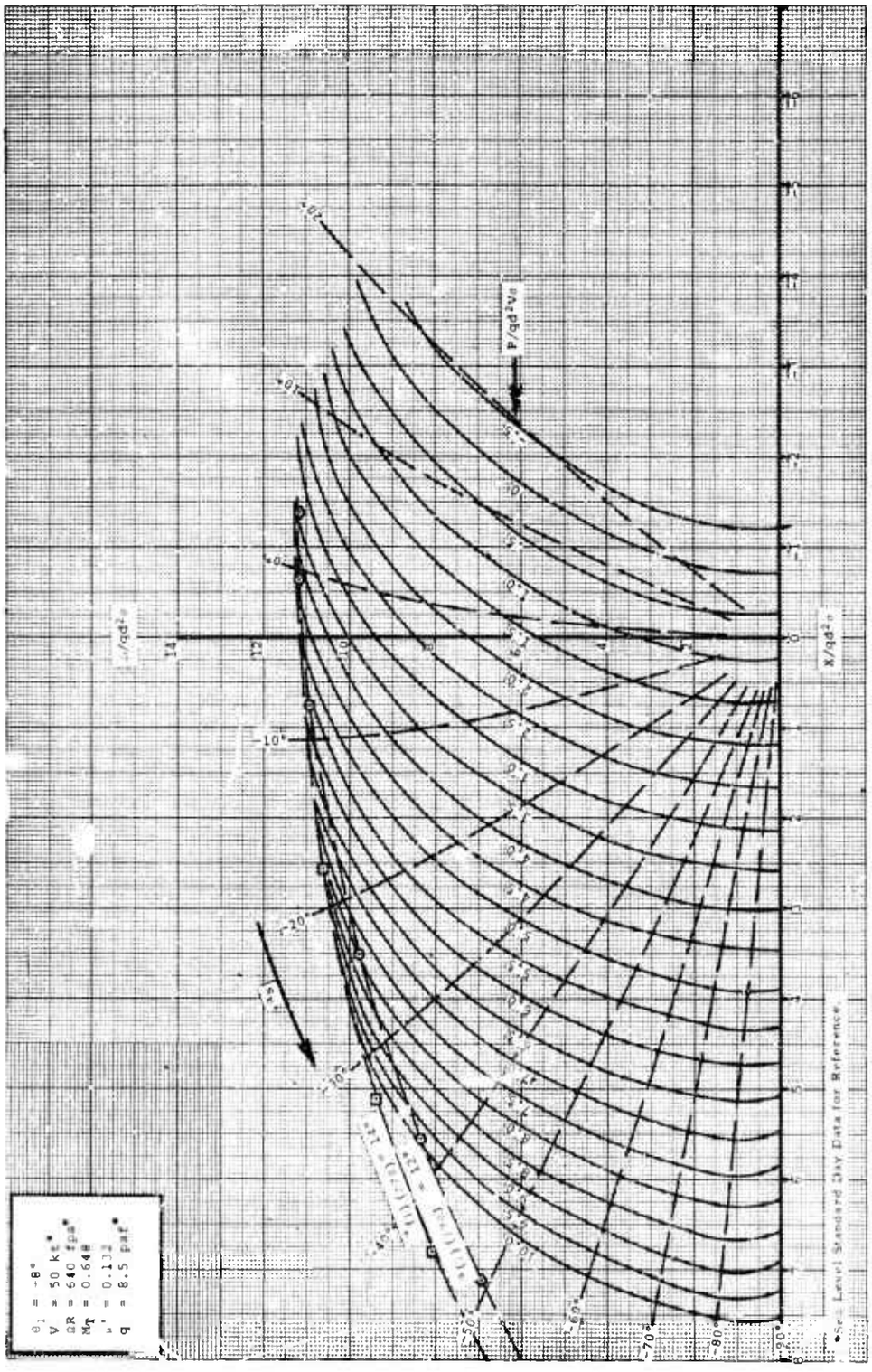
θ_1 = -8°
V = 50 kt
ΩR = 640 fps
M_T = 0.648
μ = 0.132
q = 8.5 psf
Sea Level Standard Day Data for Reference
Z/qd²
X/qd²
M/qd²v
-8°
-10°
-20°
-30°
-40°
-50°
-60°
-70°
-80°
-90°

Figure 30.

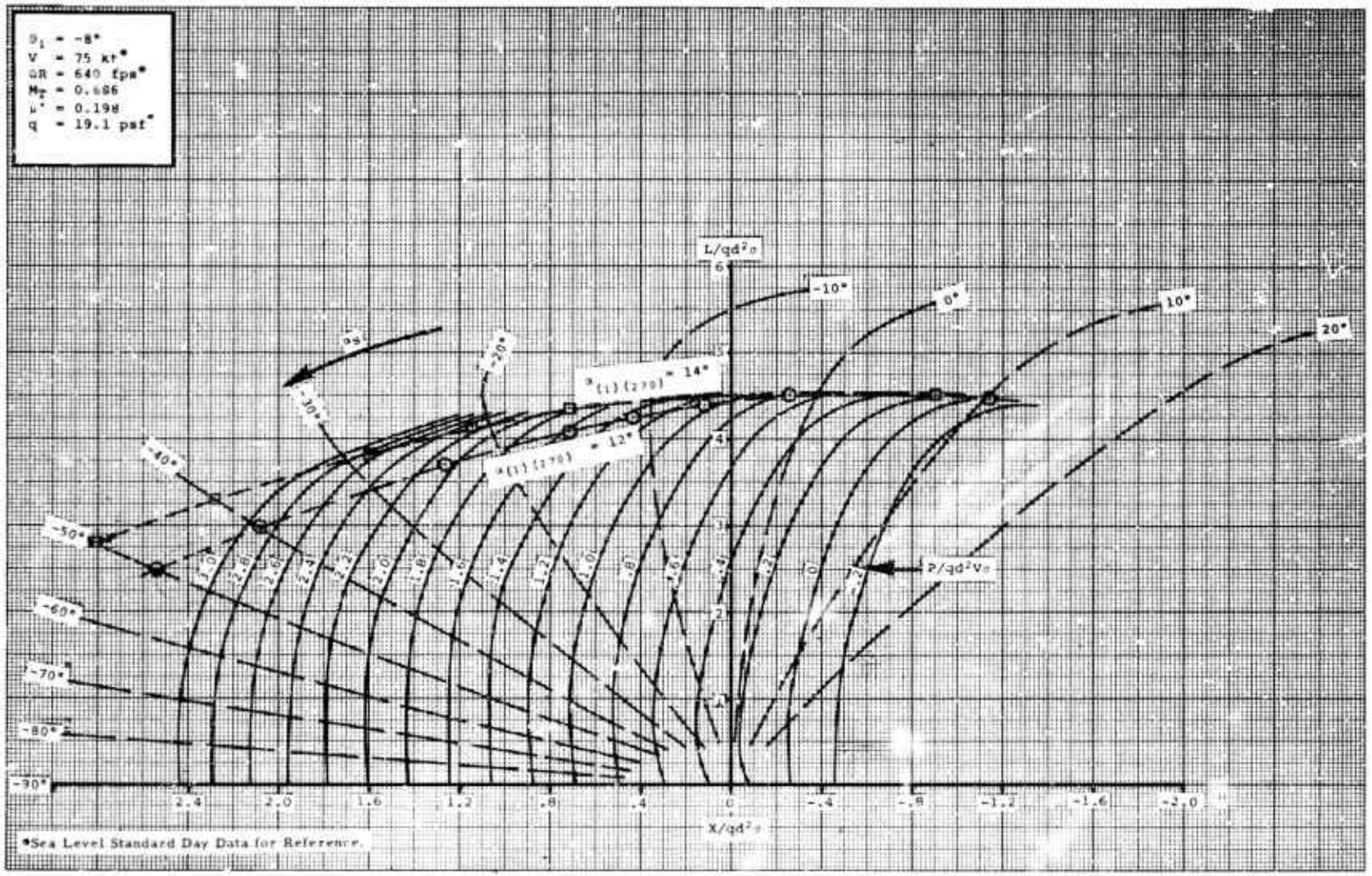
i_t = -8°
V = 75 kt*
QR = 640 fps*
M_T = 0.686
μ = 0.198
q = 19.1 psf*
L/qd²σ
X/qd²σ
P/qd²Vσ
-10°
0°
10°
20°
-30°
-40°
-50°
-60°
-70°
-80°
-90°
$i_{(1)(270)}$ = 14°
$i_{(1)(270)}$ = 12°
*Sea Level Standard Day Data for Reference.

Figure 31.

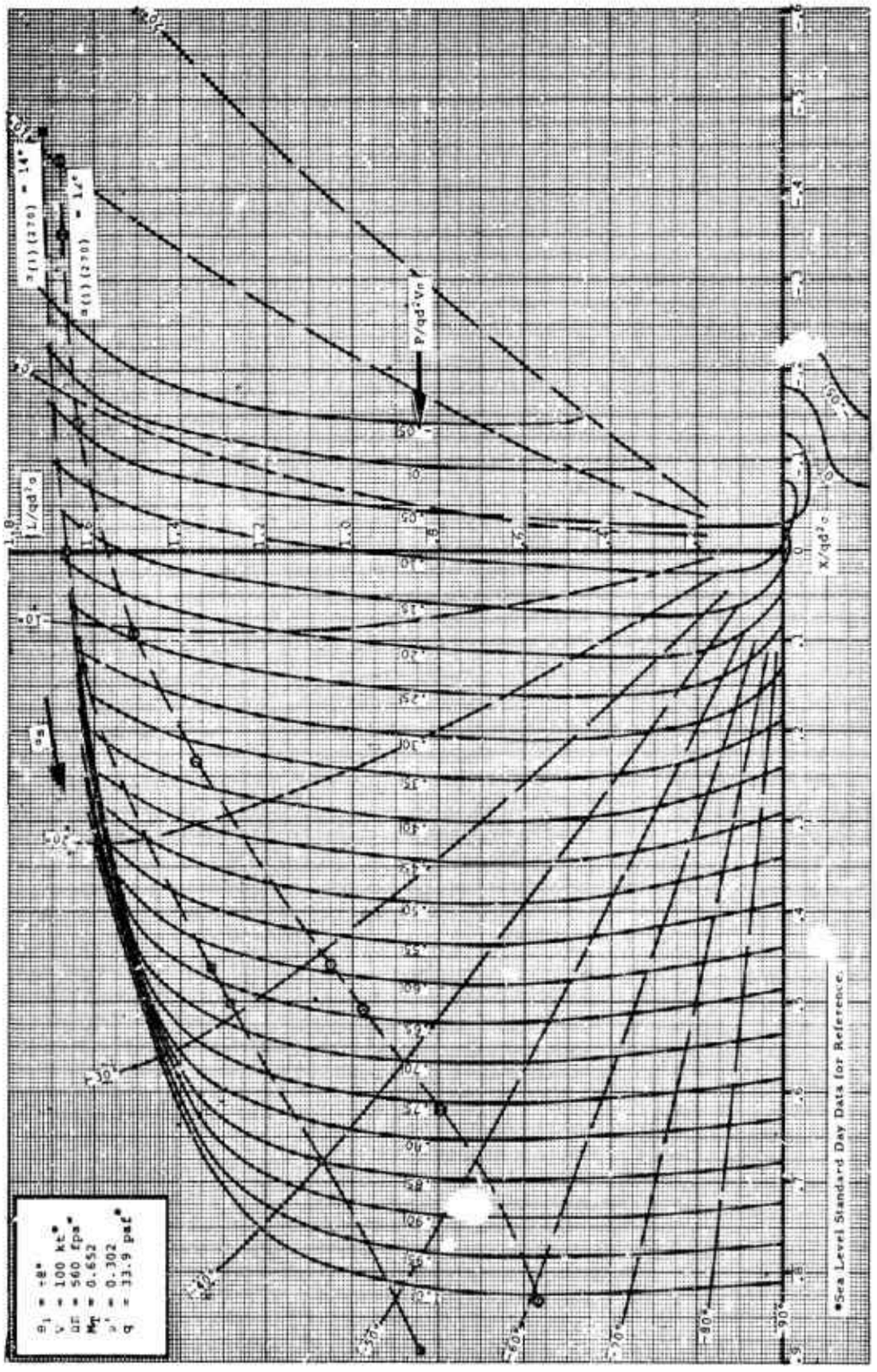
α_i = -8°
V = 100 kt*
ω_E = 560 fps*
M_{ac} = 0.652
λ' = 0.302
q = 33.9 psf*
*Sea Level Standard Day Data for Reference.
L/qd²σ
P/qd²Vσ
X/qd²σ

Figure 32.

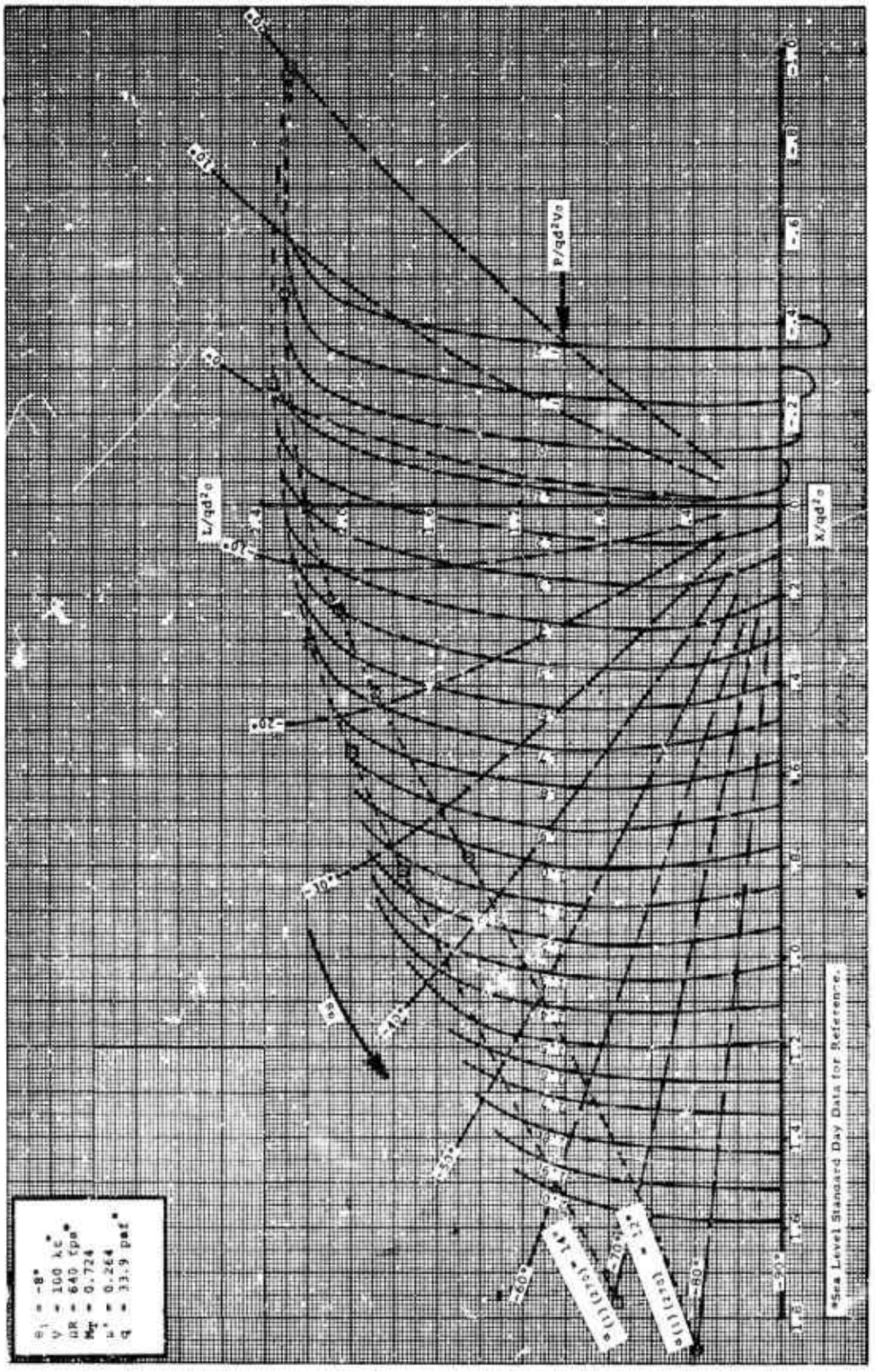
P/qd²Vσ
L/qd²σ
K/qd²σ
*Sea Level Standard Day Data for Reference.

Figure 33.

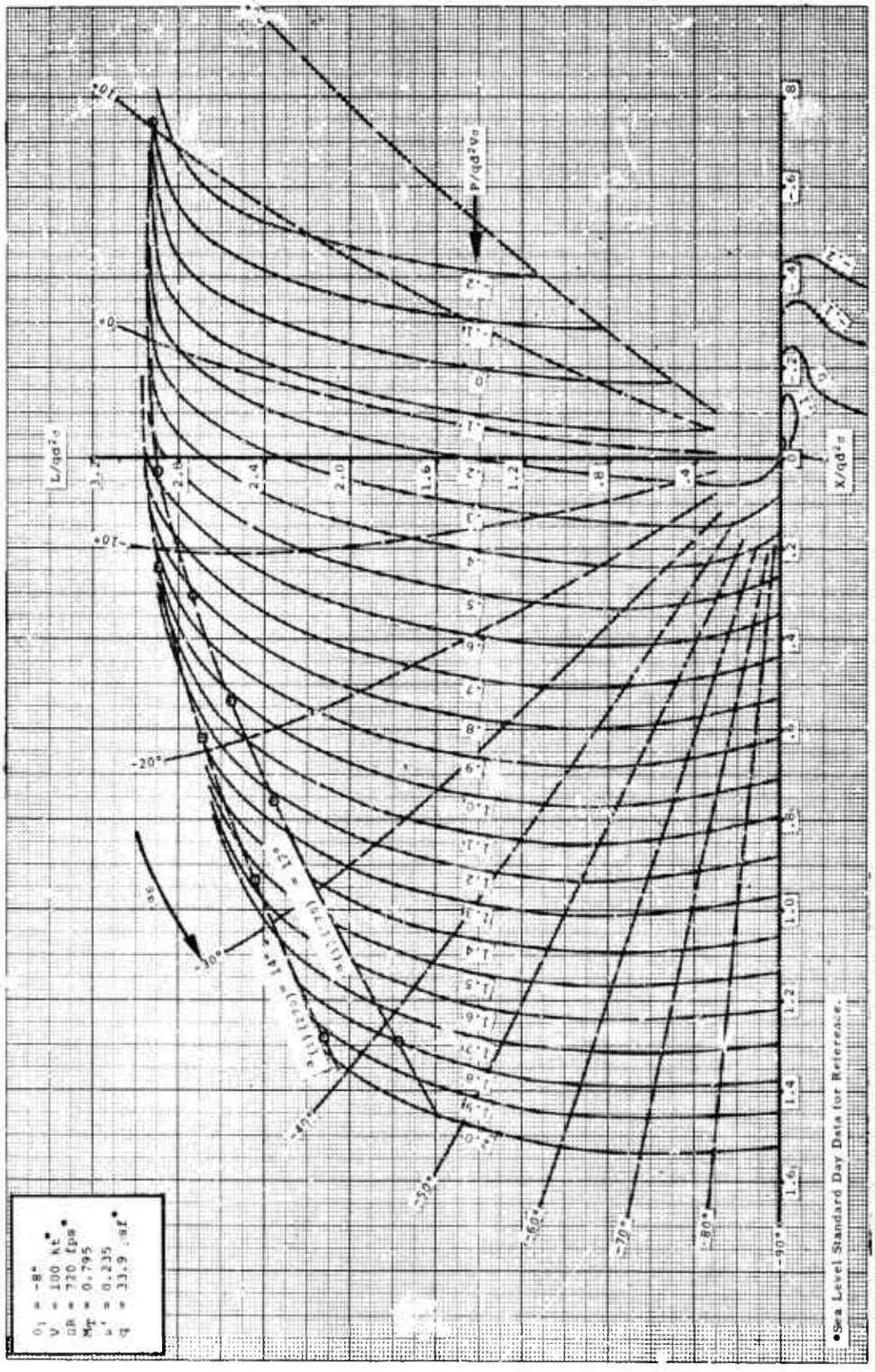
L/qd²a
X/qd²a
P/qd²Va
•Sea Level Standard Day Data for Reference.

Figure 34.

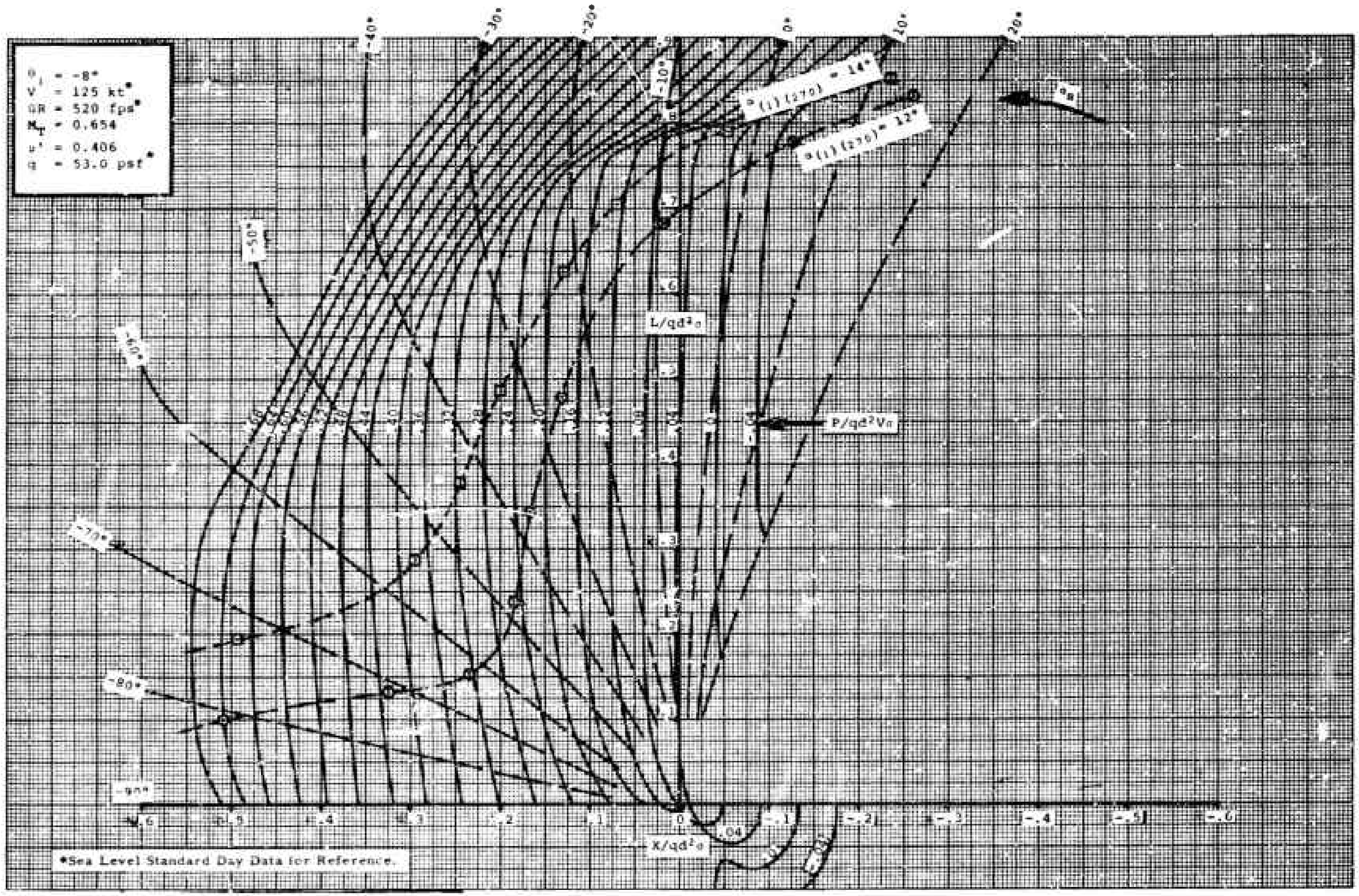

θ_i = -8°
V = 125 kt*
ΩR = 520 fps*
M_T = 0.654
μ' = 0.406
q = 53.0 psf*
L/qd²σ
P/qd²Vσ
X/qd²σ
a_s
-40°
-30°
-20°
-10°
0°
10°
20°
-50°
-60°
-70°
-80°
-90°
*Sea Level Standard Day Data for Reference.

Figure 35.

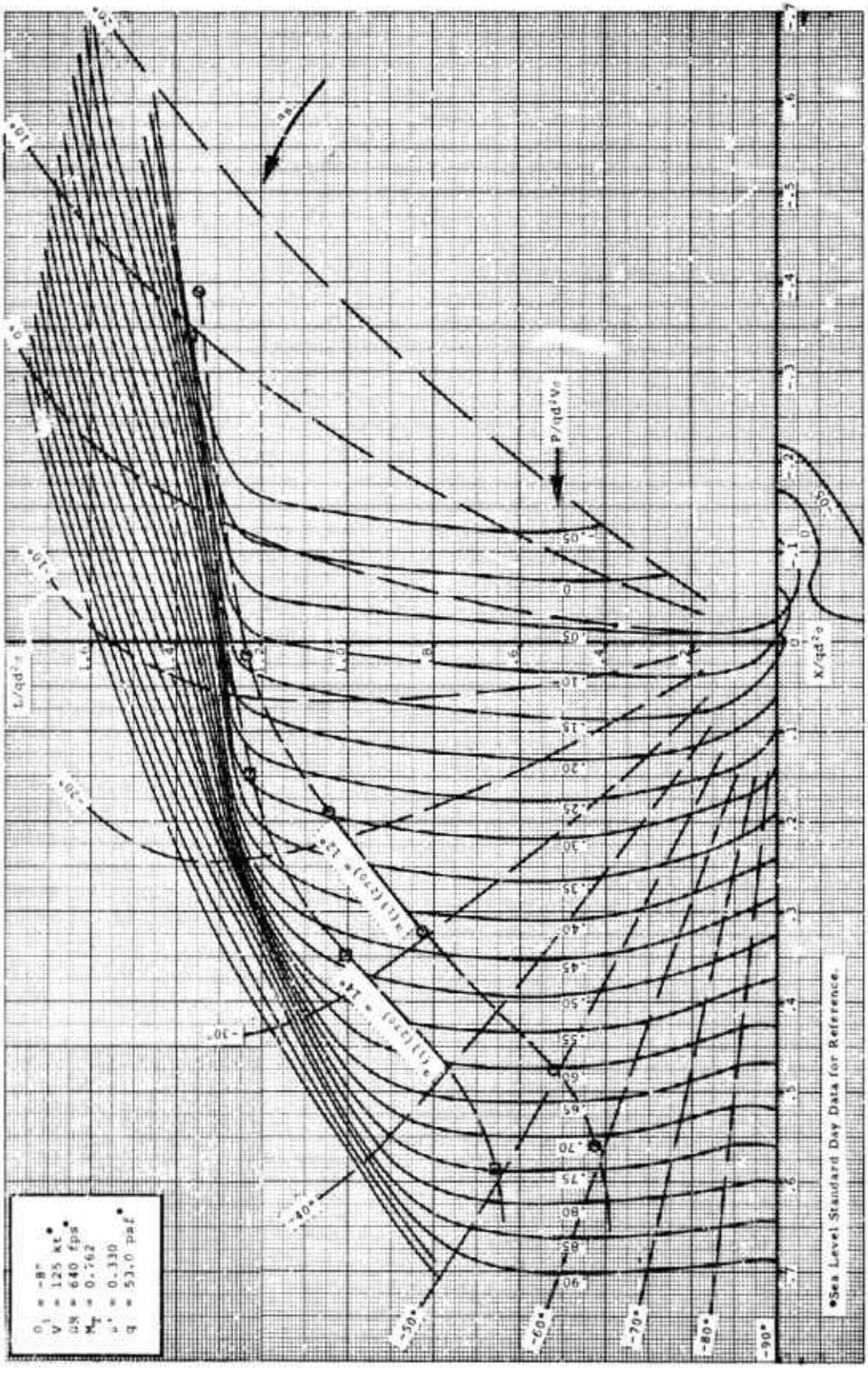
L/qd²
D/qd²
P/qd²
K/qd²
•Sea Level Standard Day Data for Reference.

Figure 36.

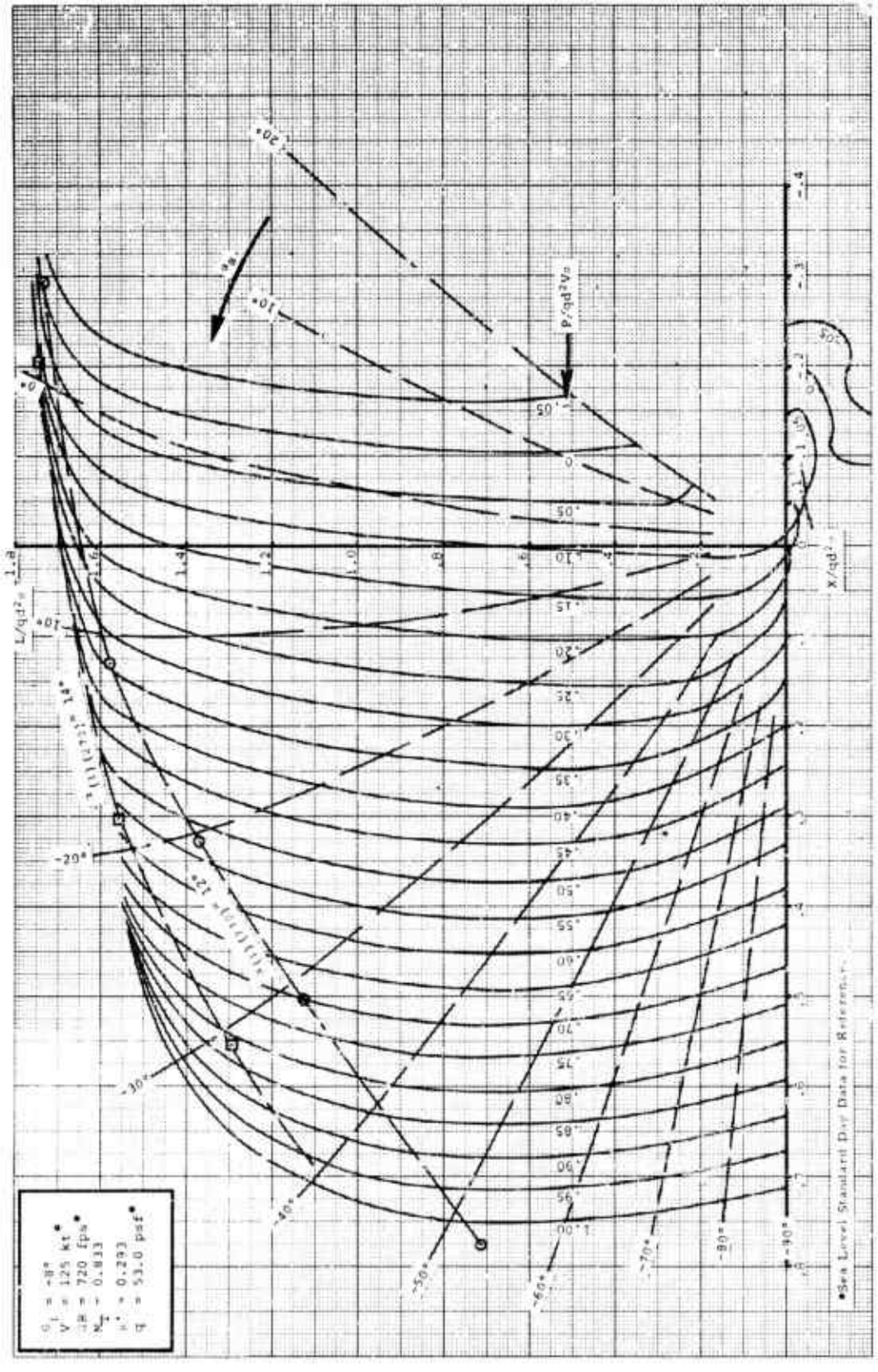
i_t = -8°
V = 125 kt
= 720 fps
N_{M_∞} = 0.293
q = 53.0 psf
*Sea Level Standard Day Data for Reference
P_i/qd^2V_∞
L/qd^2V_∞
X/qd^2V_∞

Figure 37.

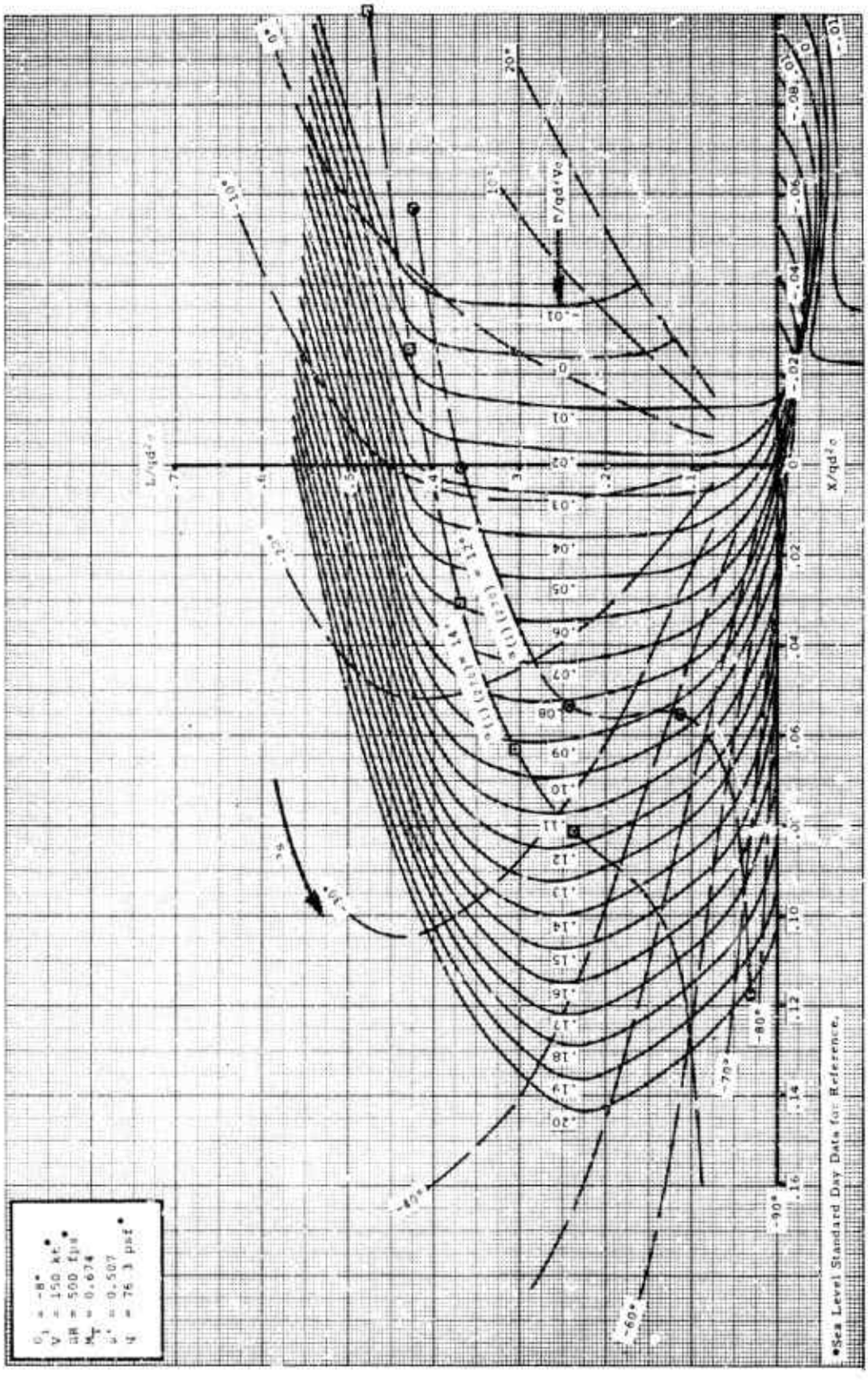
C_L = -.8°
V = 150 kt
dR = 500 fps
M_T = 0.674
$\bar{q}$ = 0.507
q = 76.3 psf
L/qd²o
D/qd²o
X/qd²o
*Sea Level Standard Day Data for Reference.

Figure 38.

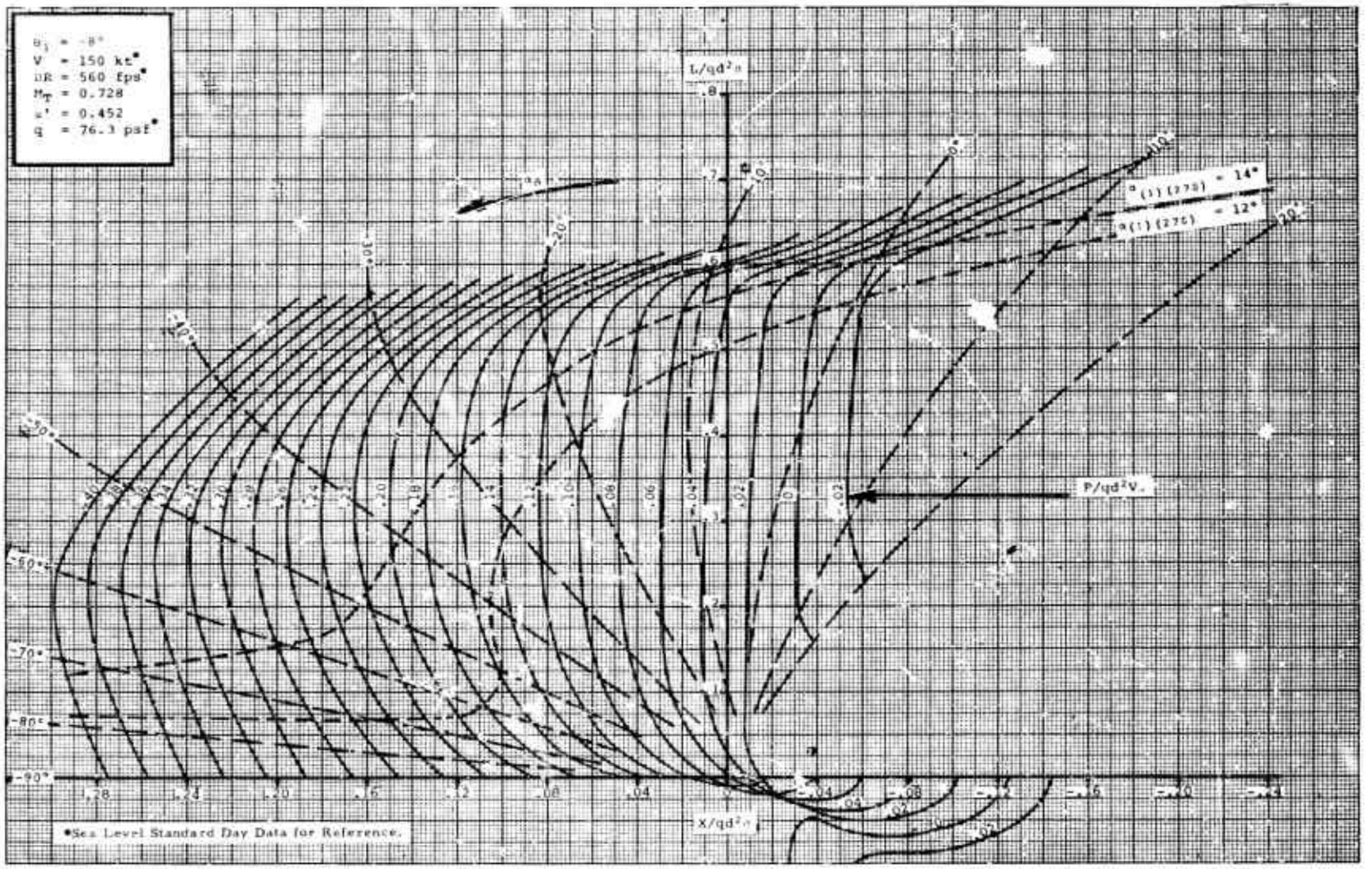
θ_j = -8°
V = 150 kt*
ΩR = 560 Eps*
M_T = 0.728
μ' = 0.452
q = 76.3 psf*
L/qd²n
P/qd²V.
X/qd²n
α(1)(27B) = 14°
α(1)(27C) = 12°
*Sea Level Standard Day Data for Reference.

Figure 39.

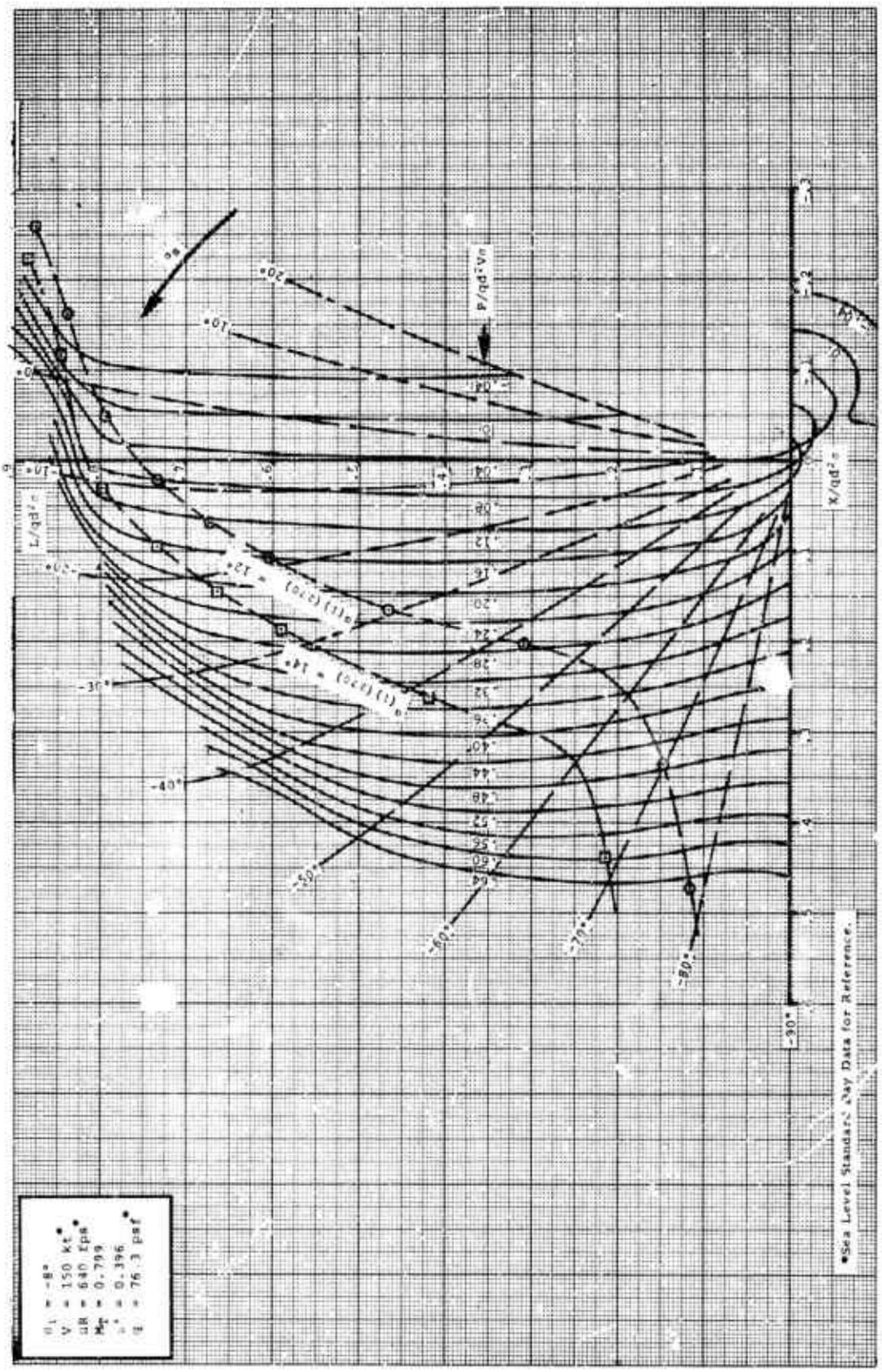

Figure 40.

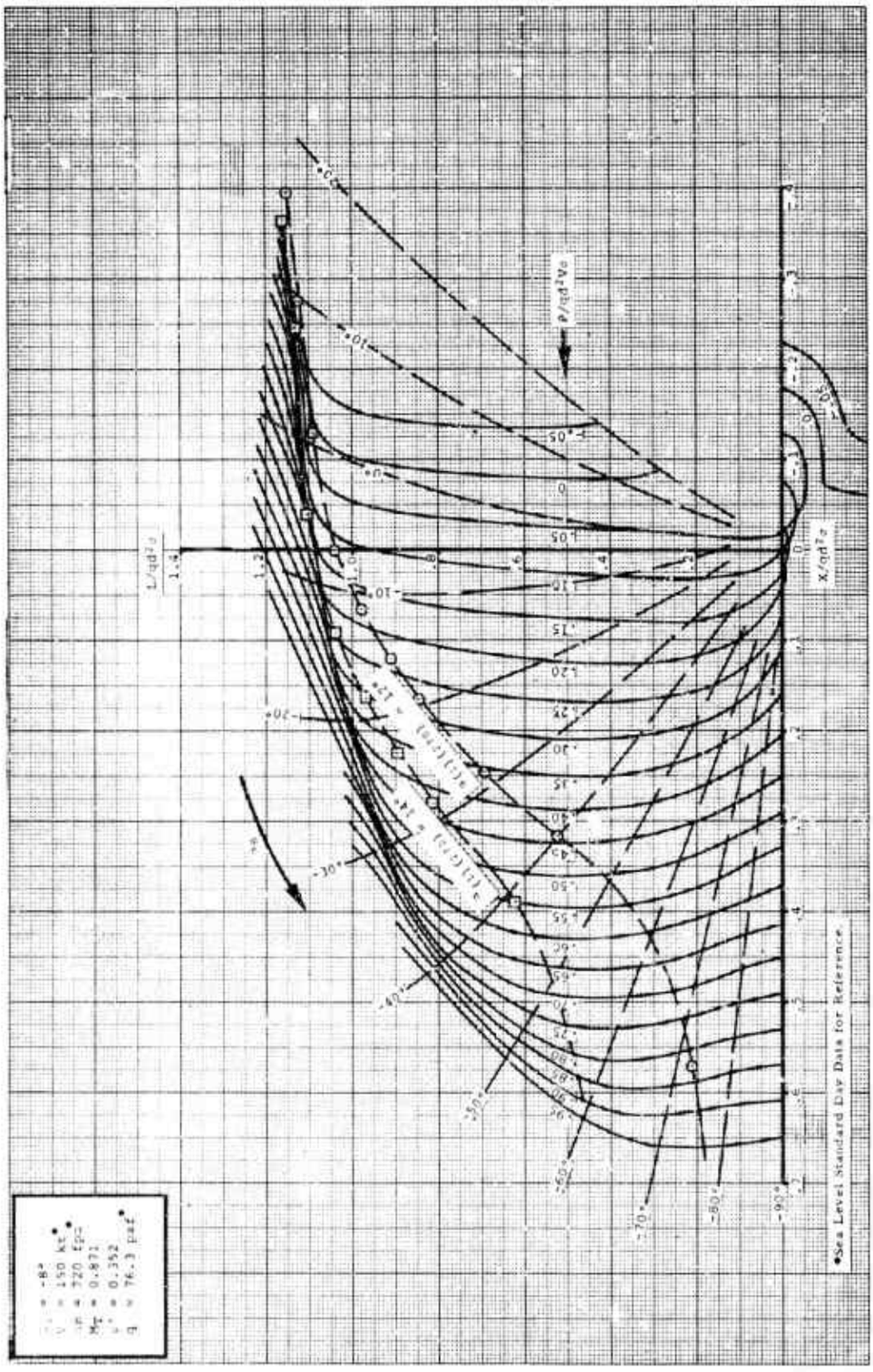
L/qd²o
D/qd²o
x/qd²o
•Sea Level Standard Day Data for Reference

Figure 41.

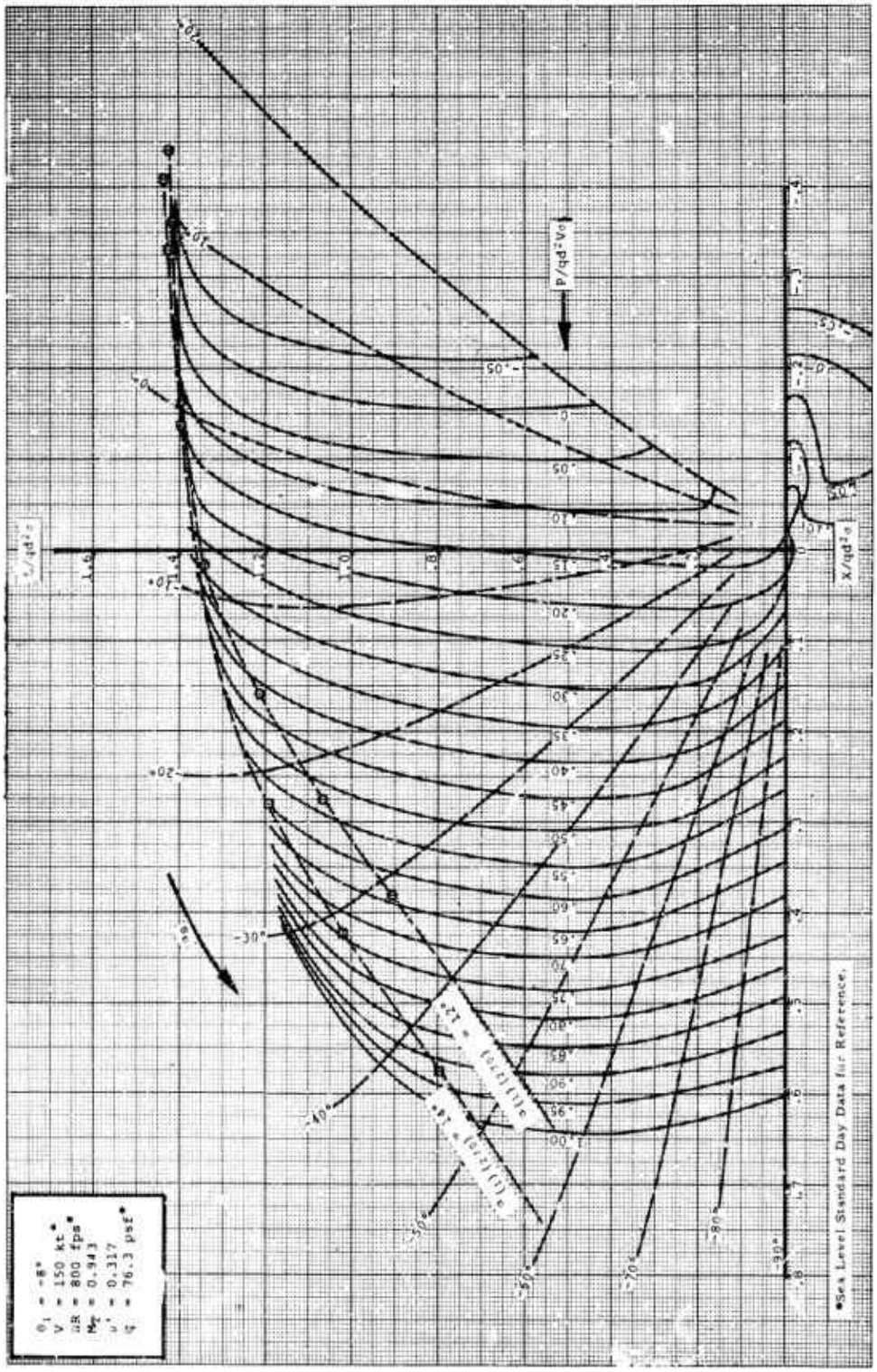
θ_1 = -8°
V = 150 kt*
ΩR = 800 fps*
M_{tip} = 0.943
μ' = 0.317
q = 76.3 psf*
Z/qd²
X/qd²
*Sea Level Standard Day Data for Reference.

Figure 42.

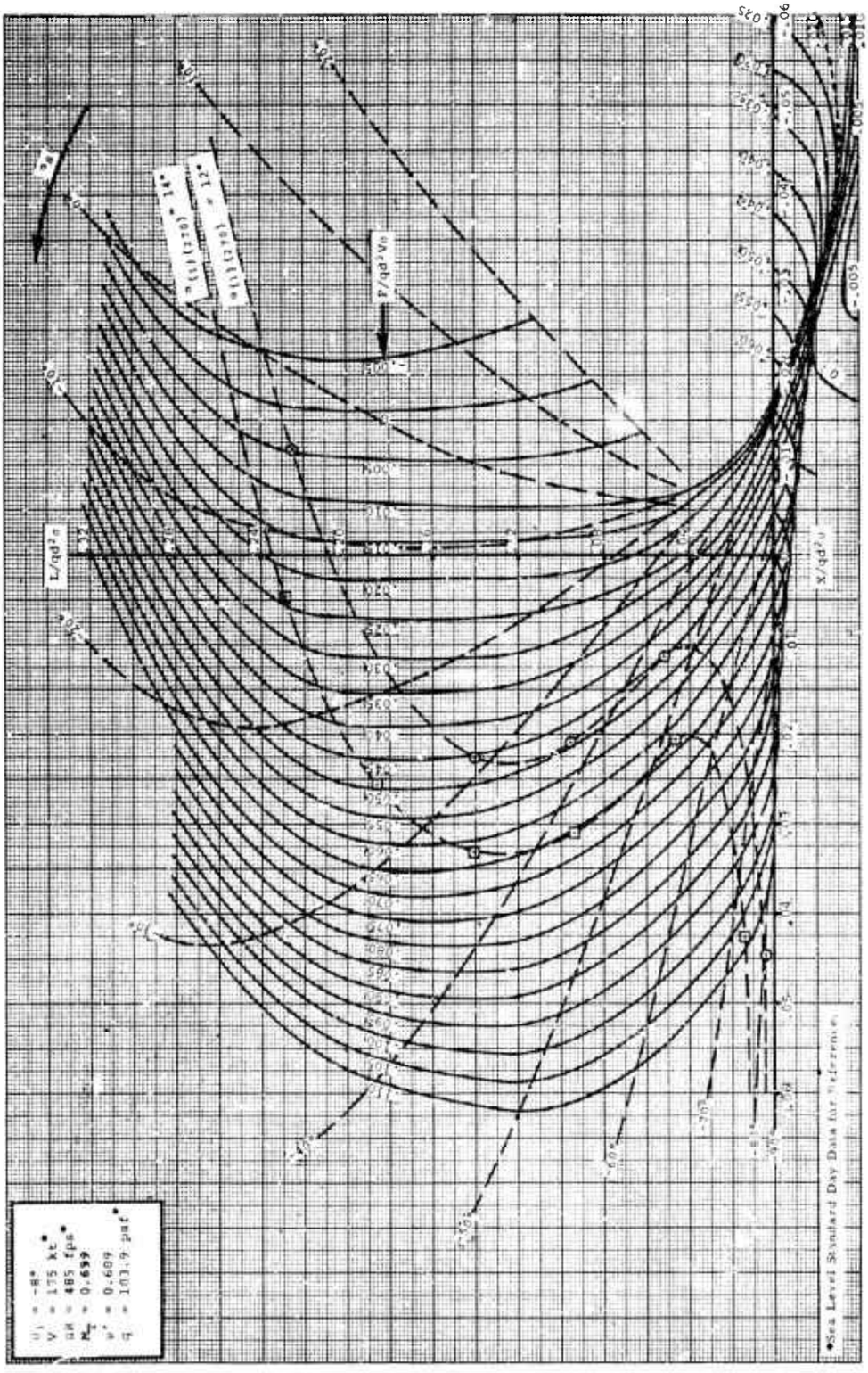
α = -8°
V = 175 kt*
ΩR = 485 fps*
M_{tip} = 0.699
μ* = 0.609
q = 103.9 psf*
*Sea Level Standard Day Data for Reference
L/qd²ₙ
D/qd²ₙ
Y/qd²ₙ
X/qd²ₙ
F/qd²Vₜ₀

Figure 43.

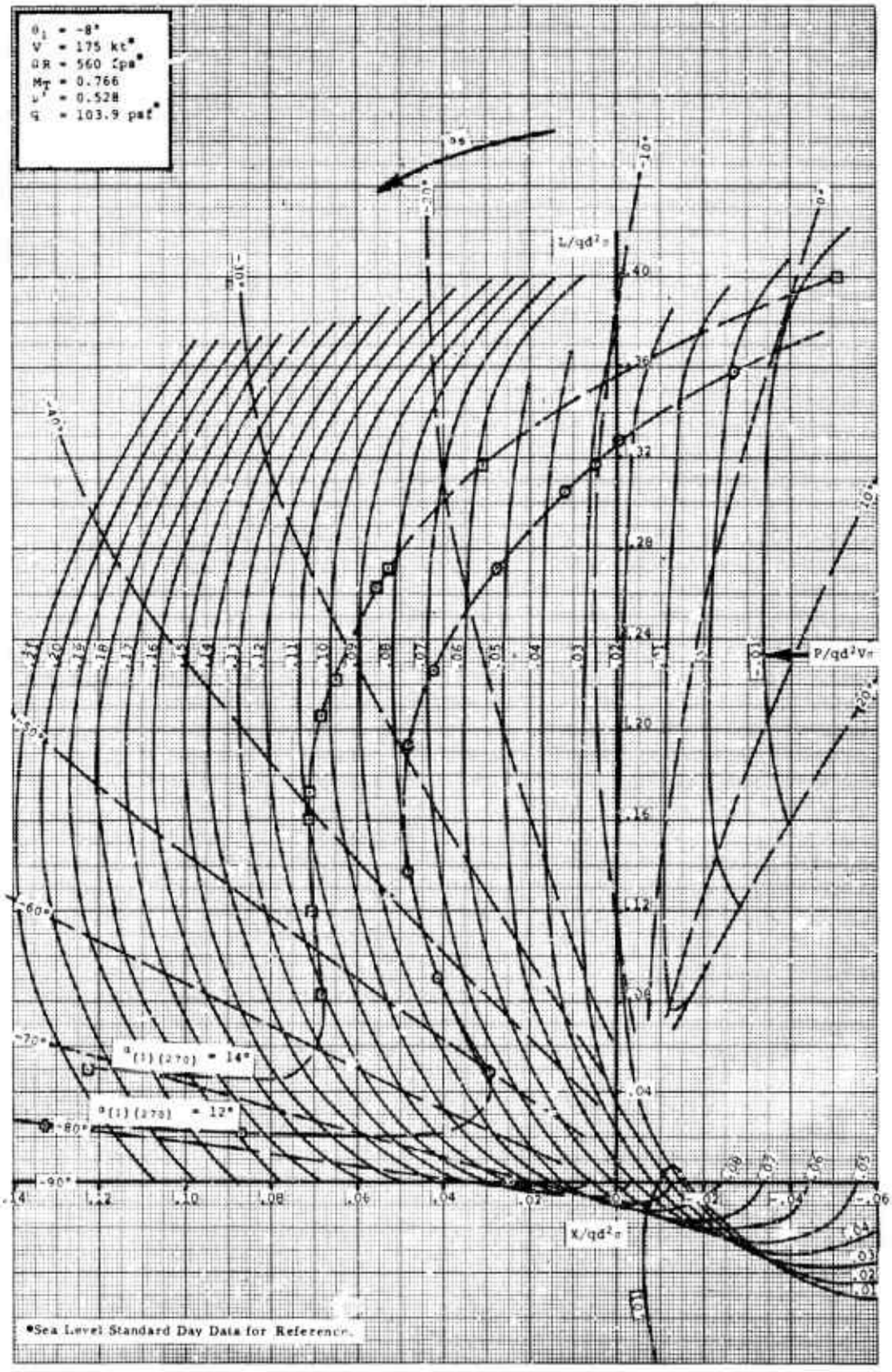
θ_i = -8°
V = 175 kt*
q_R = 560 Pa*
M_T = 0.766
ν' = 0.528
q = 103.9 psf*
α_s
L/qd²π
P/qd²Vπ
Y/qd²π
$\alpha_{(1)(270)}$ = 14°
$\alpha_{(1)(270)}$ = 12°
*Sea Level Standard Day Data for Reference.

Figure 44.

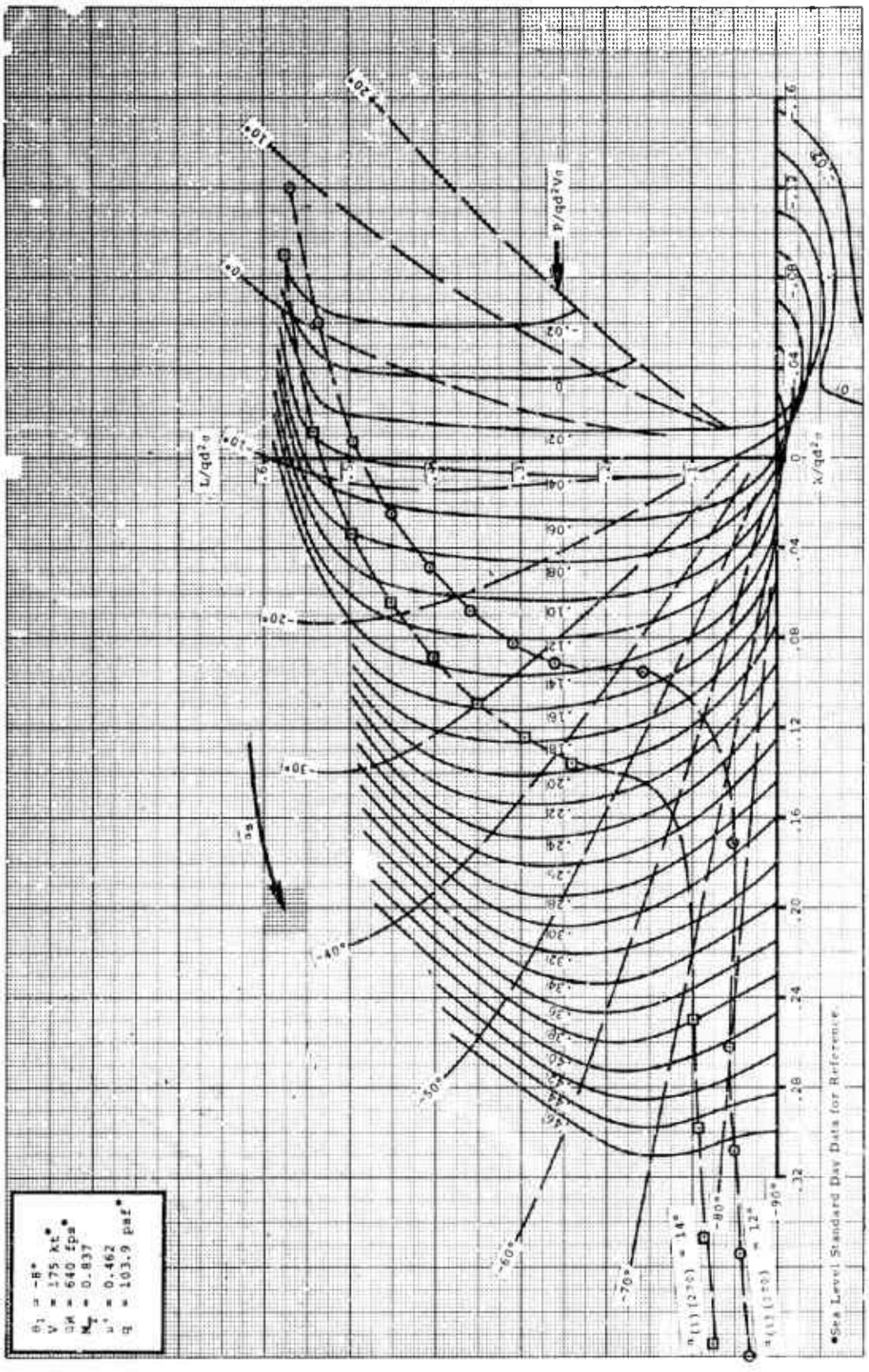
θ_1 = -8°
V = 175 kt*
q = 640 fpa*
M = 0.837
N_z = 0.462
q = 103.9 psf*
L/qd²a
M/qd²a
D/qd²a
*Sea Level Standard Day Data for Reference

Figure 45.

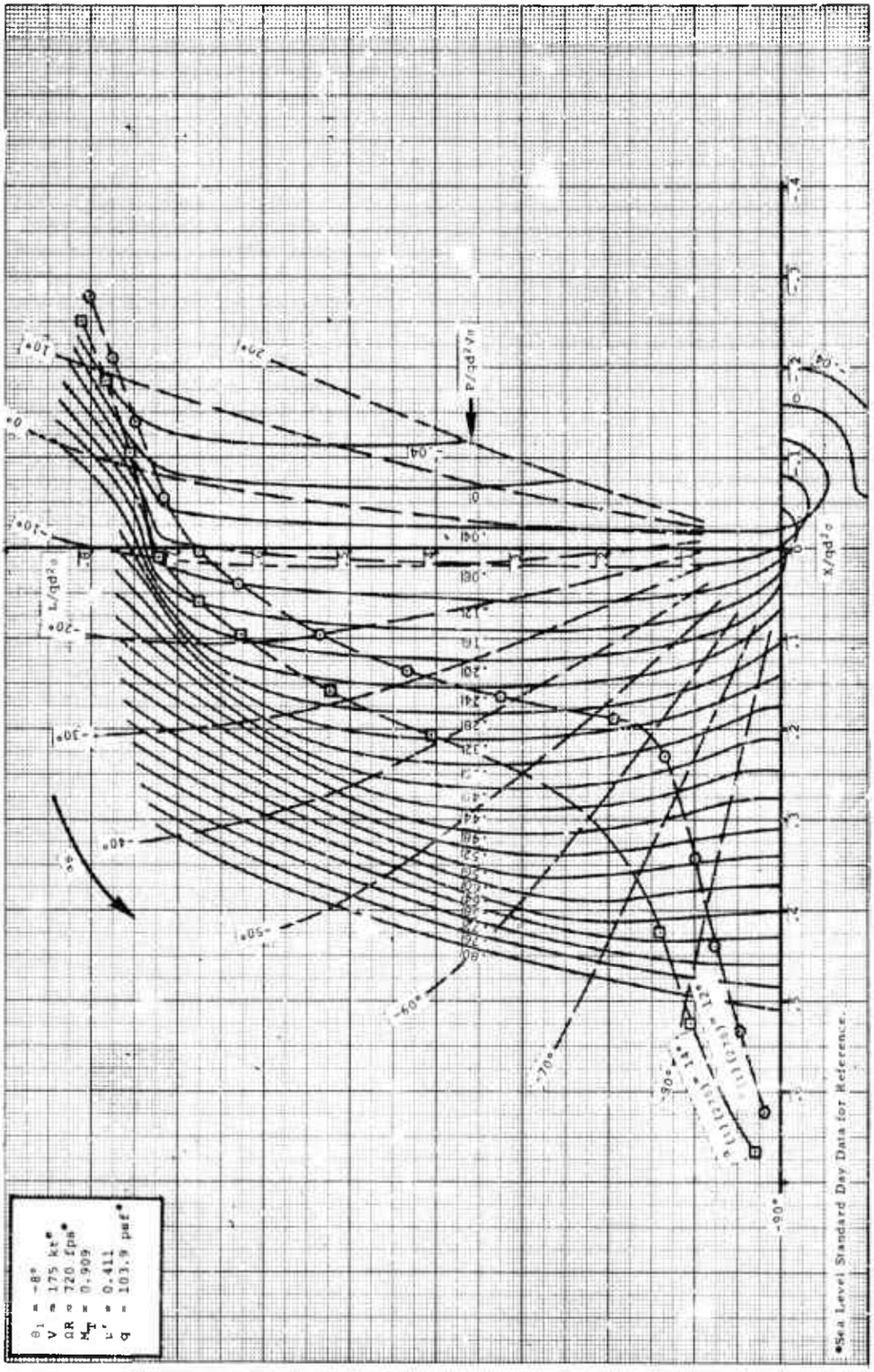
θ1 = -8°
V = 175 kt*
ΩR = 720 fps*
MT = 0.909
μ' = 0.411
q = 101.9 psf*
*Sea Level Standard Day Data for Reference.

Figure 46.

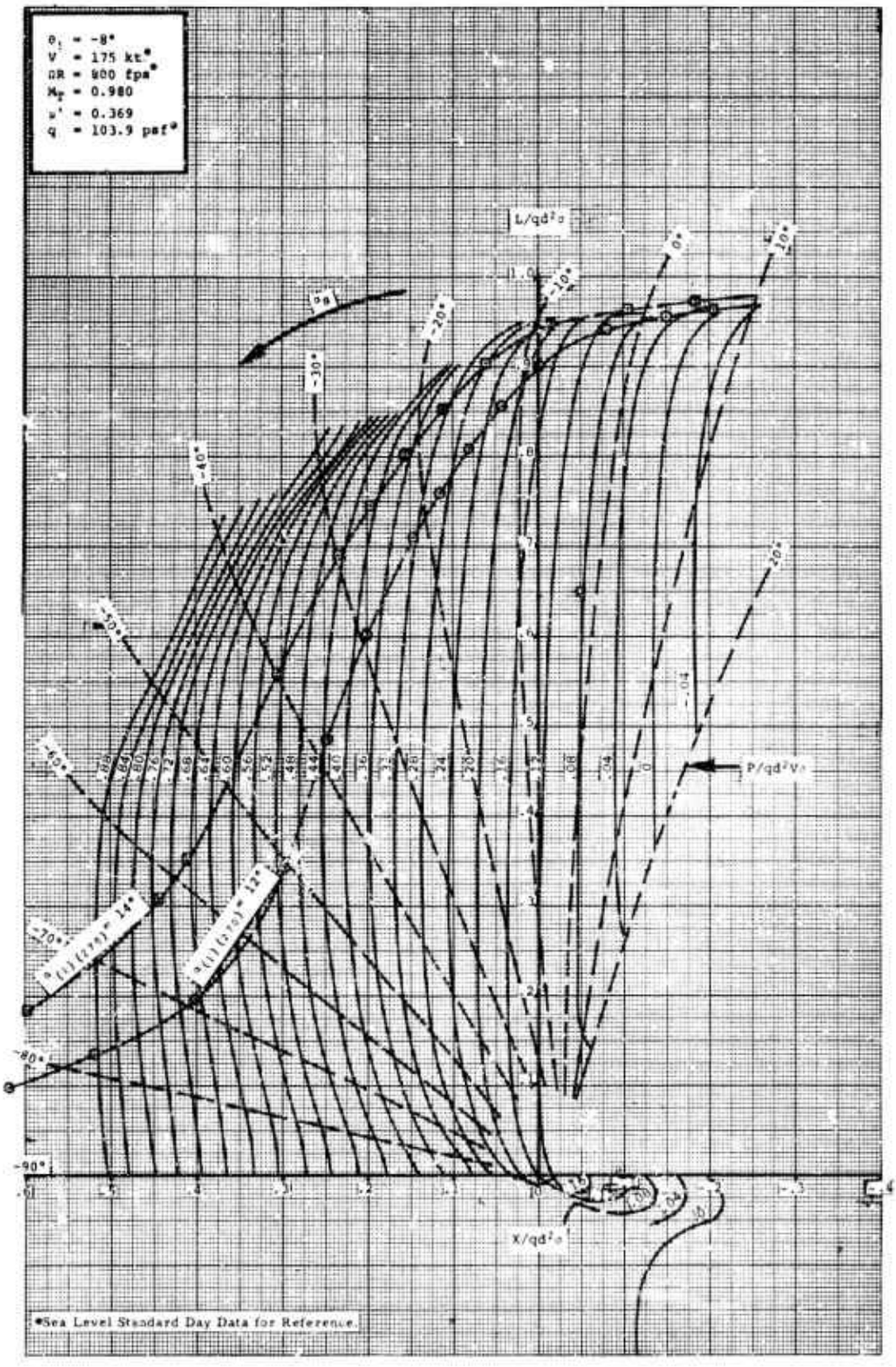
θ_i = -8°
V = 175 kt*
RR = 900 fpm*
M_F = 0.980
μ' = 0.369
q = 103.9 psf*
L/qd²ₒ
D/qd²ₒ
P/qd²ₒ
X/qd²ₒ
*Sea Level Standard Day Data for Reference

Figure 47.

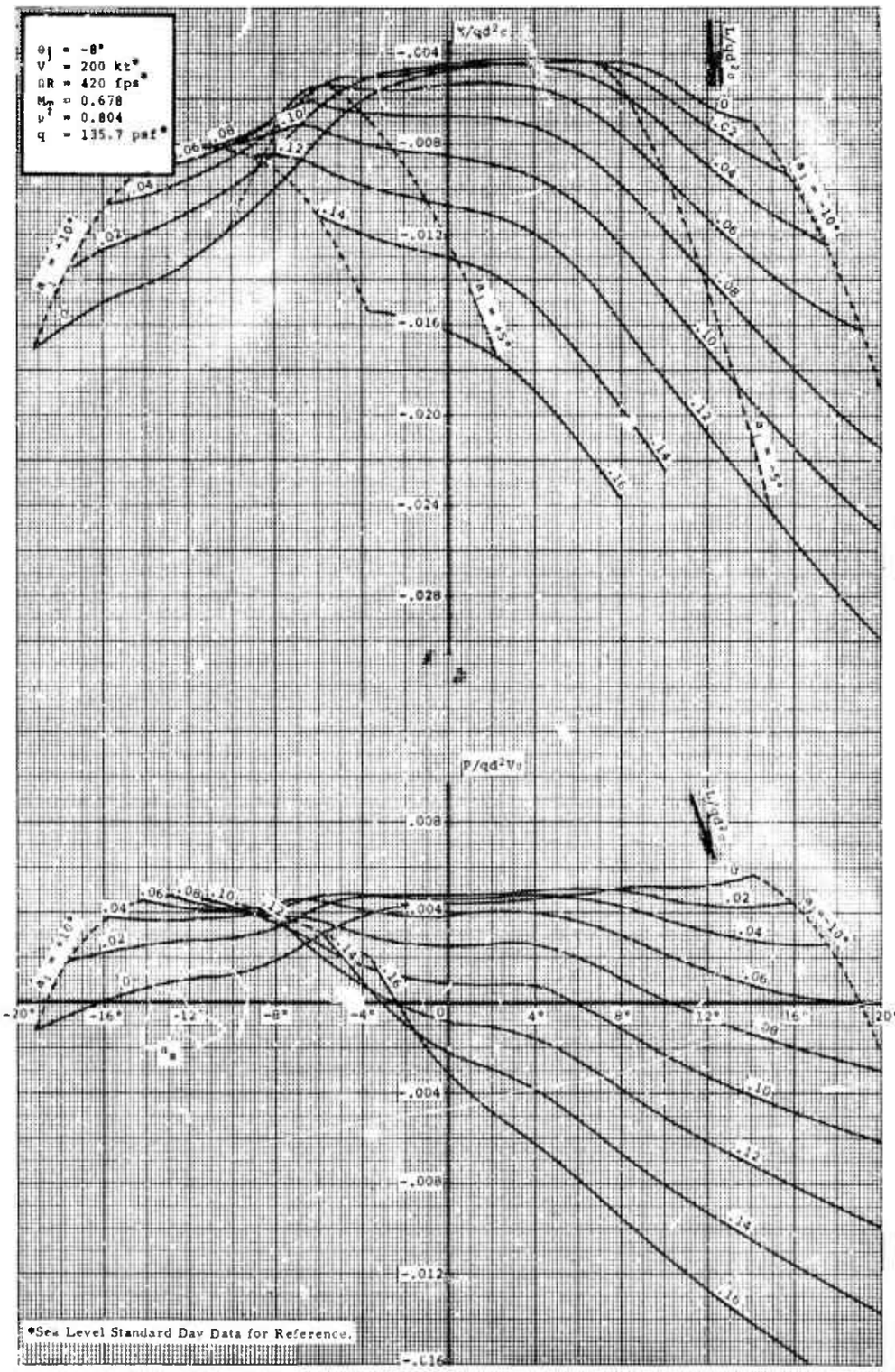
θ1 = -8°
V = 200 kt*
ΩR = 420 fps*
M = 0.678
μ = 0.804
q = 135.7 psf*
H/qd²σ
L/qd²σ
P/qd²σ
-.004
-.008
-.012
-.016
-.020
-.024
-.028
-.008
-.004
-.004
-.008
-.012
-.016
-20°
-16°
-12°
-8°
-4°
0
4°
8°
12°
16°
20°
*Sea Level Standard Day Data for Reference.

Figure 48.

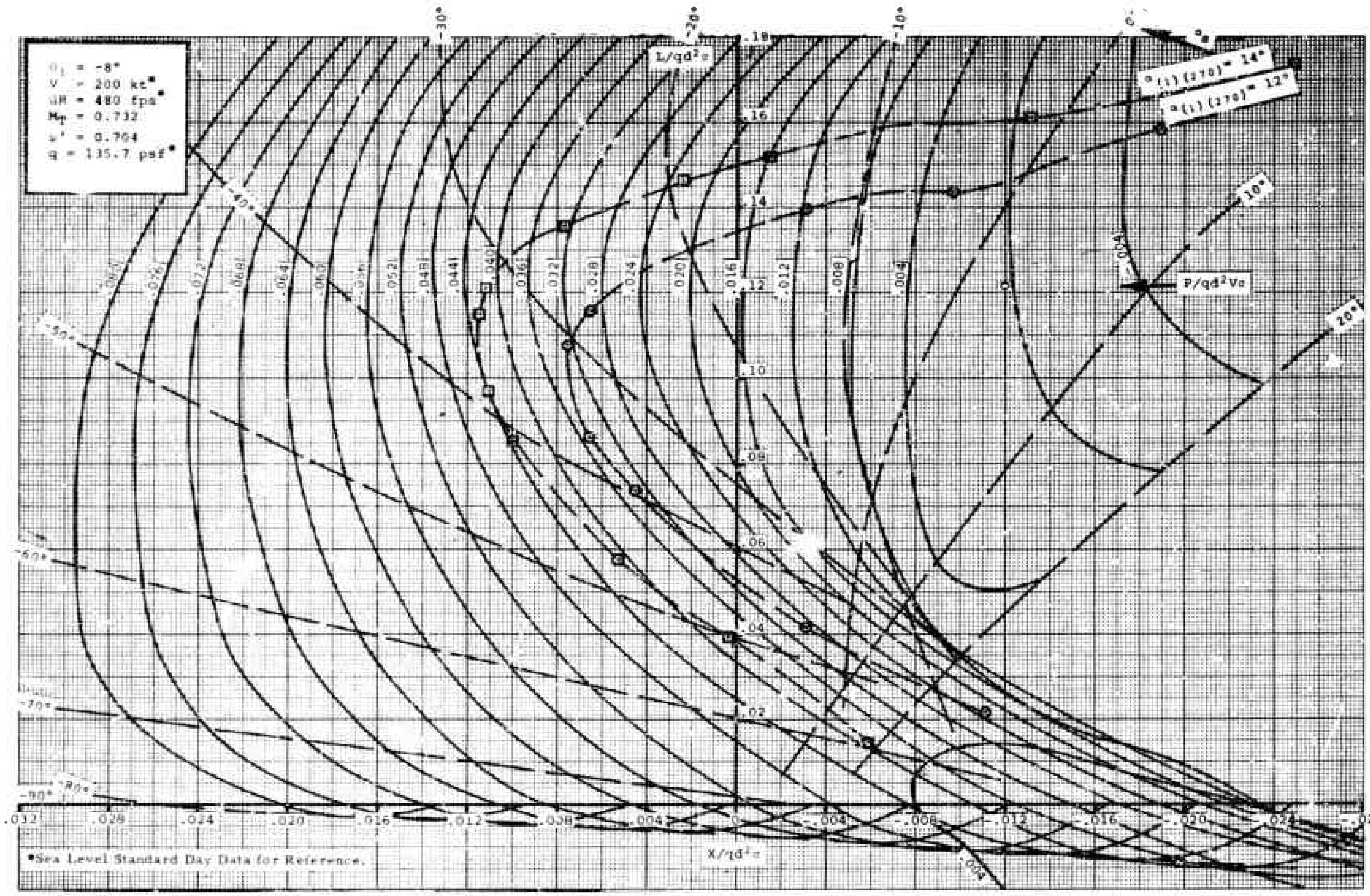
θ_1 = -8°
V = 200 kt*
ΩR = 480 fps*
M_T = 0.732
σ' = 0.704
q = 135.7 psf*
L/qd²σ
X/qd²σ
P/qd²Vσ
θ(i)(270) = 14°
θ(i)(270) = 12°
*Sea Level Standard Day Data for Reference.

Figure 49.

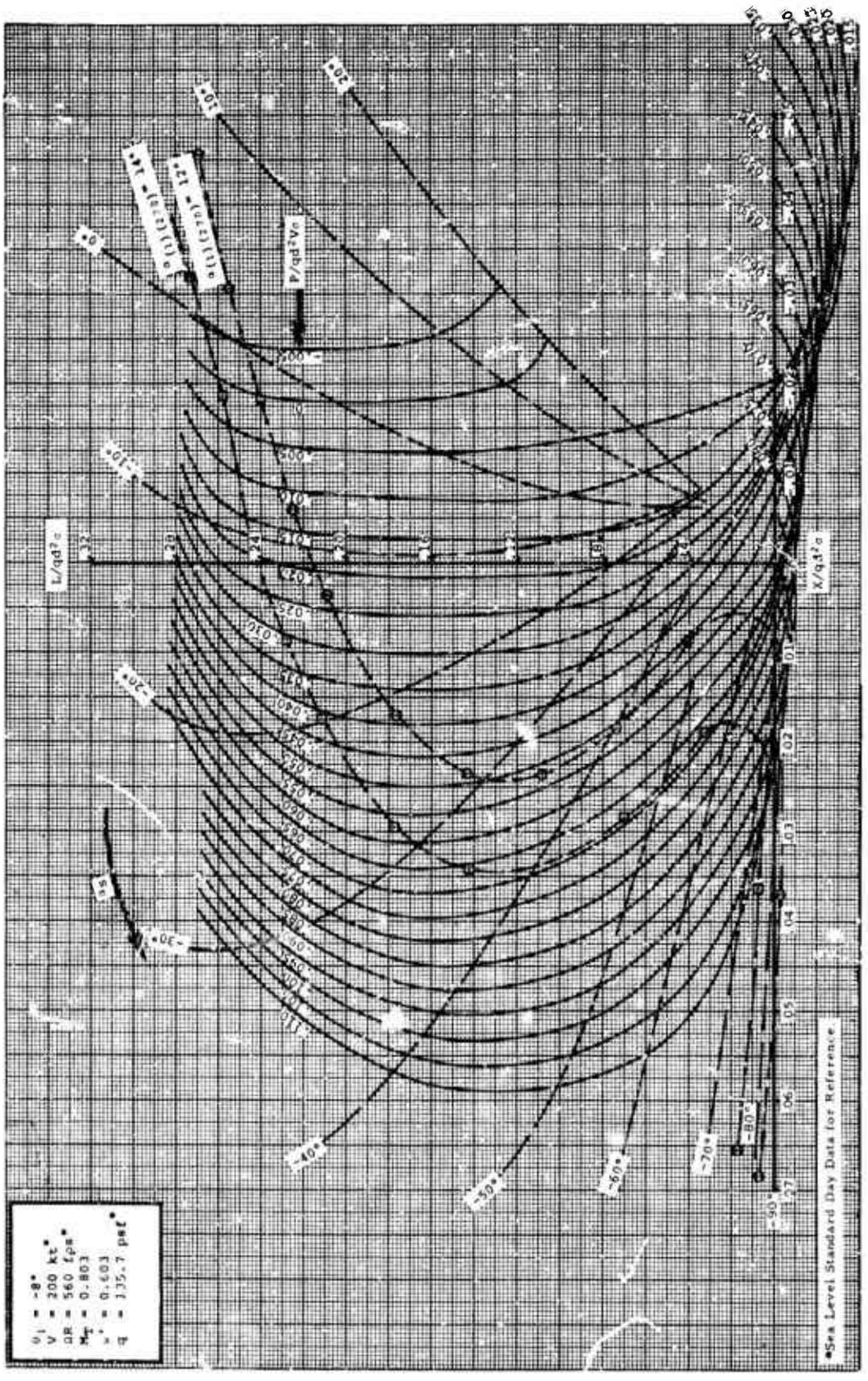
ψi = -8°
V = 200 kt*
ΩR = 560 fps*
Mt = 0.803
μ* = 0.603
q = 135.7 psf*
*Sea Level Standard Day Data for Reference

Figure 50.

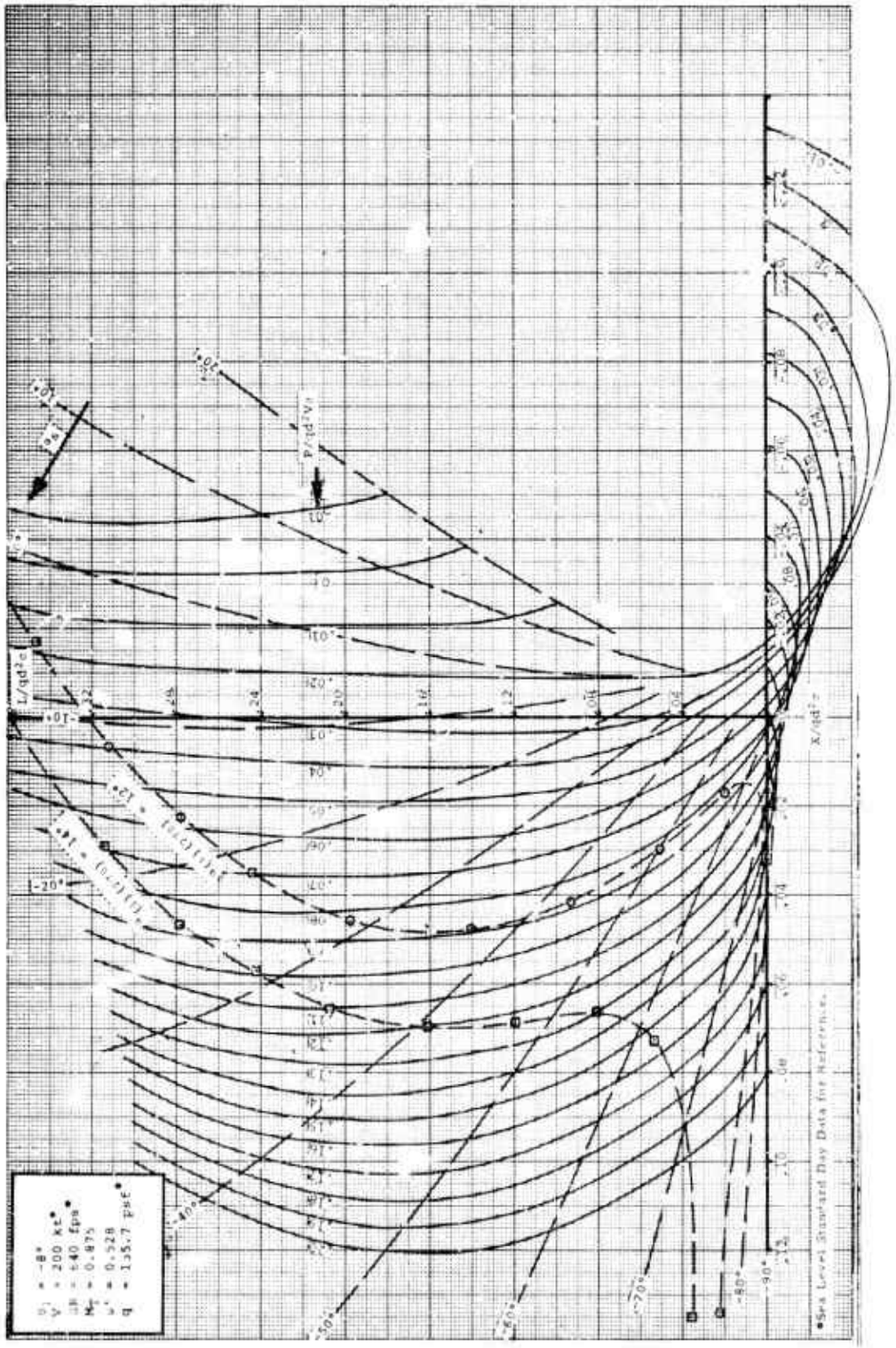

Figure 51.

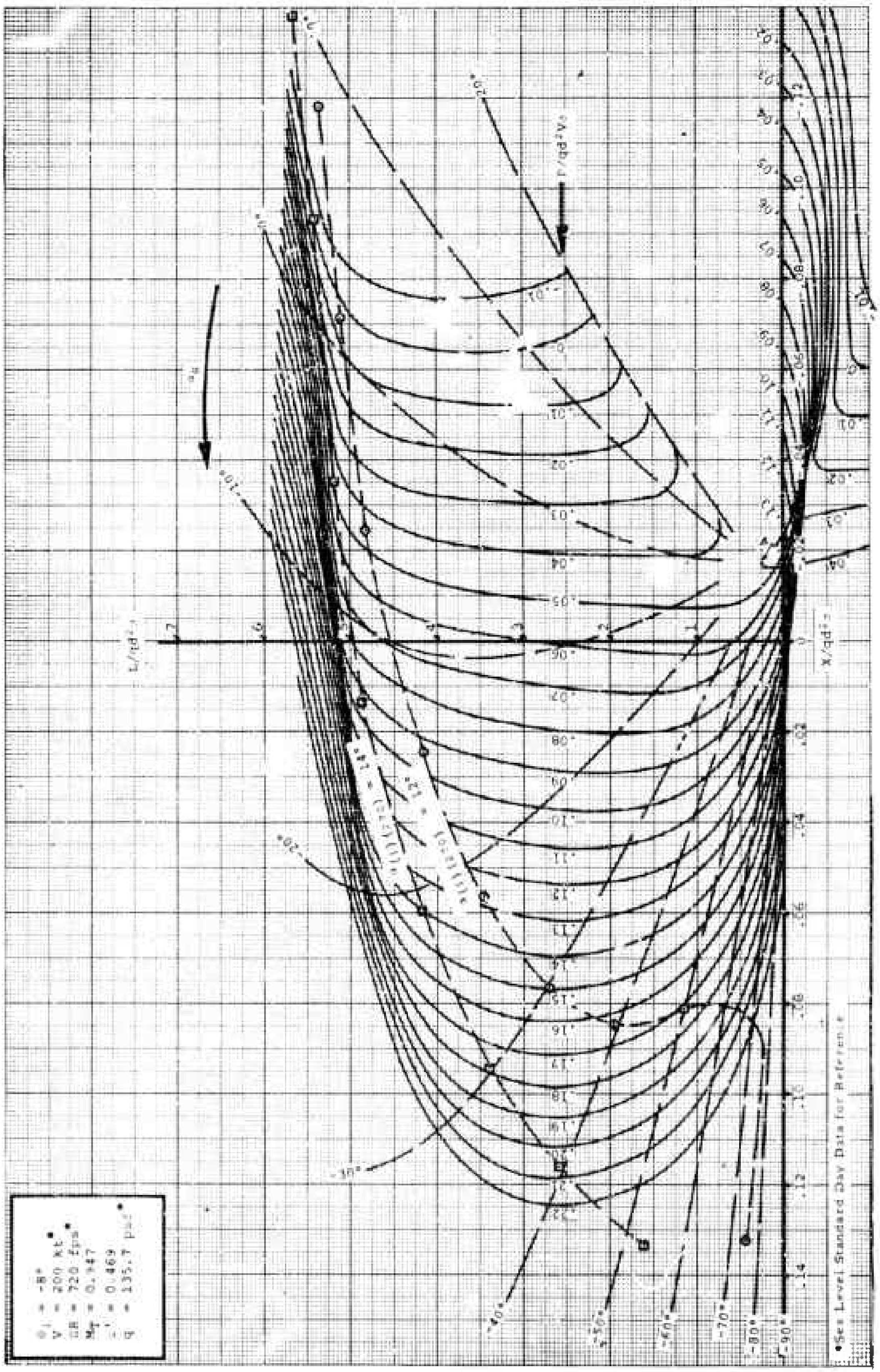

Figure 52.

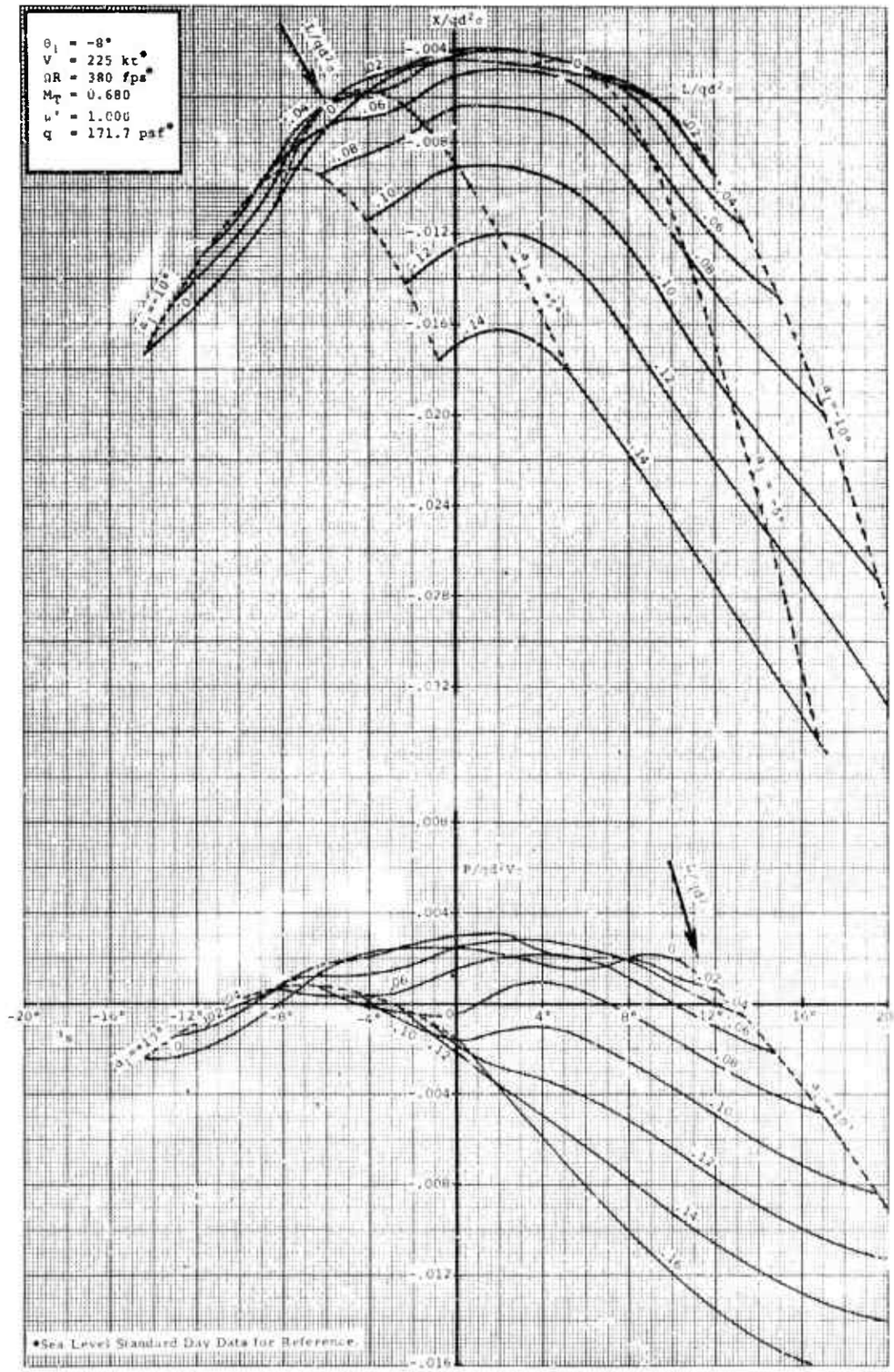
θ_1 = -8°
V = 225 kt*
ΩR = 380 fps*
M_T = 0.680
μ' = 1.000
q = 171.7 psf*
X/qd²σ
L/qd²σ
Y/qd²σ
P/ρd²V₂
*Sea Level Standard Day Data for Reference.

Figure 53.

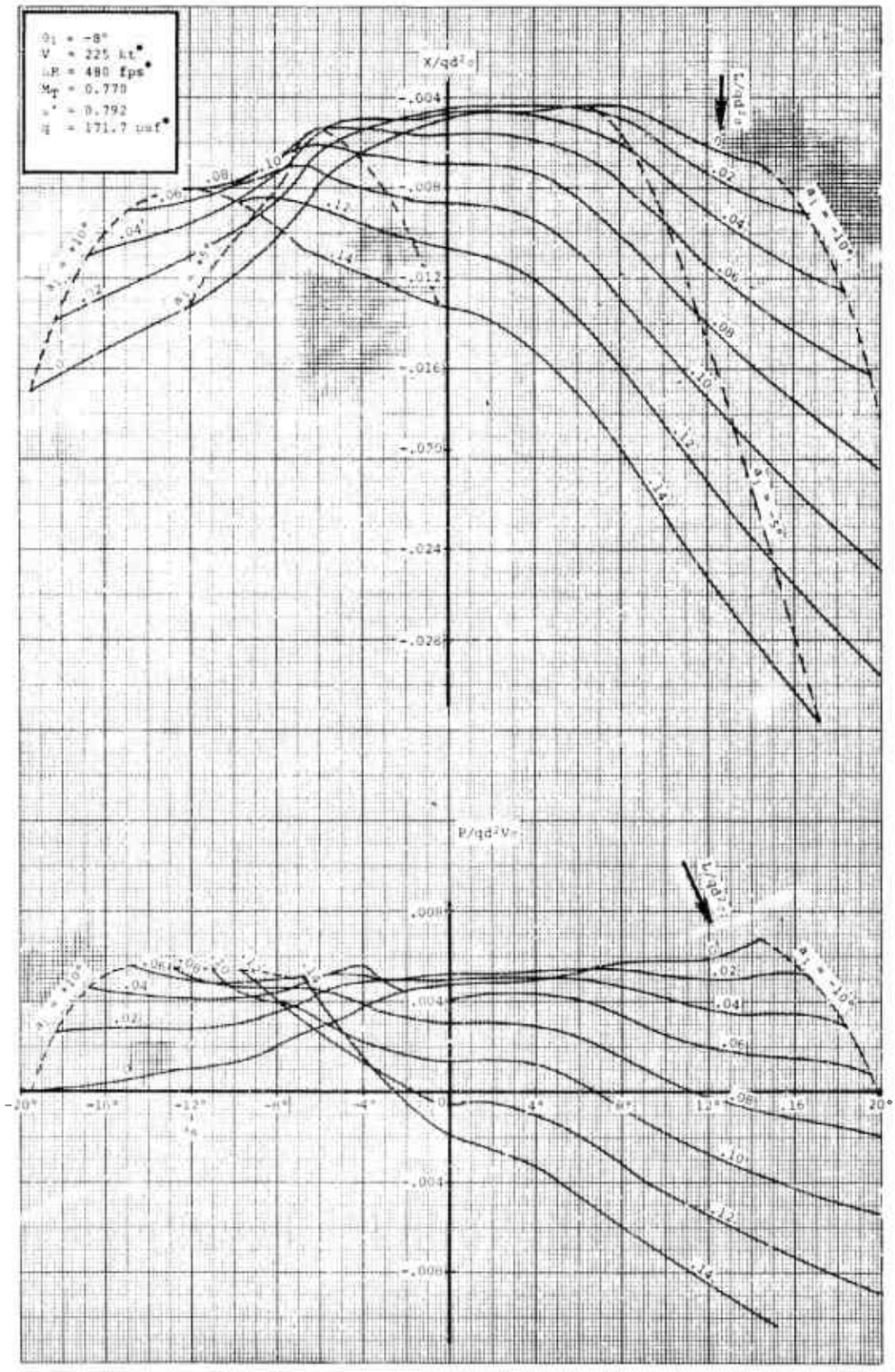
θ_1 = -8°
V = 225 kt
ΔR = 480 fps
M_T = 0.770
= 0.792
= 171.7 psf
X/qd²
P/qd²
-.004
-.008
-.012
-.016
-.020
-.024
-.028
.004
.008
-20°
-16°
-12°
-8°
-4°
0°
4°
8°
12°
16°
20°
α

Figure 54.

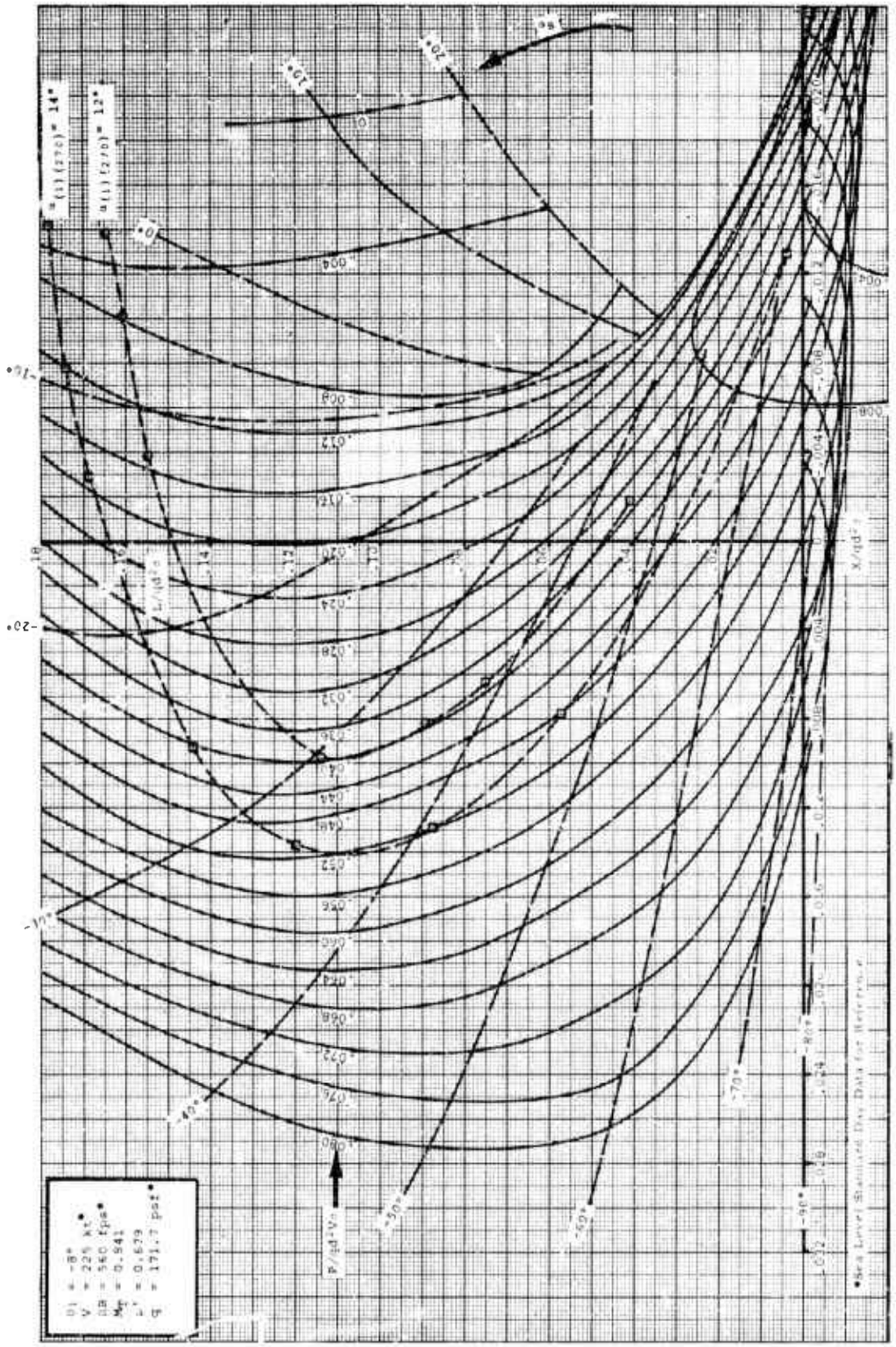

Figure 55.

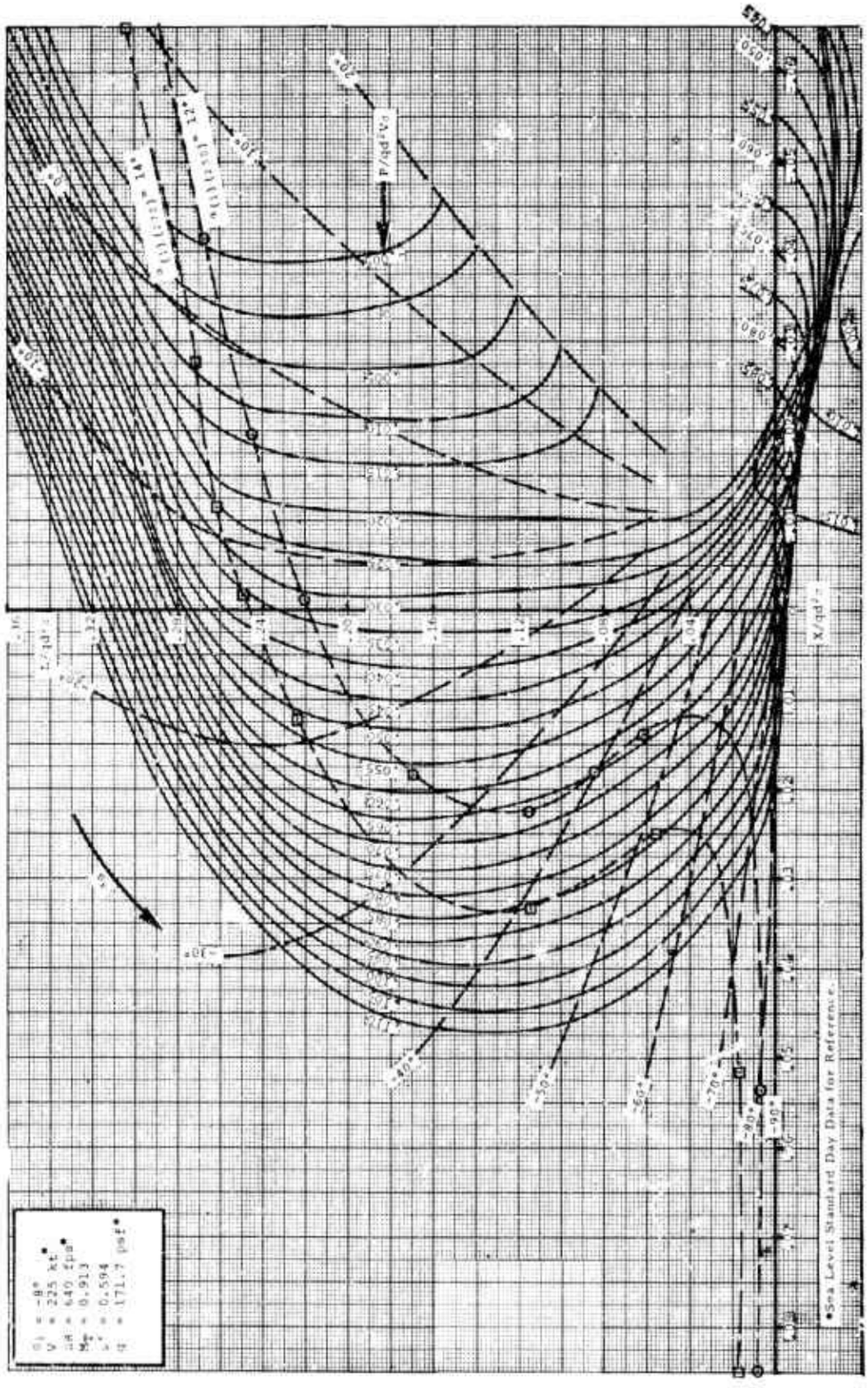

Figure 56.

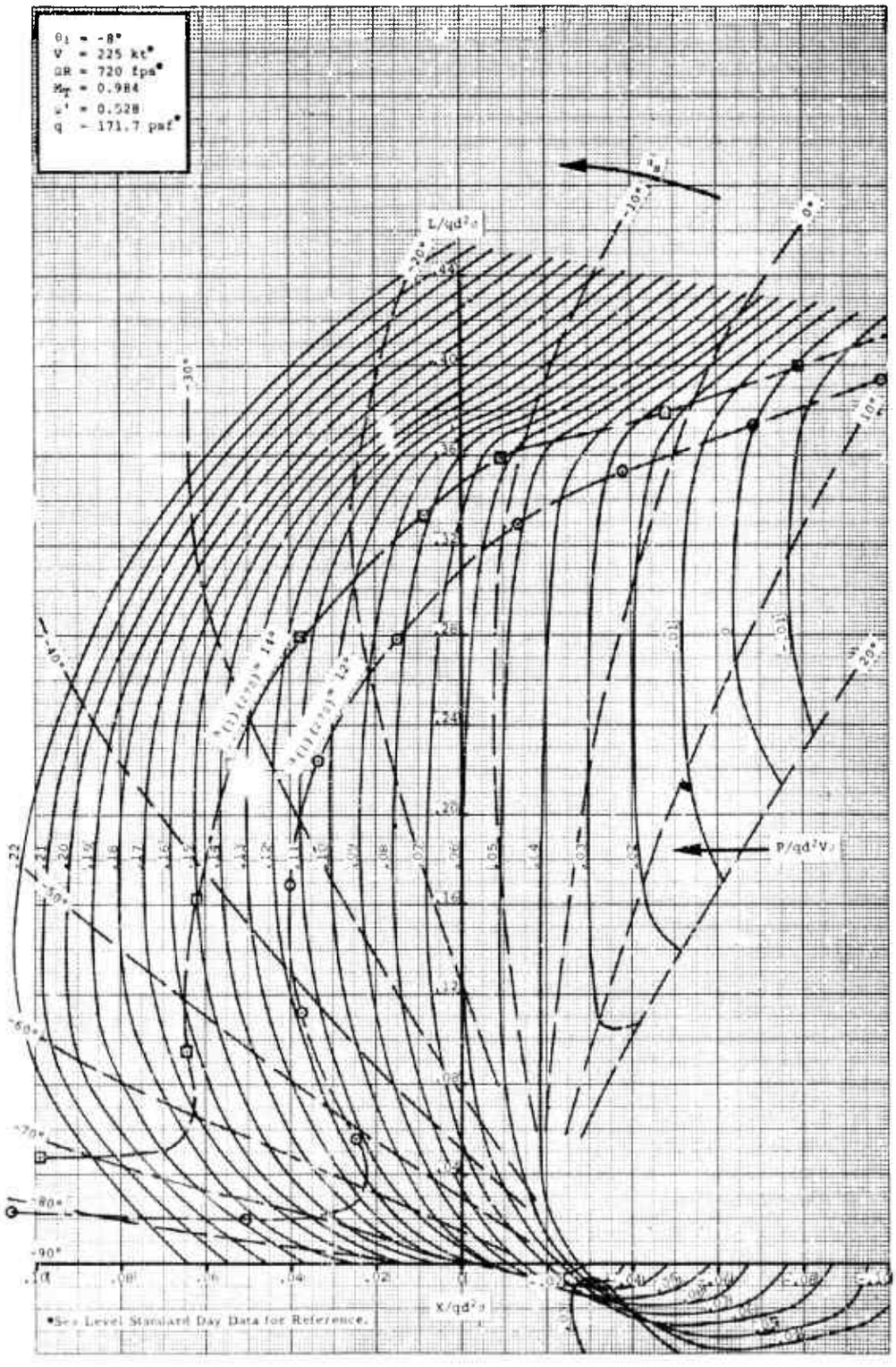
θ1 = -8°
V = 225 kt*
QR = 720 fps*
MT = 0.984
ω' = 0.528
q = 171.7 psf*
L/qd²
P/qd²
X/qd²
*Sea Level Standard Day Data for Reference.

Figure 57.

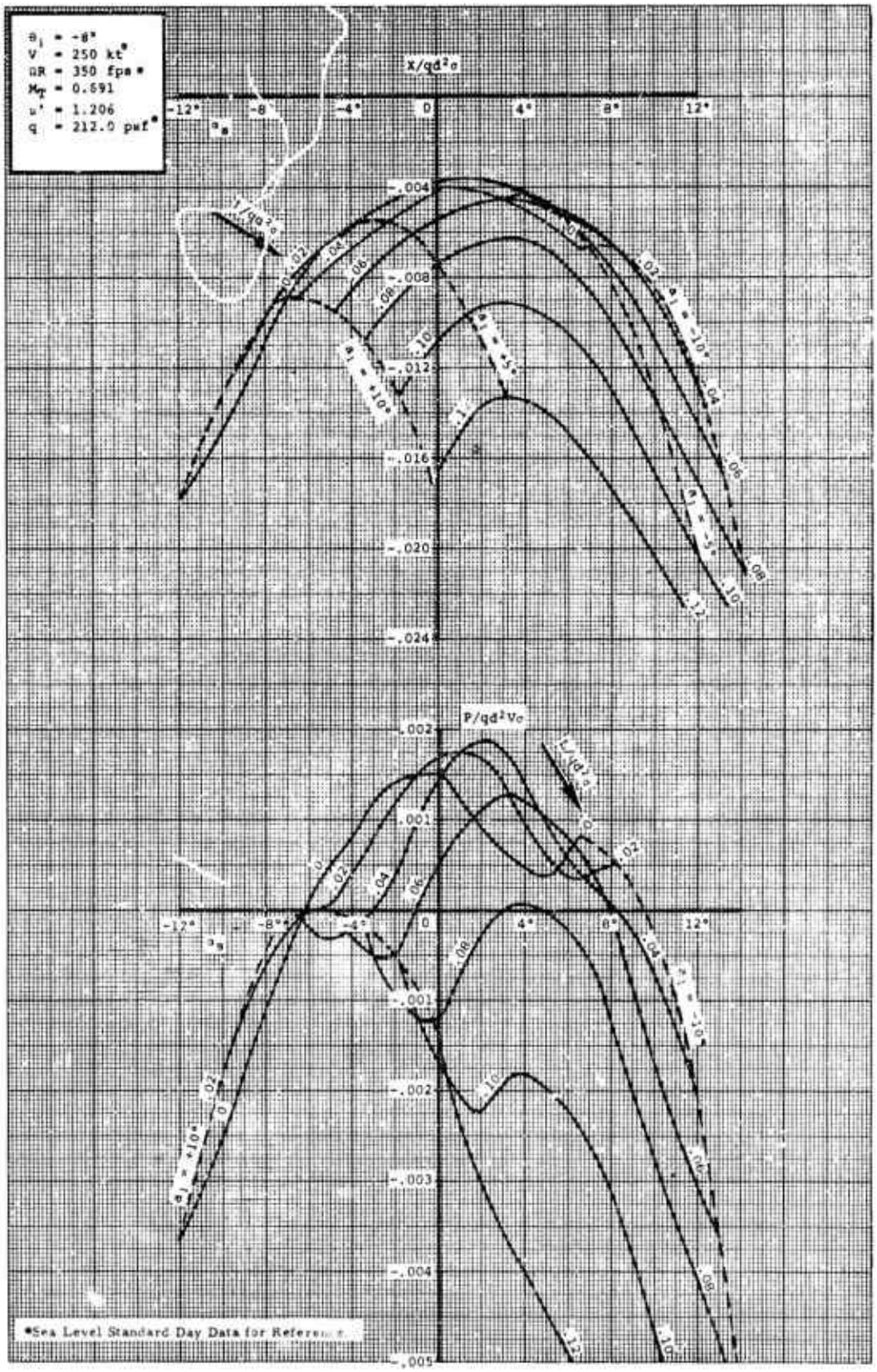
θ_1 = -8°
V = 250 kt*
RR = 350 fps*
M_T = 0.691
u' = 1.206
q = 212.0 psf*
X/qd²σ
T/qd²σ
P/qd²Vσ
L/qd²σ
α_s
*Sea Level Standard Day Data for Reference

Figure 58.

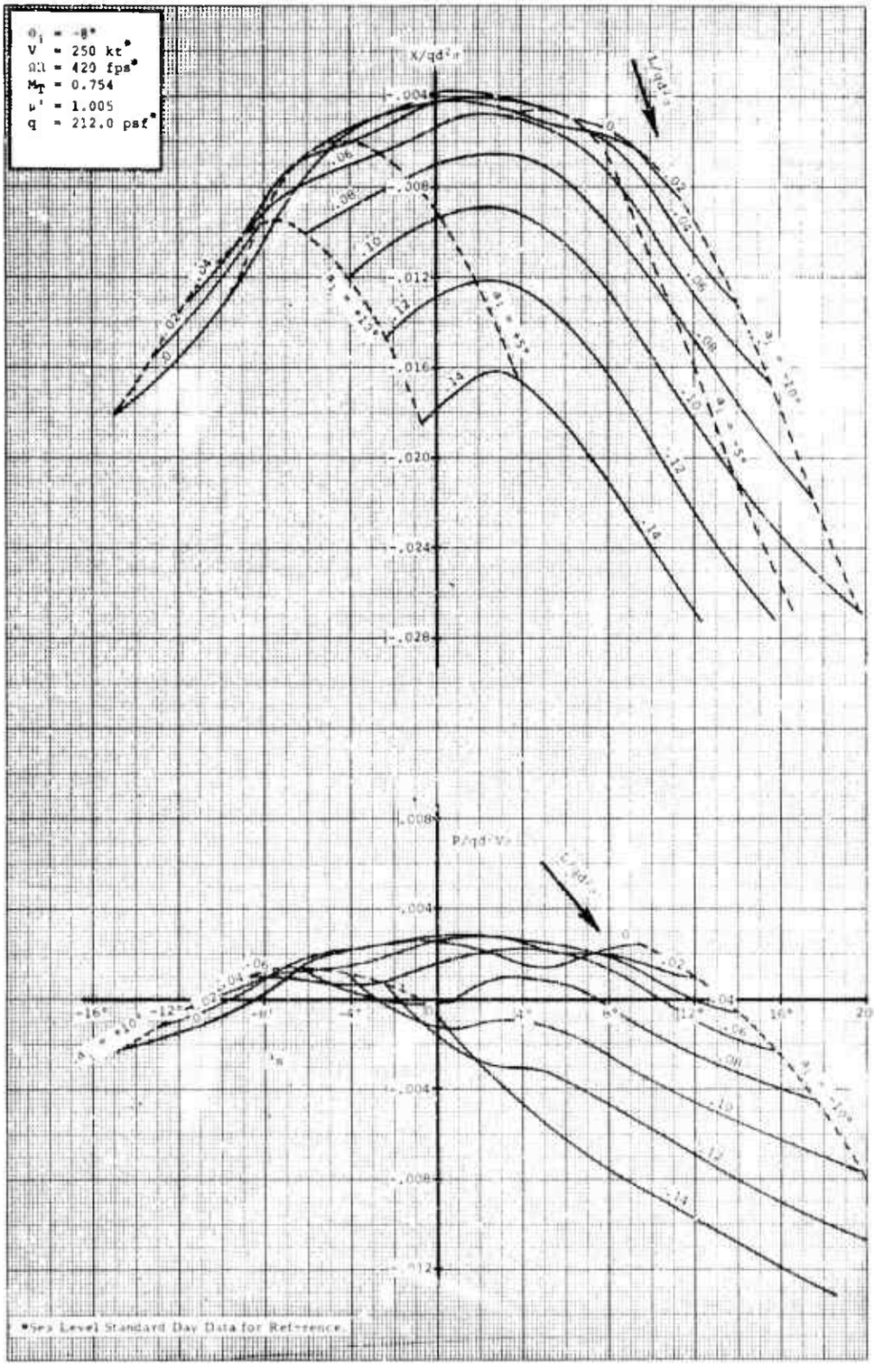
θ_i = -8°
V = 250 kt*
Ω = 420 fps*
M_T = 0.754
μ' = 1.005
q = 212.0 psf*
X/qd²σ
L/qd²σ
P/qd²V²
*Sea Level Standard Day Data for Reference

Figure 59.

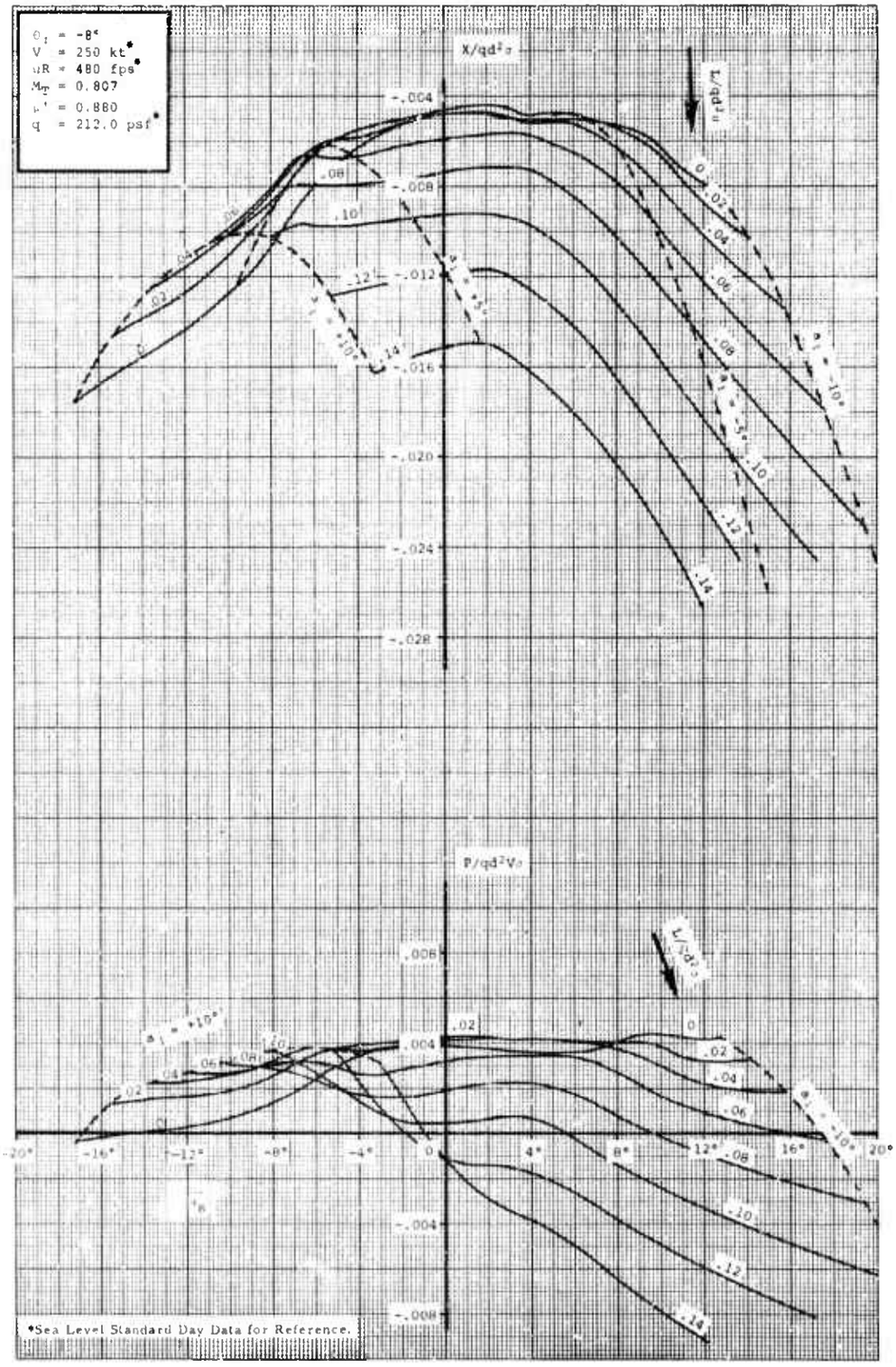
i_t = -8°
V = 250 kt*
uR = 480 fps*
M_T = 0.807
μ' = 0.880
q = 212.0 psf*
X/qd²σ
L/qd²σ
P/qd²Vσ
L/Vd²σ
*Sea Level Standard Day Data for Reference.

Figure 60.

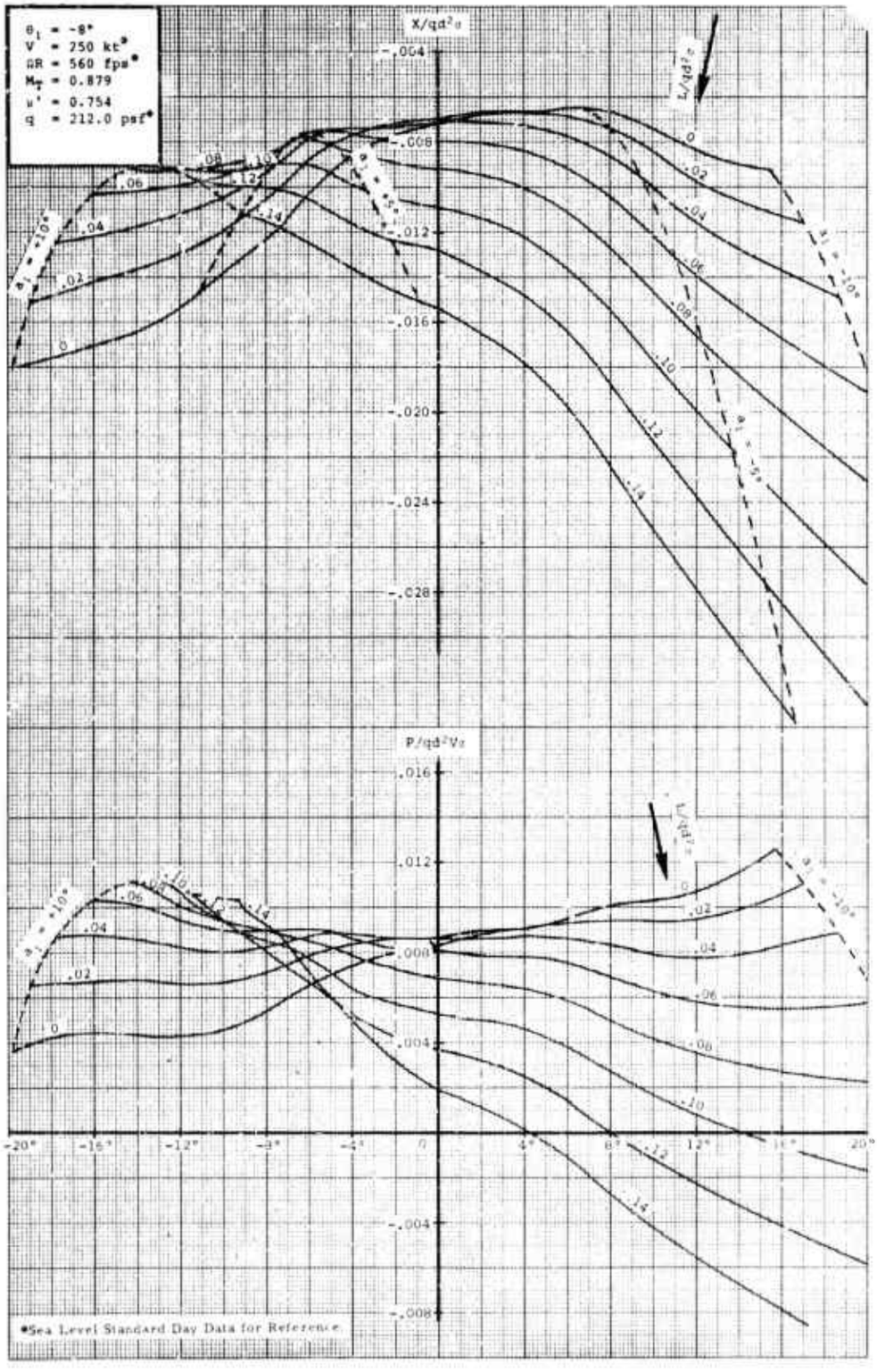
θ_i = -8°
V = 250 kt*
RR = 560 fpa*
M_∞ = 0.879
u' = 0.754
q = 212.0 psf*
X/qd²σ
L/qd²σ
P/qd²Vσ
a_i = +10°
a_i = -5°
a_i = -10°
-.004
-.008
-.012
-.016
-.020
-.024
-.028
.016
.012
.008
.004
-.004
-.008
-20°
-16°
-12°
-8°
-4°
0
4°
8°
12°
16°
20°
*Sea Level Standard Day Data for Reference

Figure 61.

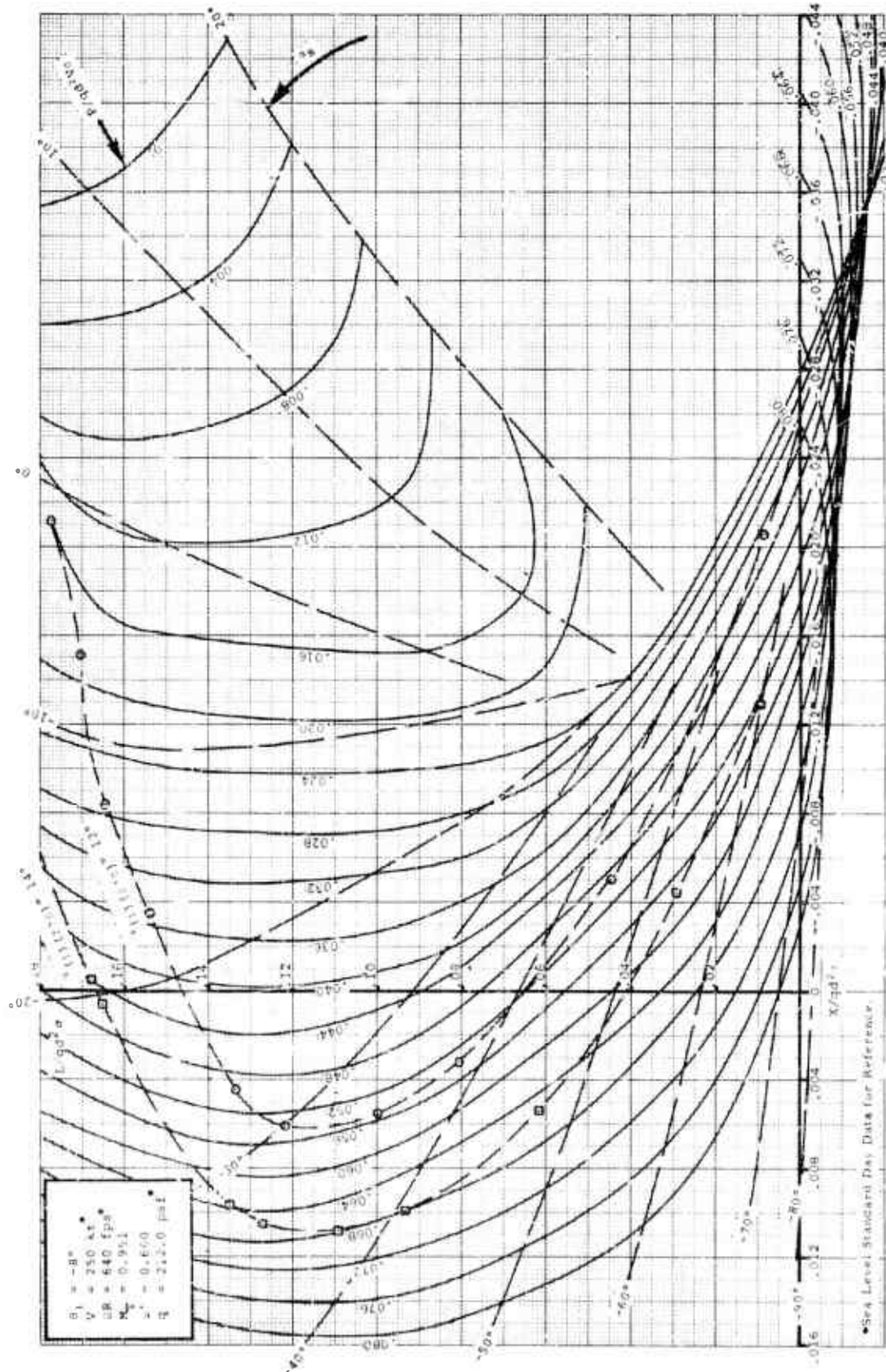

Figure 62.

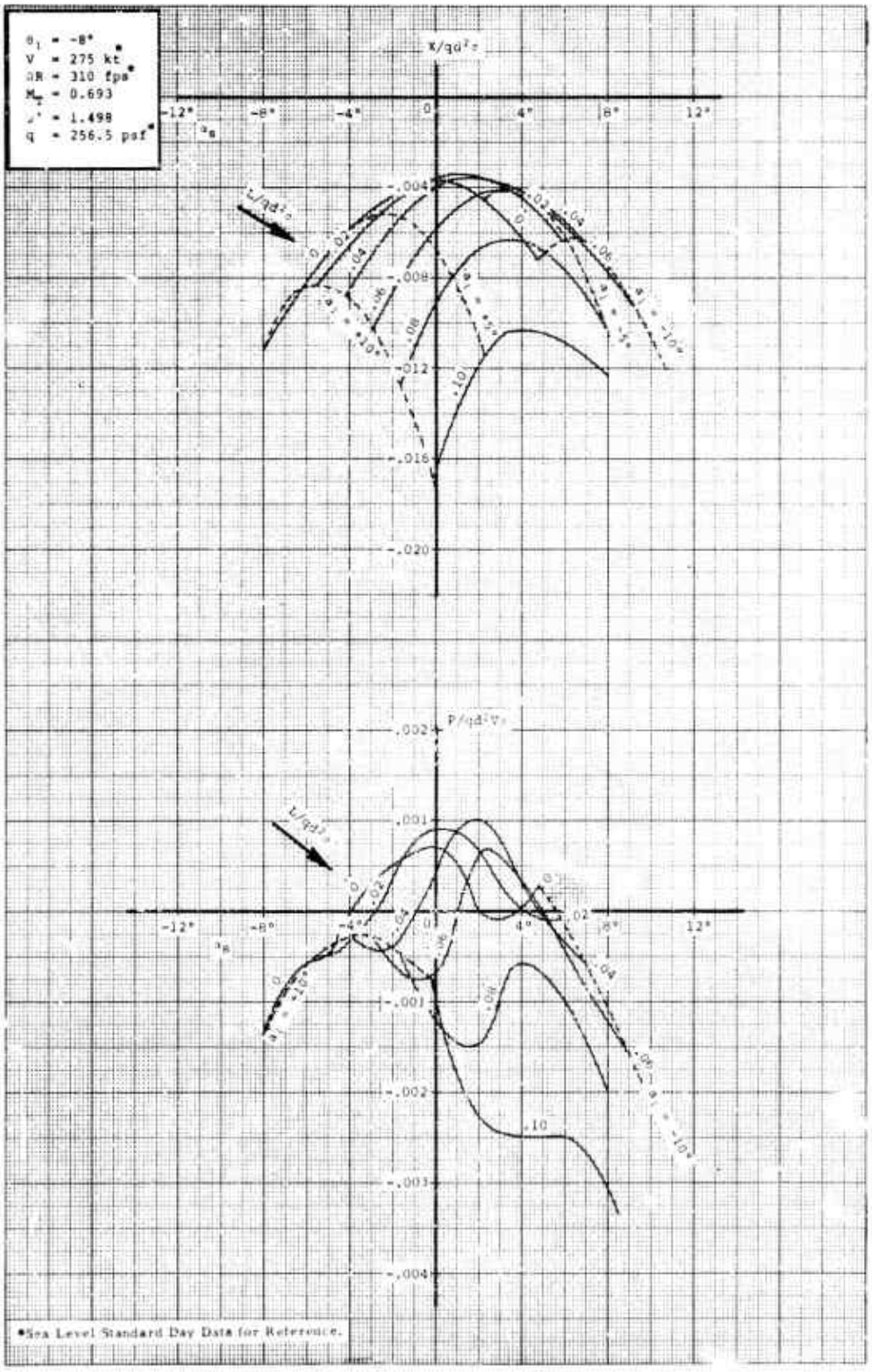
θ_1 = -8°
V = 275 kt
ΩR = 310 fps
M_T = 0.693
σ' = 1.498
q = 256.5 psf
X/qd²σ
L/qd²σ
P/qd²Vσ
α_s
-12°
-8°
-4°
0
4°
8°
12°
•Sea Level Standard Day Data for Reference.

Figure 63.

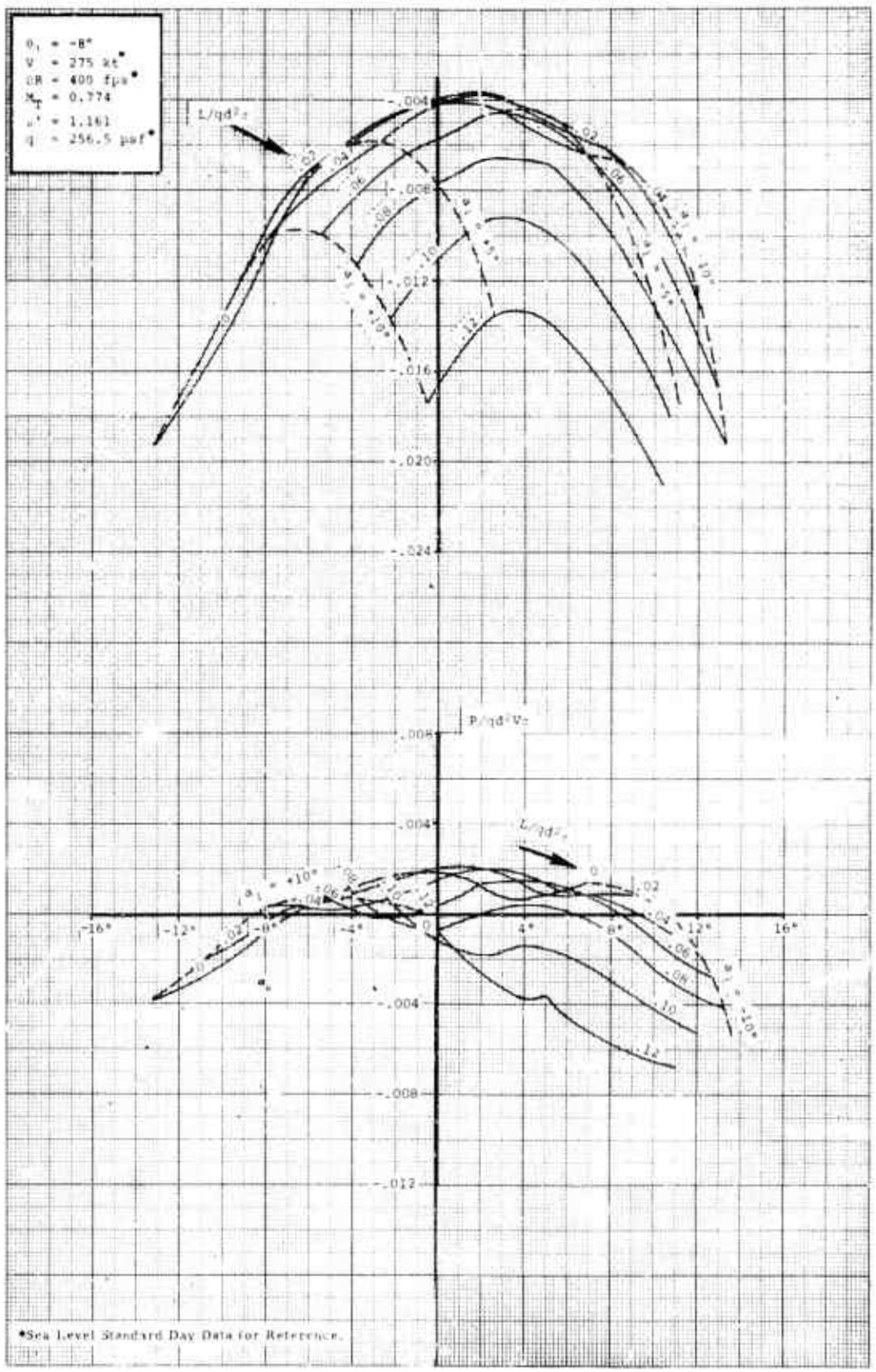
i_t = -8°
V = 275 kt*
aR = 400 fps*
M_T = 0.774
ρ' = 1.161
q = 256.5 psf*
L/qd²=
P/qd²V=
*Sea Level Standard Day Data for Reference.

Figure 64.

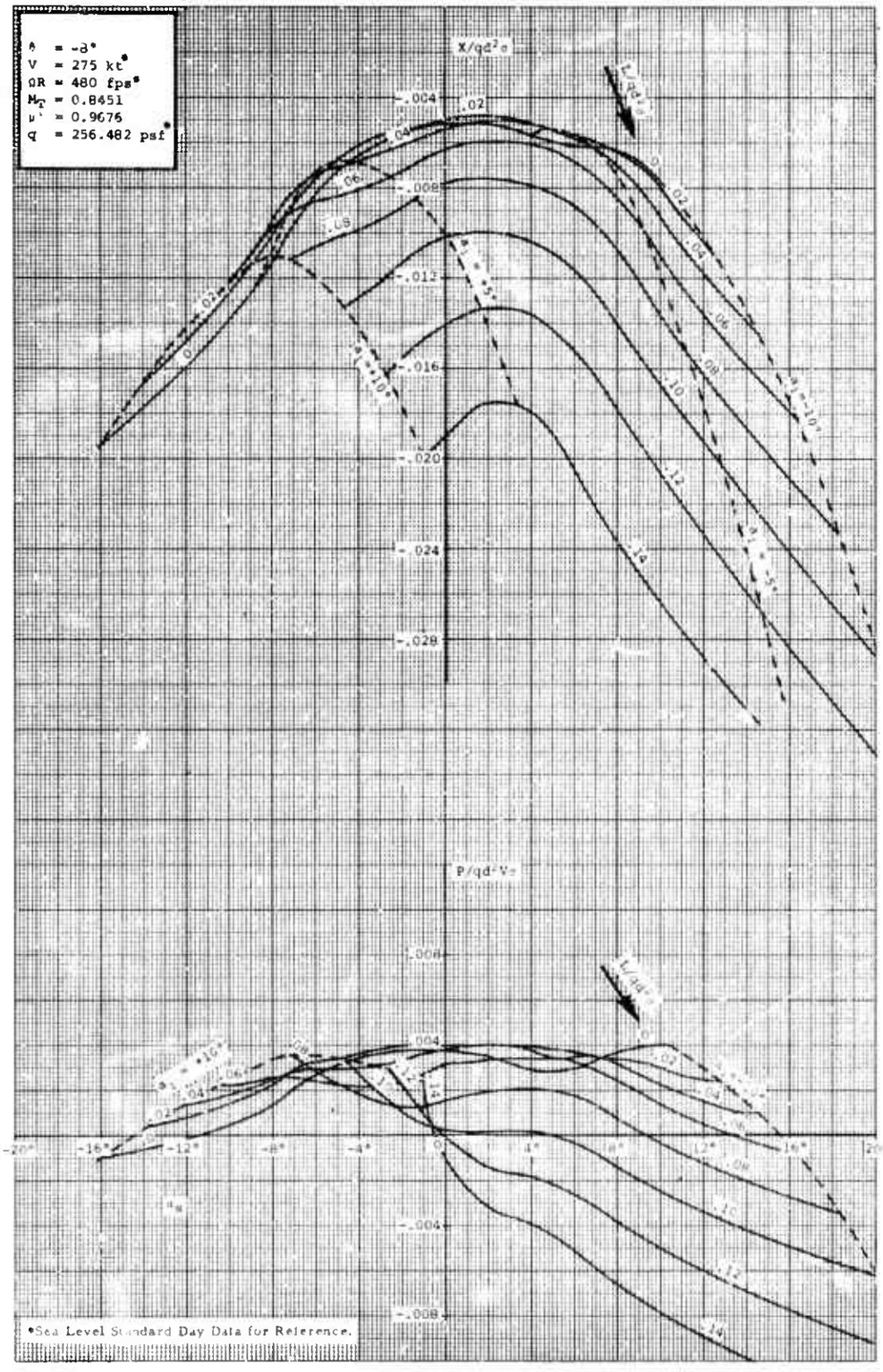
θ = -8°
V = 275 kt*
ΩR = 480 fps*
M_T = 0.8451
μ = 0.9676
q = 256.482 psf*
X/qd²σ
L/qd²σ
P/qd²V∞
*Sea Level Standard Day Data for Reference.

Figure 65.

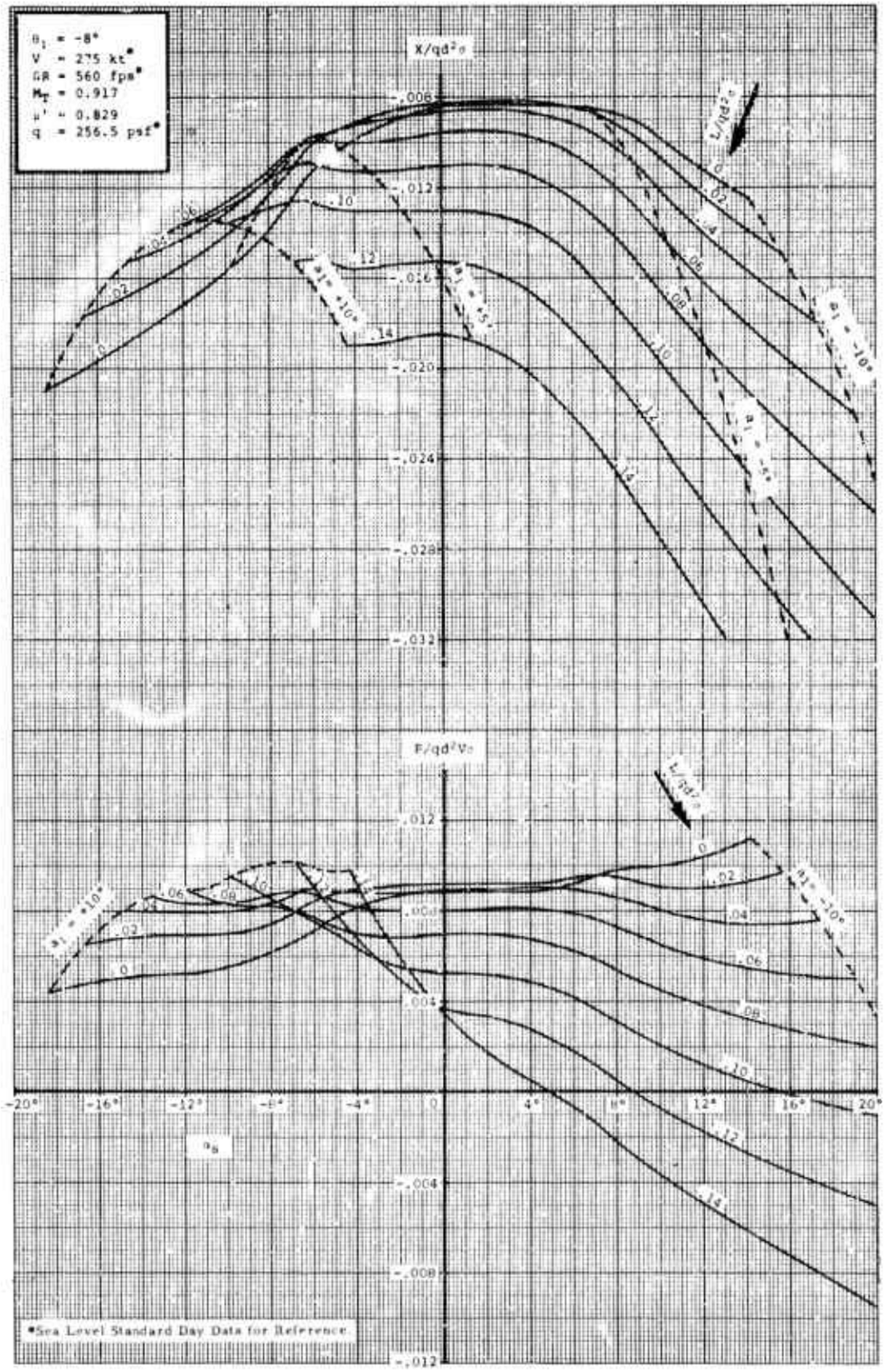
θ_i = -8°
V = 275 kt*
RR = 560 fpm*
M_T = 0.917
μ' = 0.829
q = 256.5 psf*
X/qd²σ
L/qd²σ
F/qd²Vσ
α_s
*Sea Level Standard Day Data for Reference

Figure 66.

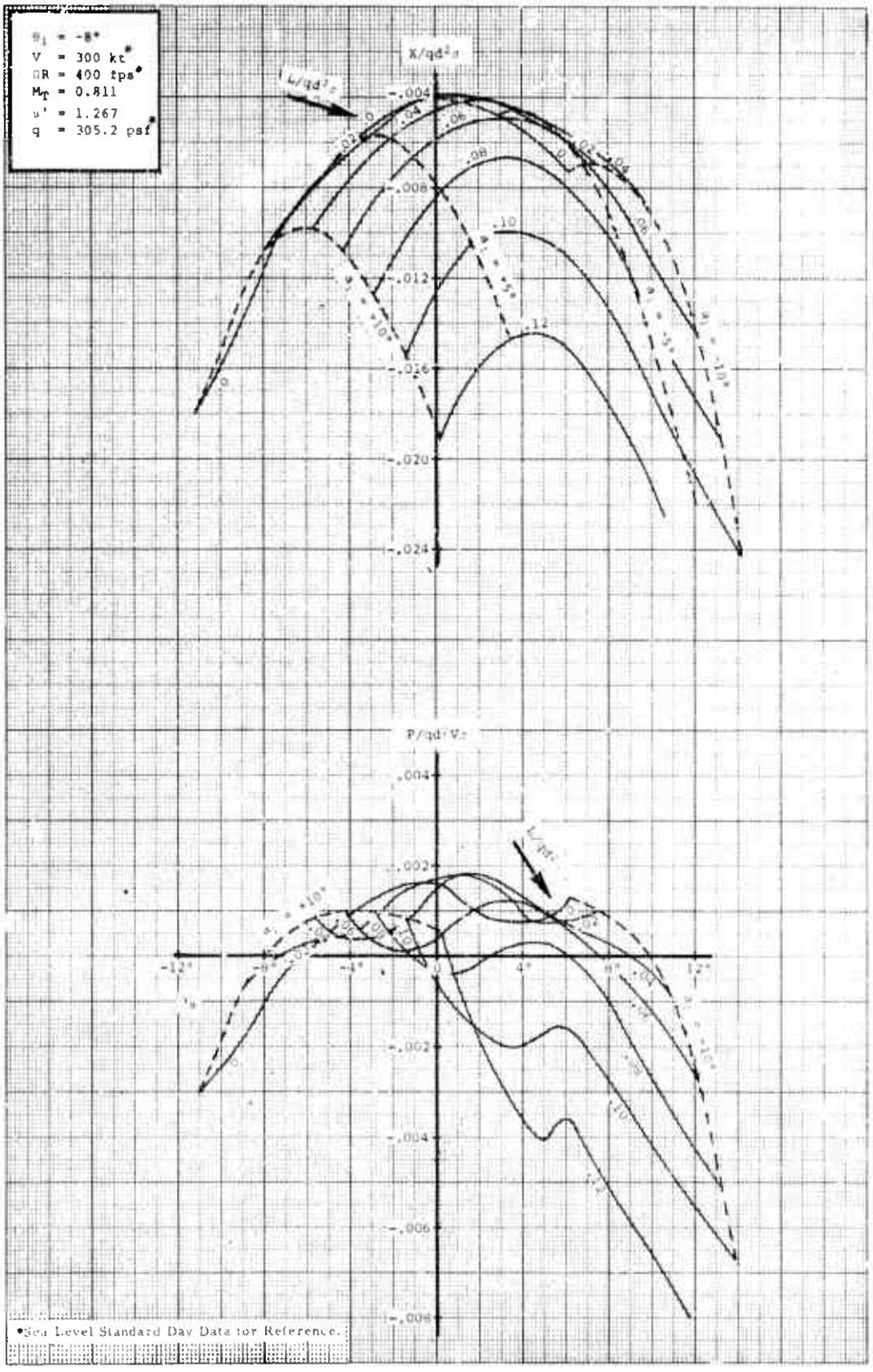
θ_1 = -8°
V = 300 kt*
ΩR = 400 fps*
M_T = 0.811
μ' = 1.267
q = 305.2 psf*
K/qd²σ
L/qd²σ
P/qdrV₂
L/qd
*Sea Level Standard Day Data for Reference.

Figure 67.

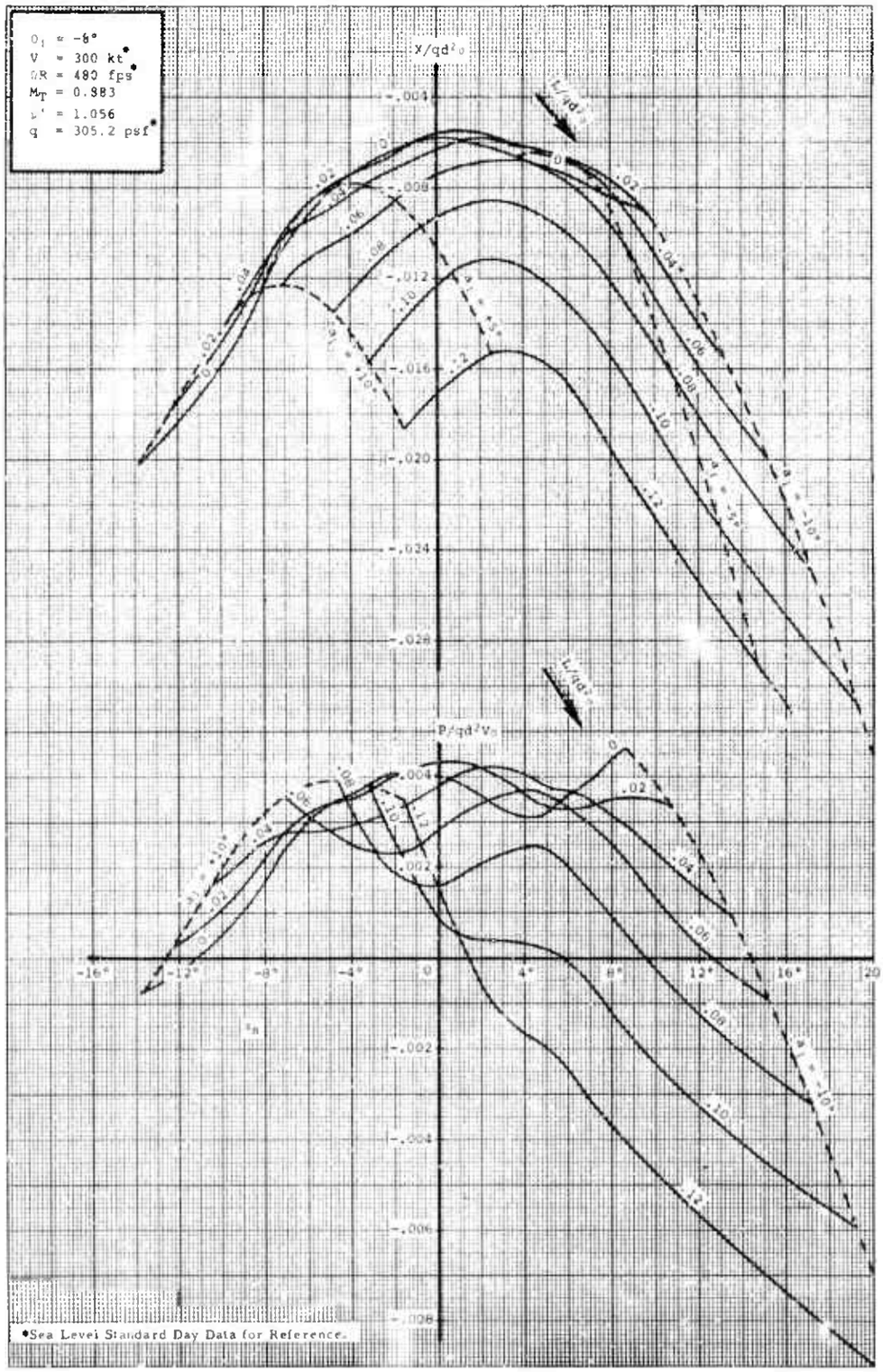
α_i = -6°
V = 300 kt*
ΩR = 480 fps*
M_T = 0.983
μ = 1.056
q = 305.2 psf*
X/qd²
L/qd²
P/qd²
-.004
-.008
-.012
-.016
-.020
-.024
-.028
.004
.002
-.002
-.004
-.006
-.008
-16°
-12°
-8°
-4°
0
4°
8°
12°
16°
20°
α_R
*Sea Level Standard Day Data for Reference.

Figure 68.

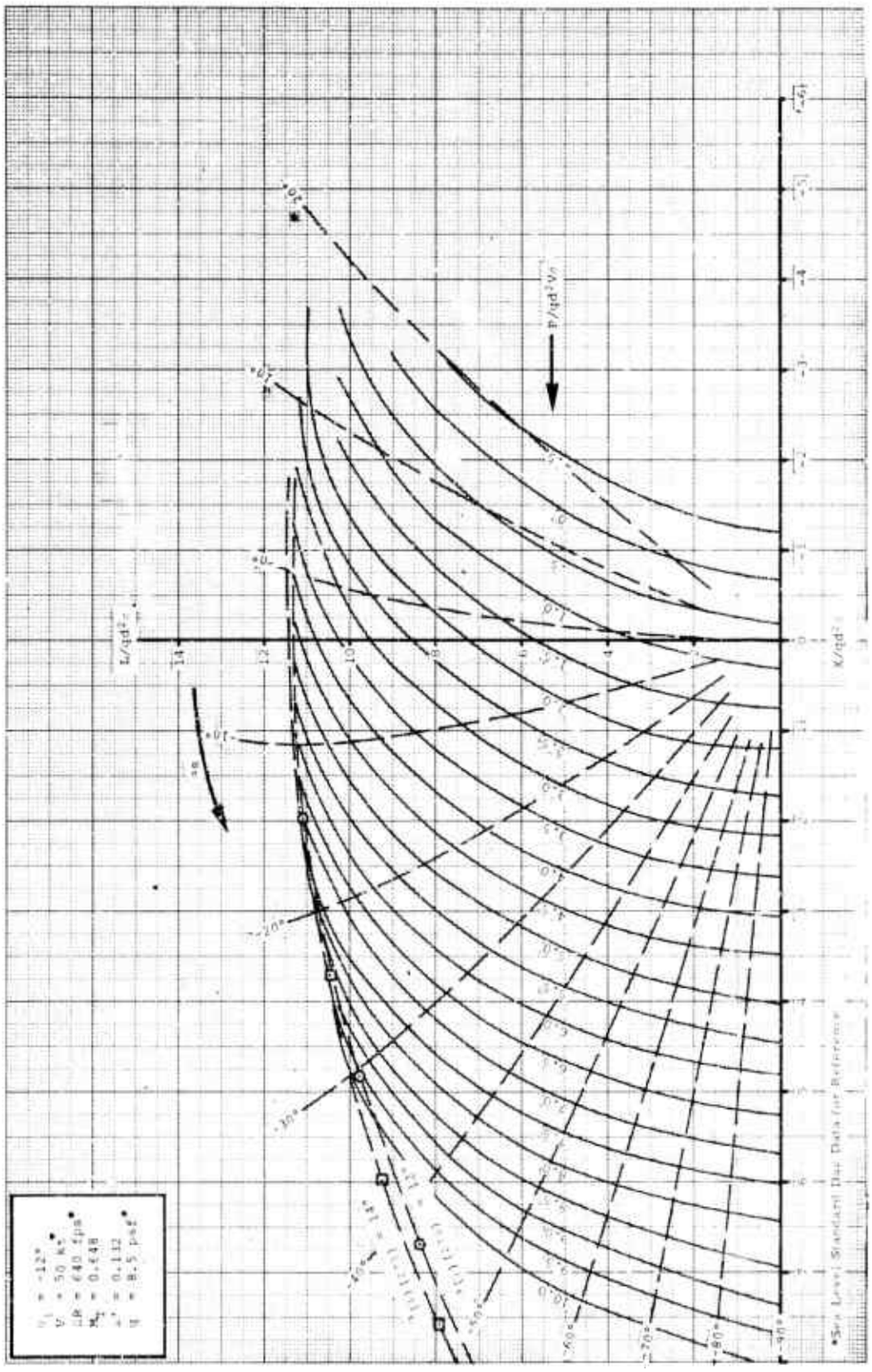

Figure 69.

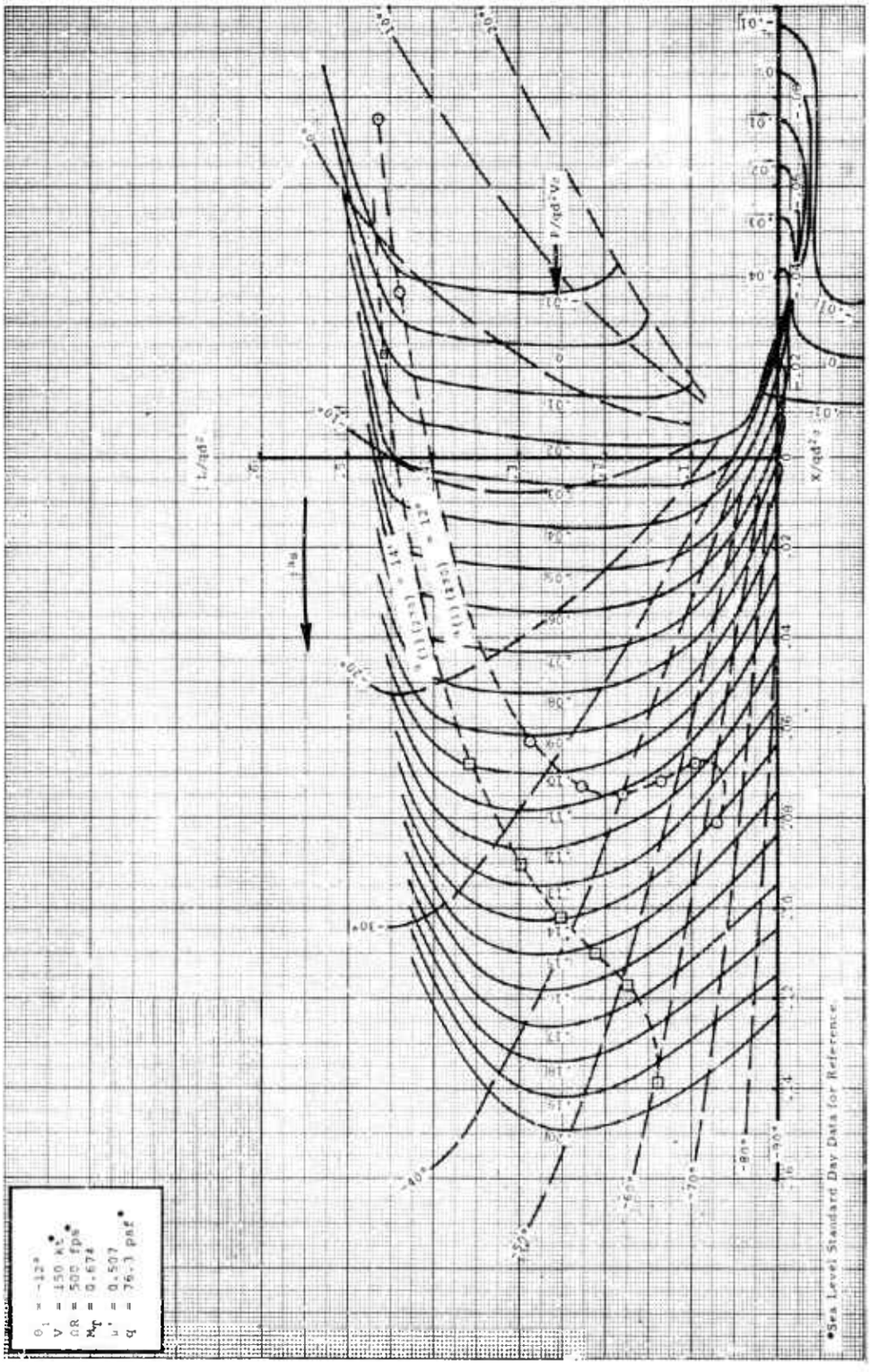
θ_i = -12°
V = 450 KE*
QR = 500 fps*
M_∞ = 0.674
u' = 0.507
q = 76.3 psf*
*Sea Level Standard Day Data for Reference

Figure 70.

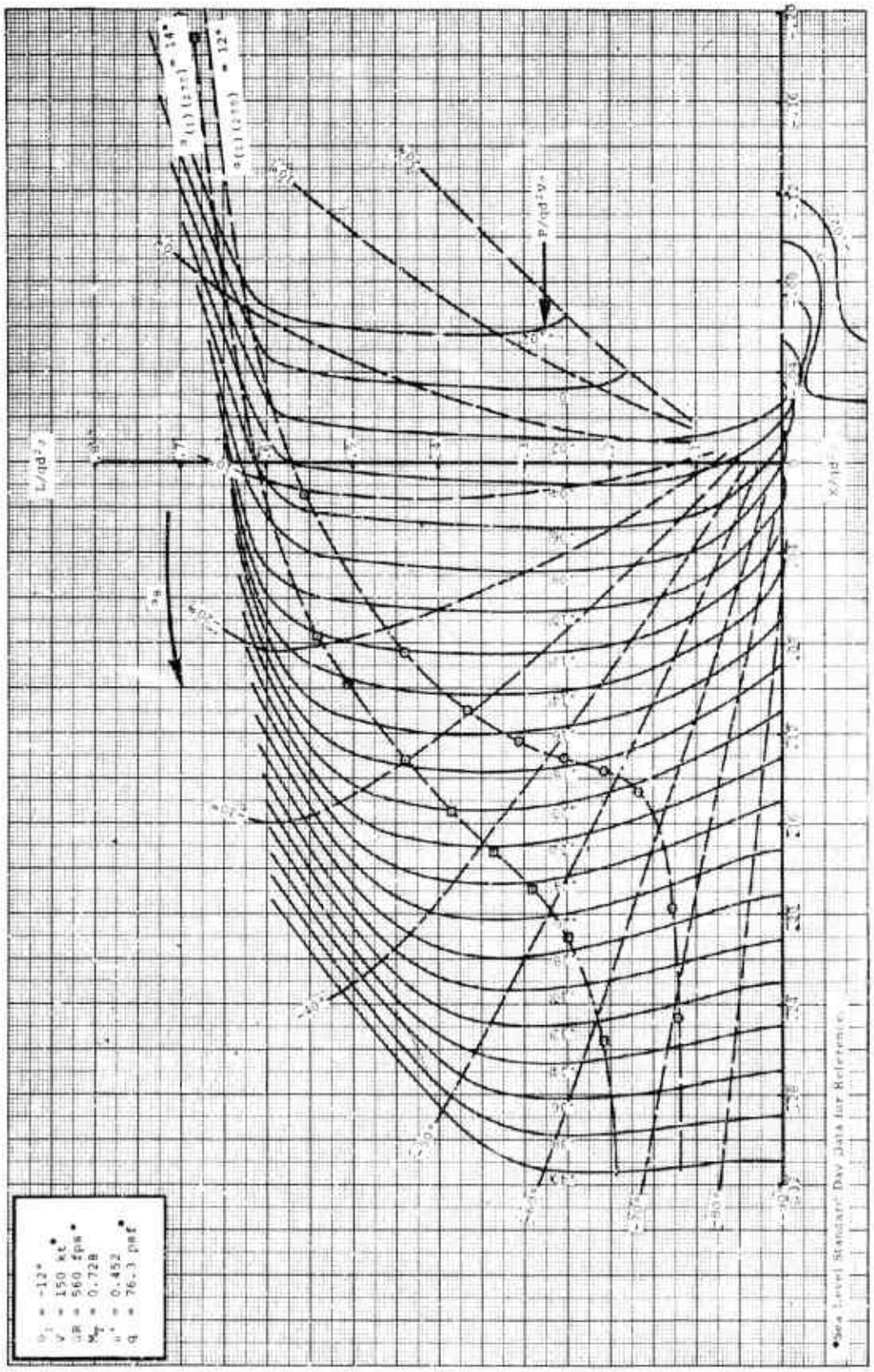
α = -12°
V = 150 kt*
R = 560 fps*
M = 0.728
μ = 0.452
q = 76.3 psf*
L/qd²
P/qd²
X/d
*Sea Level Standard Day Data for Reference

Figure 71.

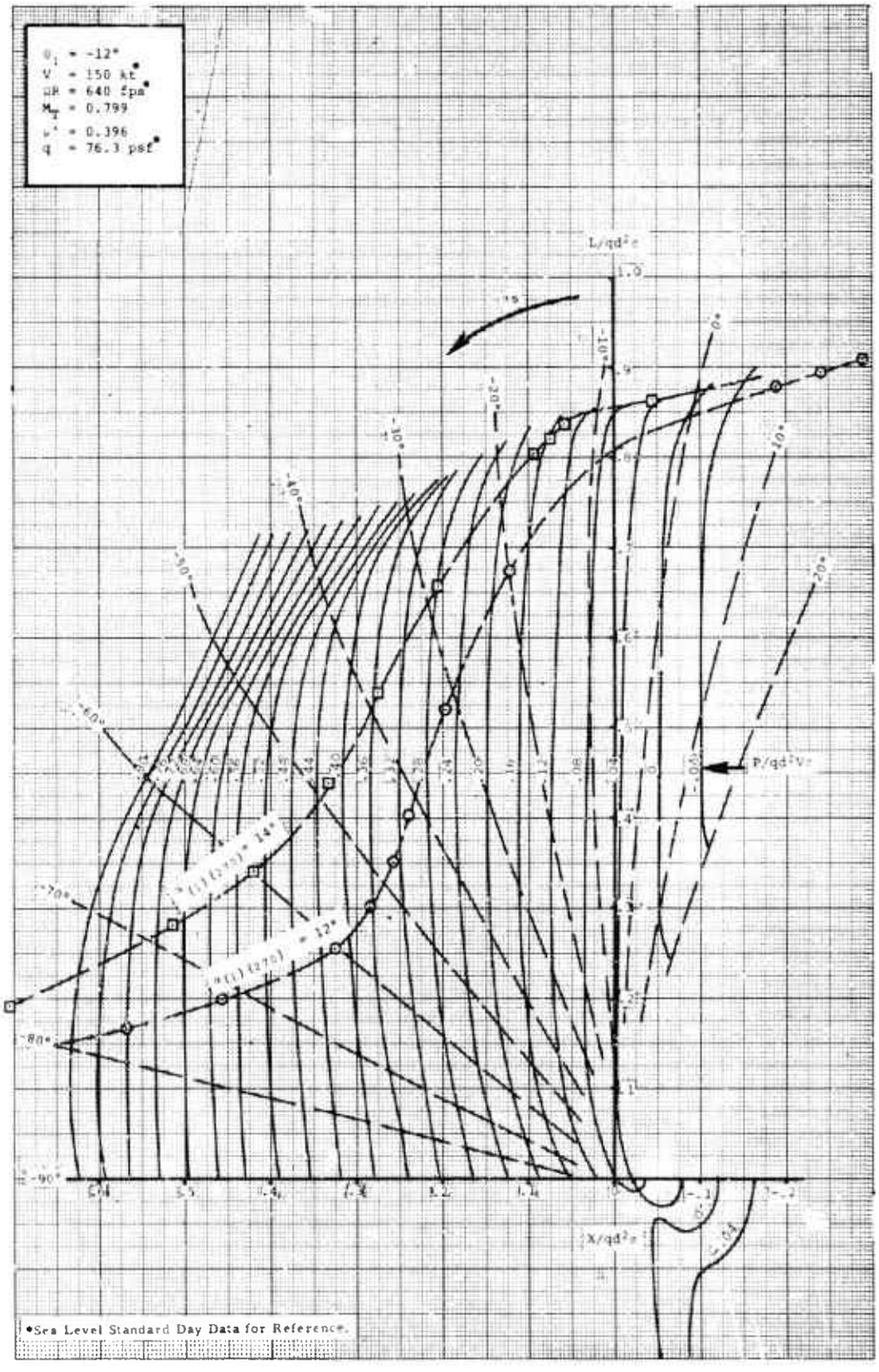
θ_i = -12°
V = 150 kt*
ΩR = 640 fps*
M_T = 0.799
μ^2 = 0.396
q = 76.3 psf*
L/qd²
P/qd²
X/qd²
*Sea Level Standard Day Data for Reference.

Figure 72.

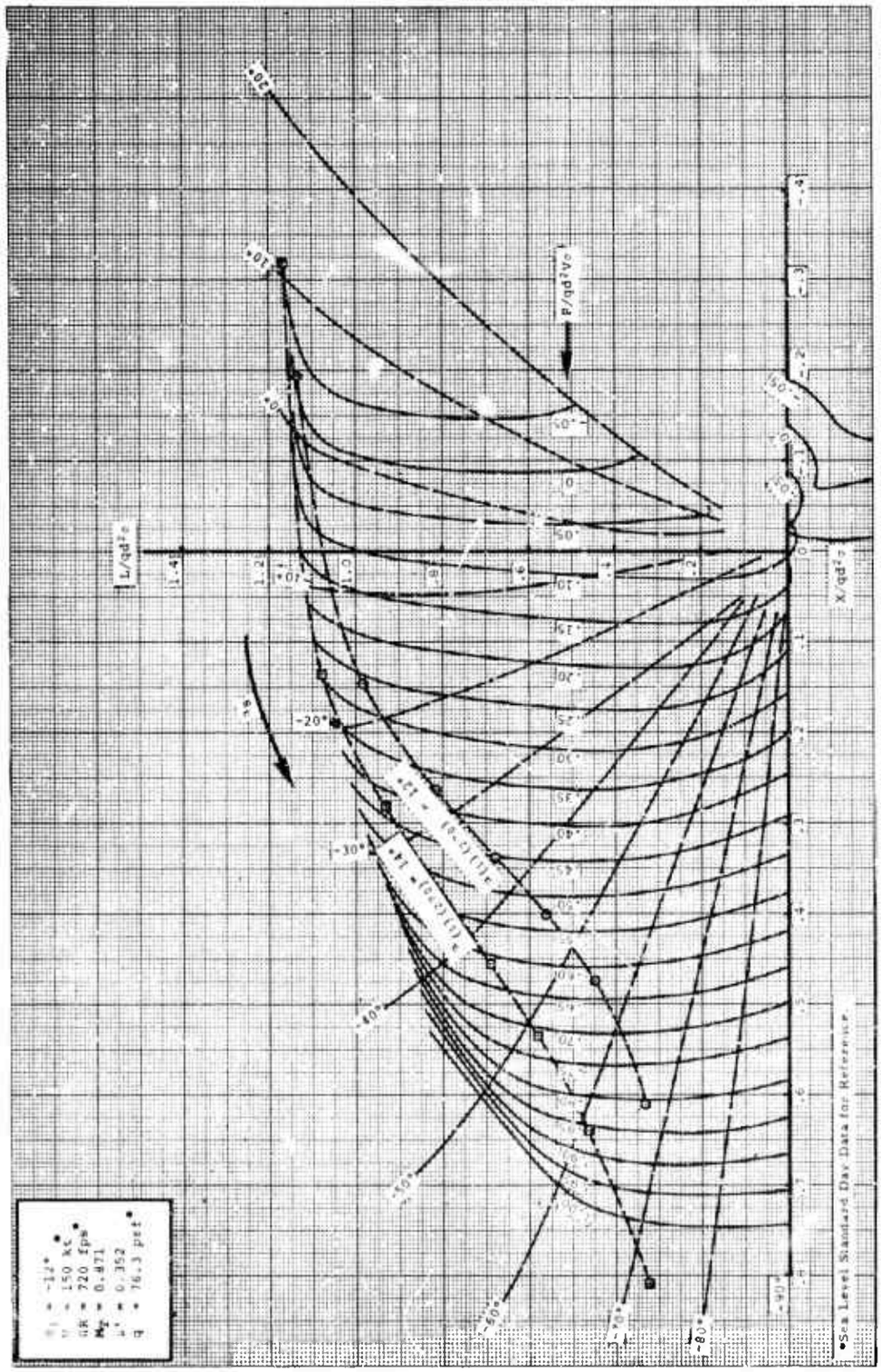
L/qd²s
D/qd²s
X/qd²s
*Sea Level Standard Day Data for Reference

Figure 73.

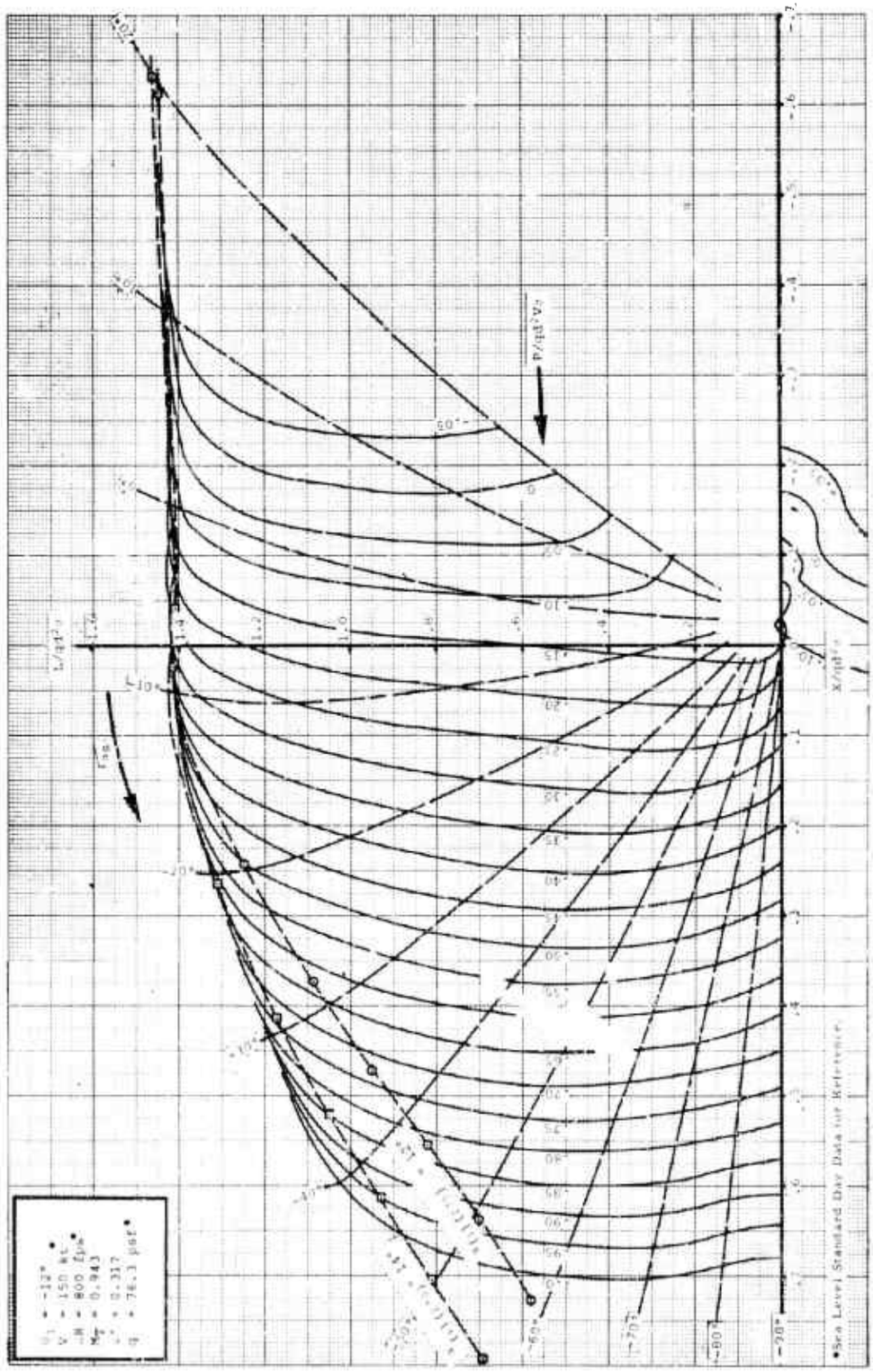

Figure 74.

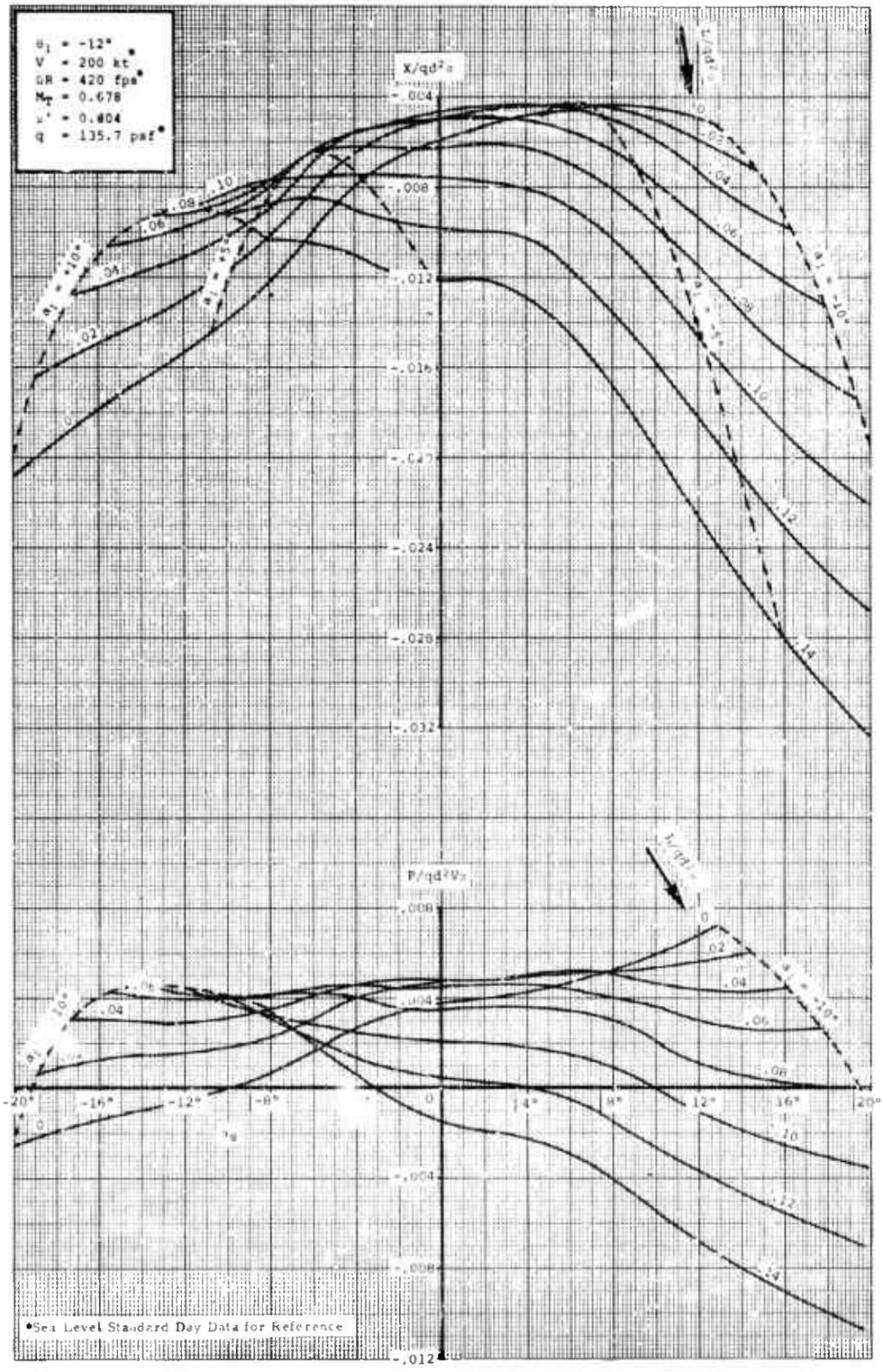
θ_1 = -12°
V = 200 kt
GR = 420 fps*
M_T = 0.678
μ' = 0.804
q = 135.7 psf*
X/qd²σ
P/qd²V₂
*Sea Level Standard Day Data for Reference

Figure 75.

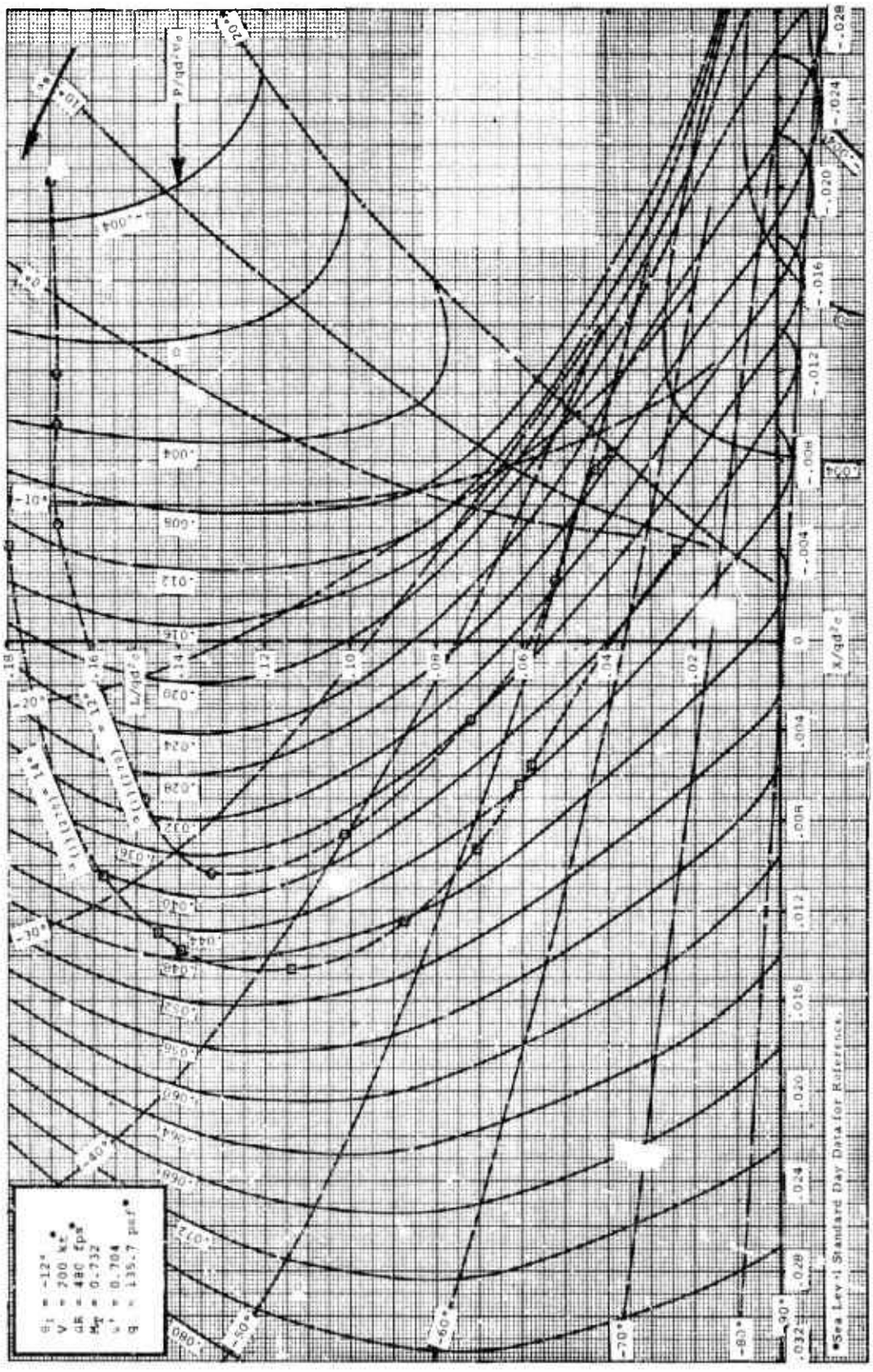
P/qd²e
L/qd²e
Y/qd²e
X/qd²e
Sea Level Standard Day Data for Reference.

Figure 76.

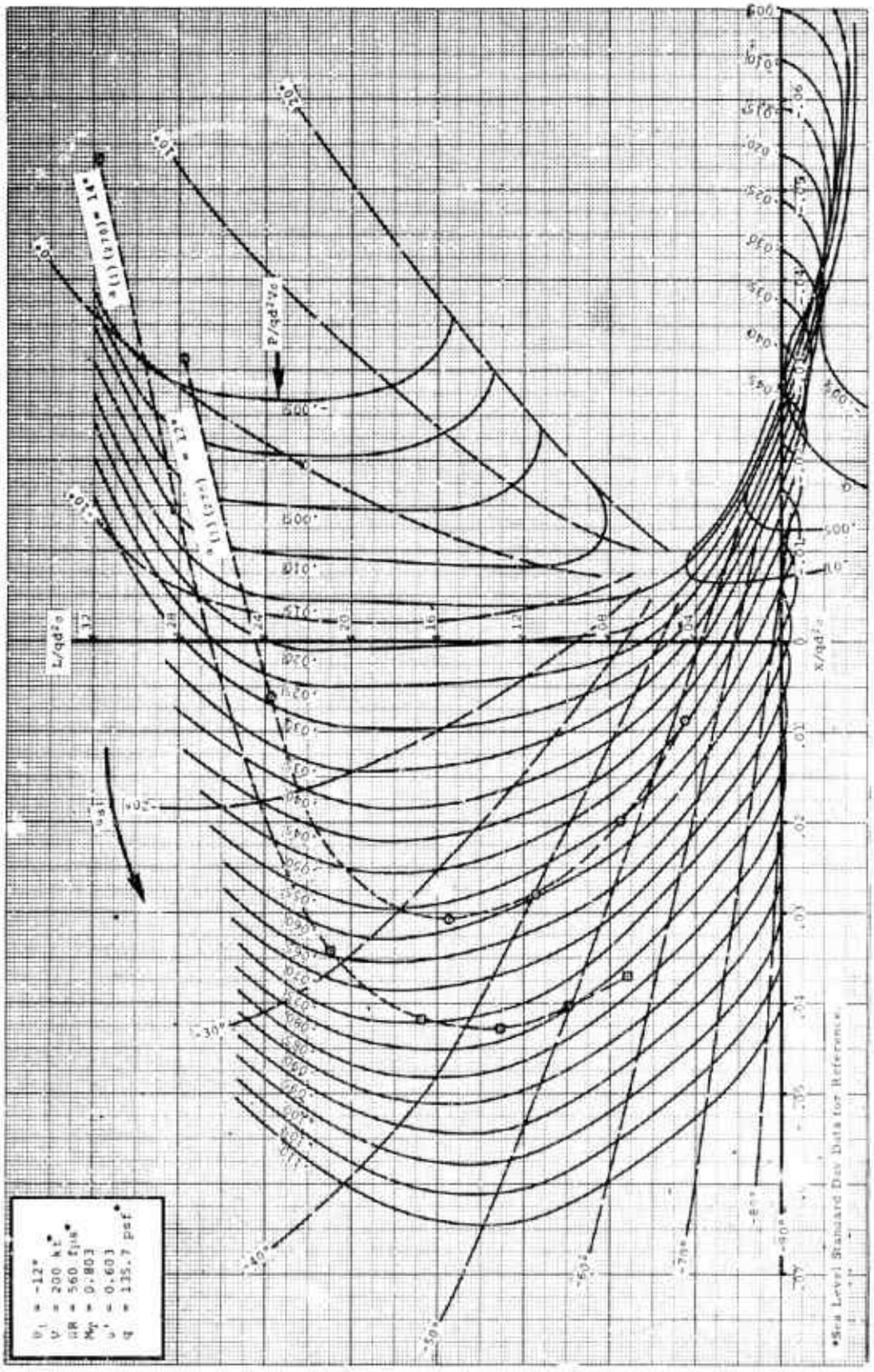

Figure 77.

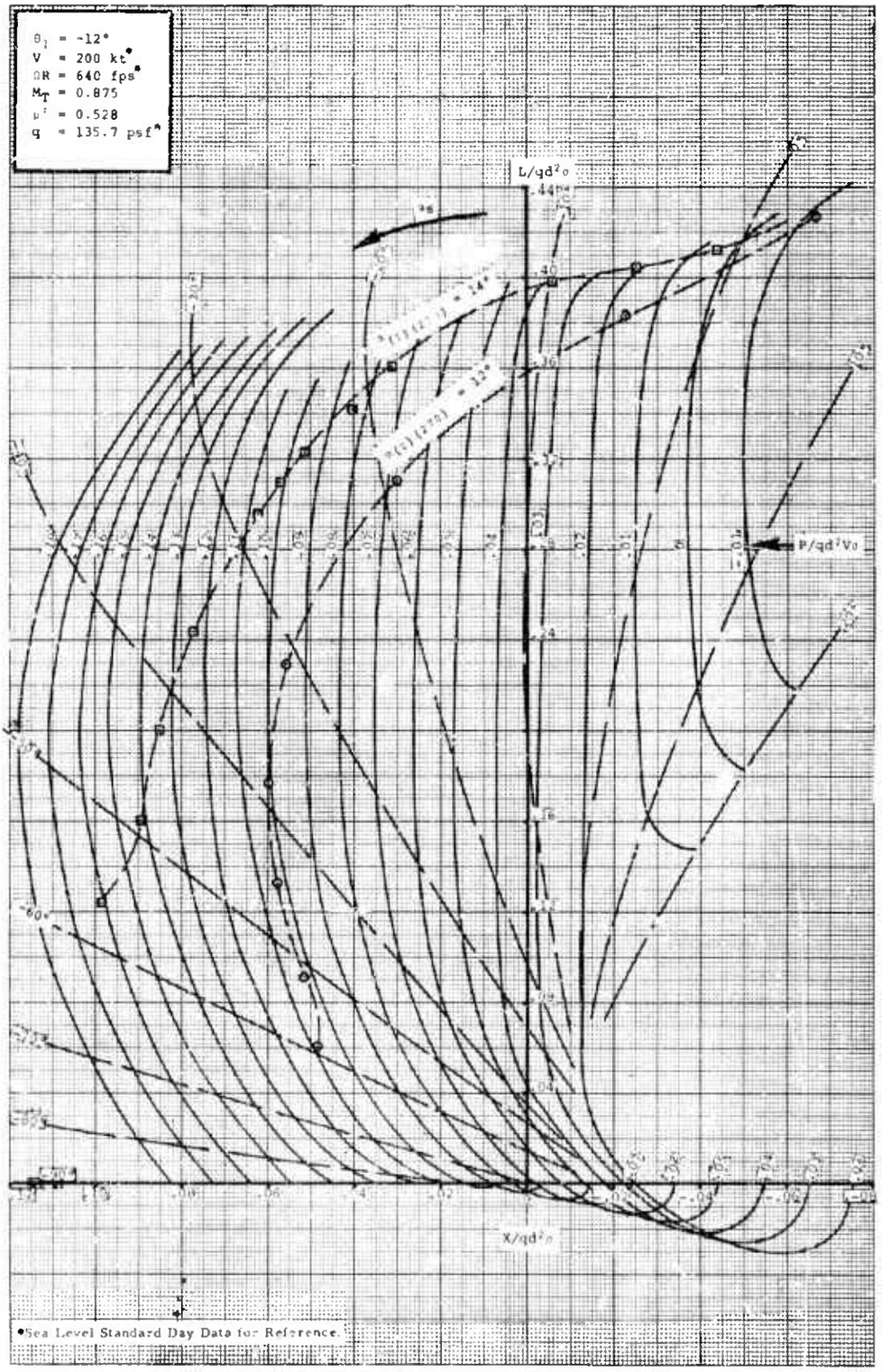
θ_i = -12°
V = 200 kt*
ΩR = 640 fps*
M_T = 0.875
μ^2 = 0.528
q = 135.7 psf*
L/qd^2_0
P/qd^2V_0
X/qd^2_0
*Sea Level Standard Day Data for Reference.

Figure 78.

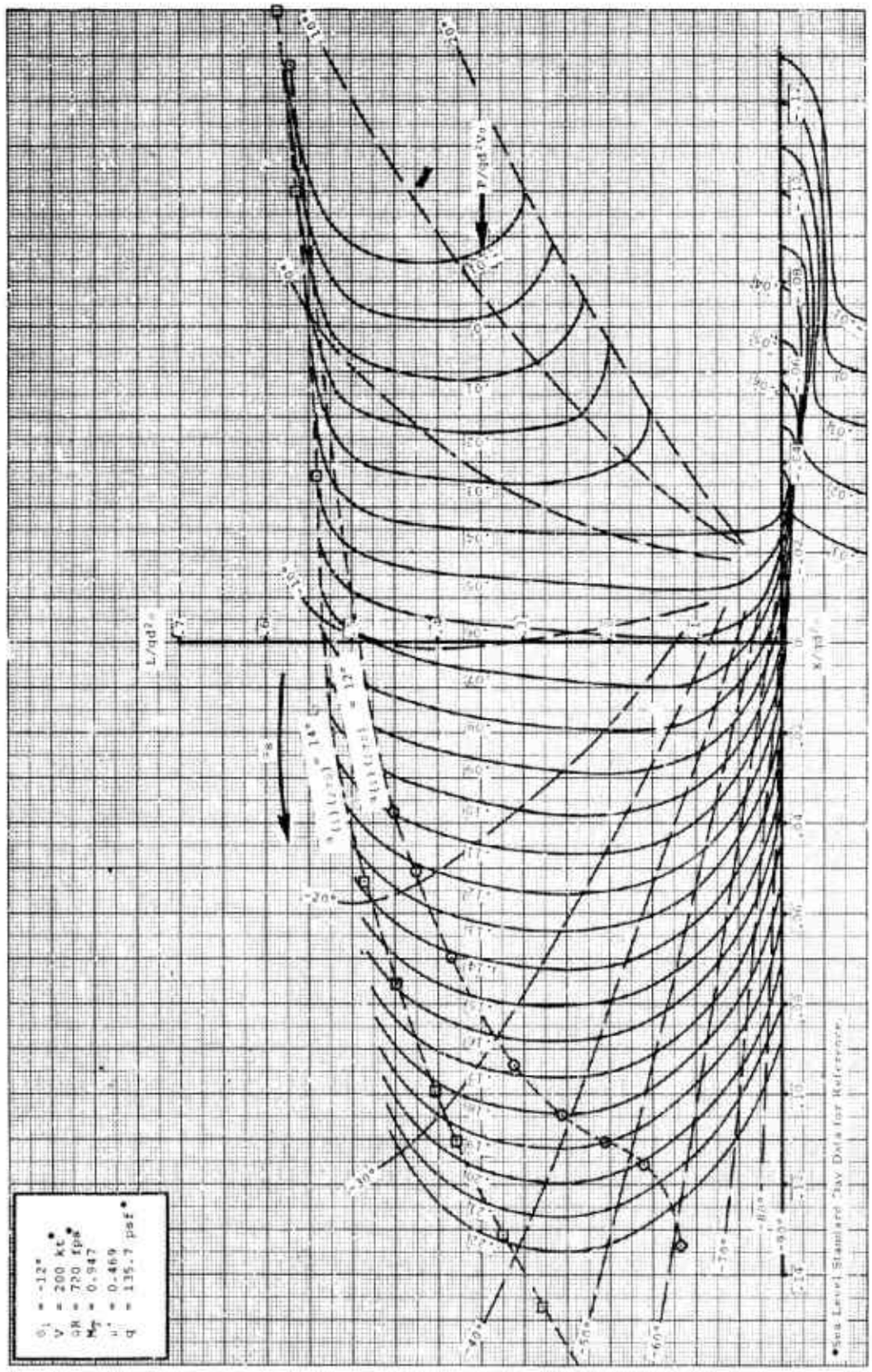
i_t = -12°
V = 200 kt*
aR = 720 fps*
M_{aR} = 0.947
μ' = 0.469
q = 135.7 psf*
L/qd²
P/qd²V₀
*Sea Level Standard Day Data for Reference

Figure 79.

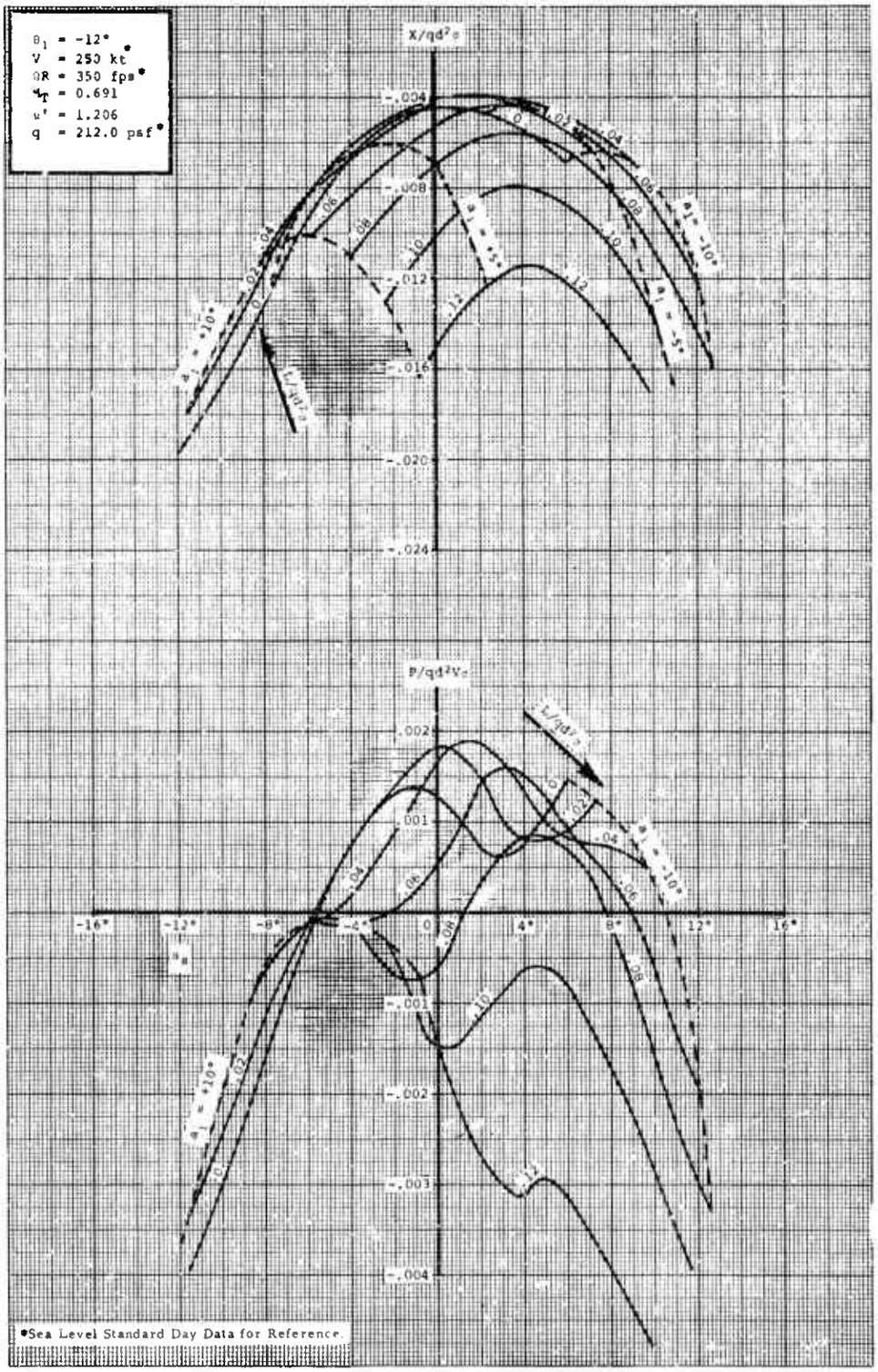
θ1 = -12°
V = 250 kt
ΩR = 350 fps
μT = 0.691
w' = 1.206
q = 212.0 psf
X/qd²σ
-.004
-.008
-.012
-.016
-.020
-.024
P/qd²Vσ
.002
.001
-.001
-.002
-.003
-.004
-16°
-12°
-8°
-4°
0
4°
8°
12°
16°
α1 = +10°
α1 = +5°
α1 = -5°
α1 = -10°
L/qd²σ
*Sea Level Standard Day Data for Reference.

Figure 80.

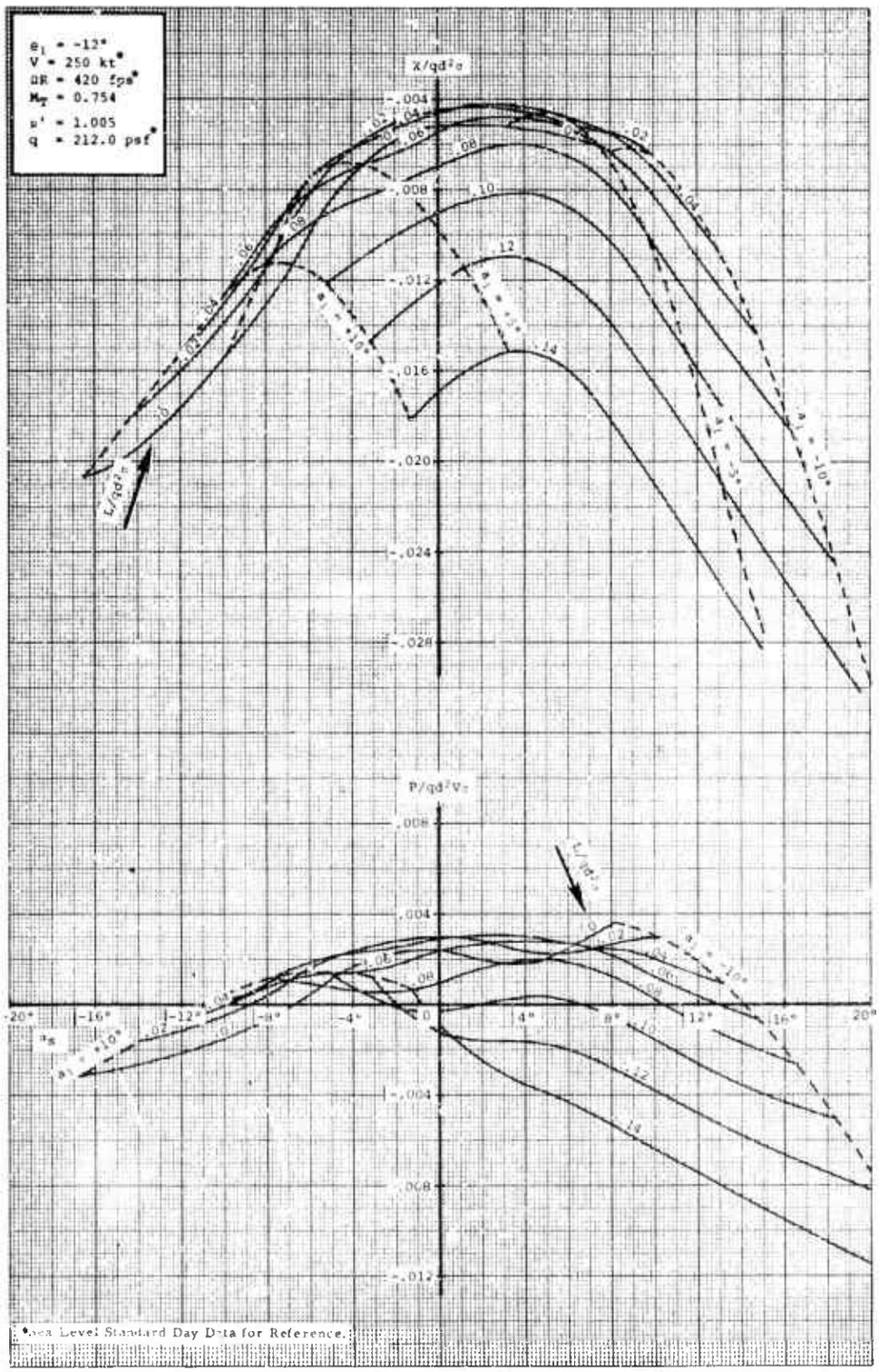
θ_l = -12°
V = 250 kt*
dR = 420 fps*
M_T = 0.754
σ' = 1.005
q = 212.0 psf*
X/qd²σ
-.004
-.008
-.012
-.016
-.020
-.024
-.028
L/qd²σ
P/qd²σ
.008
.004
-.004
-.008
-.012
-20°
-16°
-12°
-8°
-4°
0
4°
8°
12°
16°
20°
α_s
*Sea Level Standard Day Data for Reference.

Figure 81.

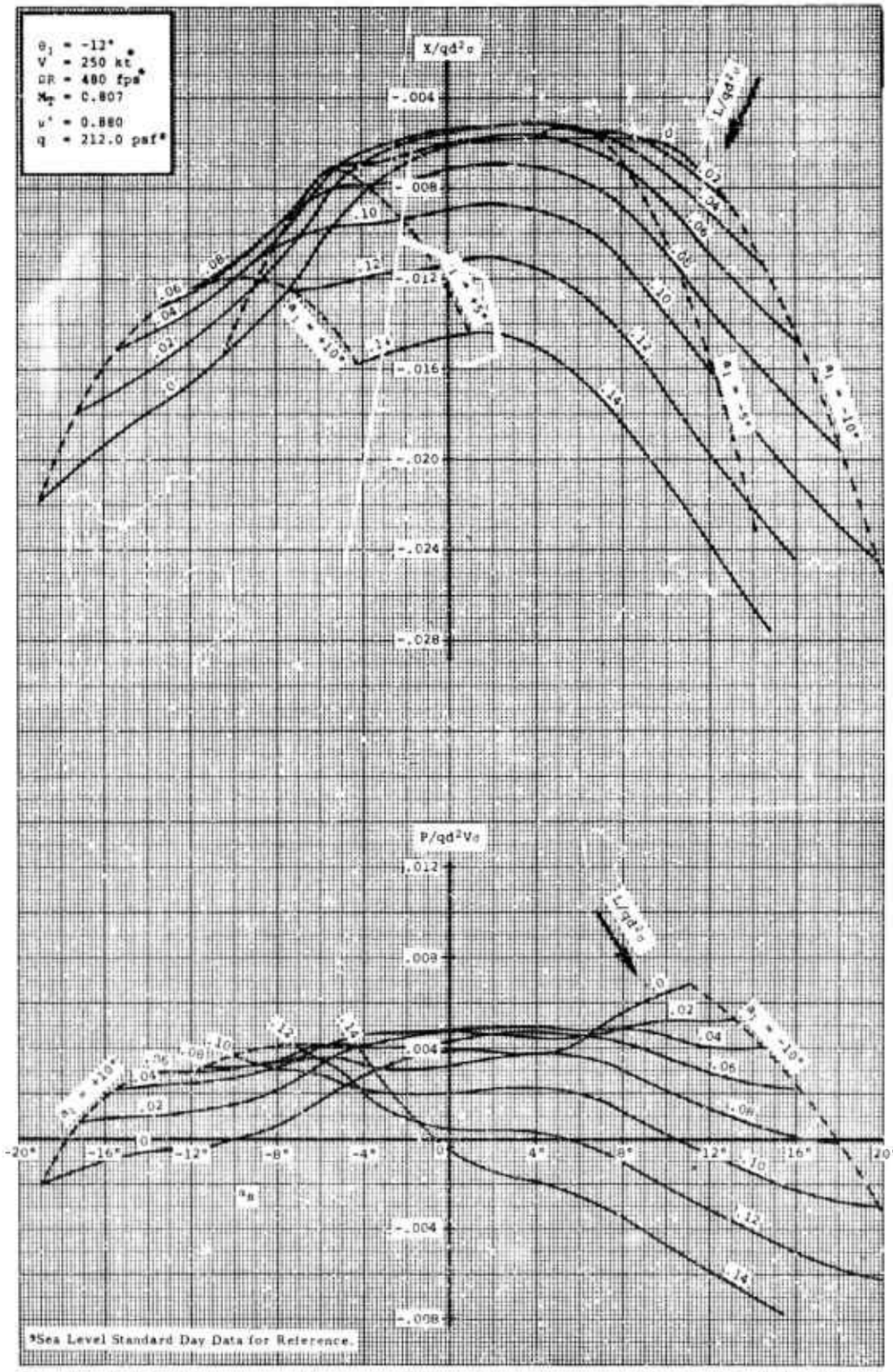
θ_1 = -12°
V = 250 kt*
ΩR = 480 fps*
M_T = 0.807
μ = 0.880
q = 212.0 psf*
X/qd²σ
P/qd²Vσ
L/qd²σ
θ_1 = +10°
θ_1 = +5°
θ_1 = -5°
θ_1 = -10°
α_s
-20°
-16°
-12°
-8°
-4°
0
4°
8°
12°
16°
20°
*Sea Level Standard Day Data for Reference.

Figure 82.

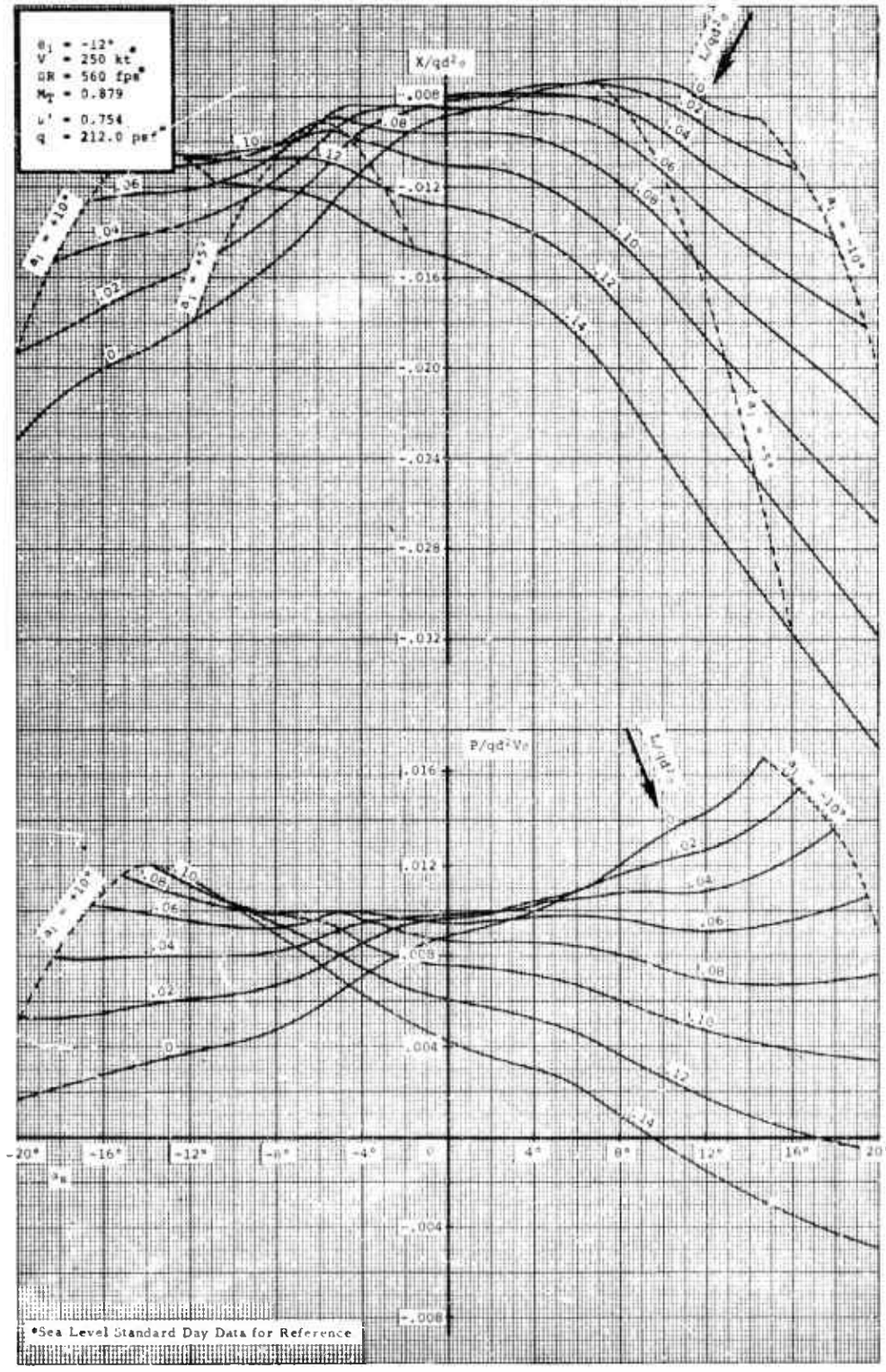
θ_j = -12°
V = 250 kt*
GR = 560 fps*
M_T = 0.879
ω' = 0.754
q = 212.0 psf*
X/qd²e
P/qd²Ve
L/qd²e
α_j = +10°
α_j = +5°
α_j = 0°
α_j = -5°
α_j = -10°
-20°
-16°
-12°
-8°
-4°
0
4°
8°
12°
16°
20°
α_s
*Sea Level Standard Day Data for Reference

Figure 83.

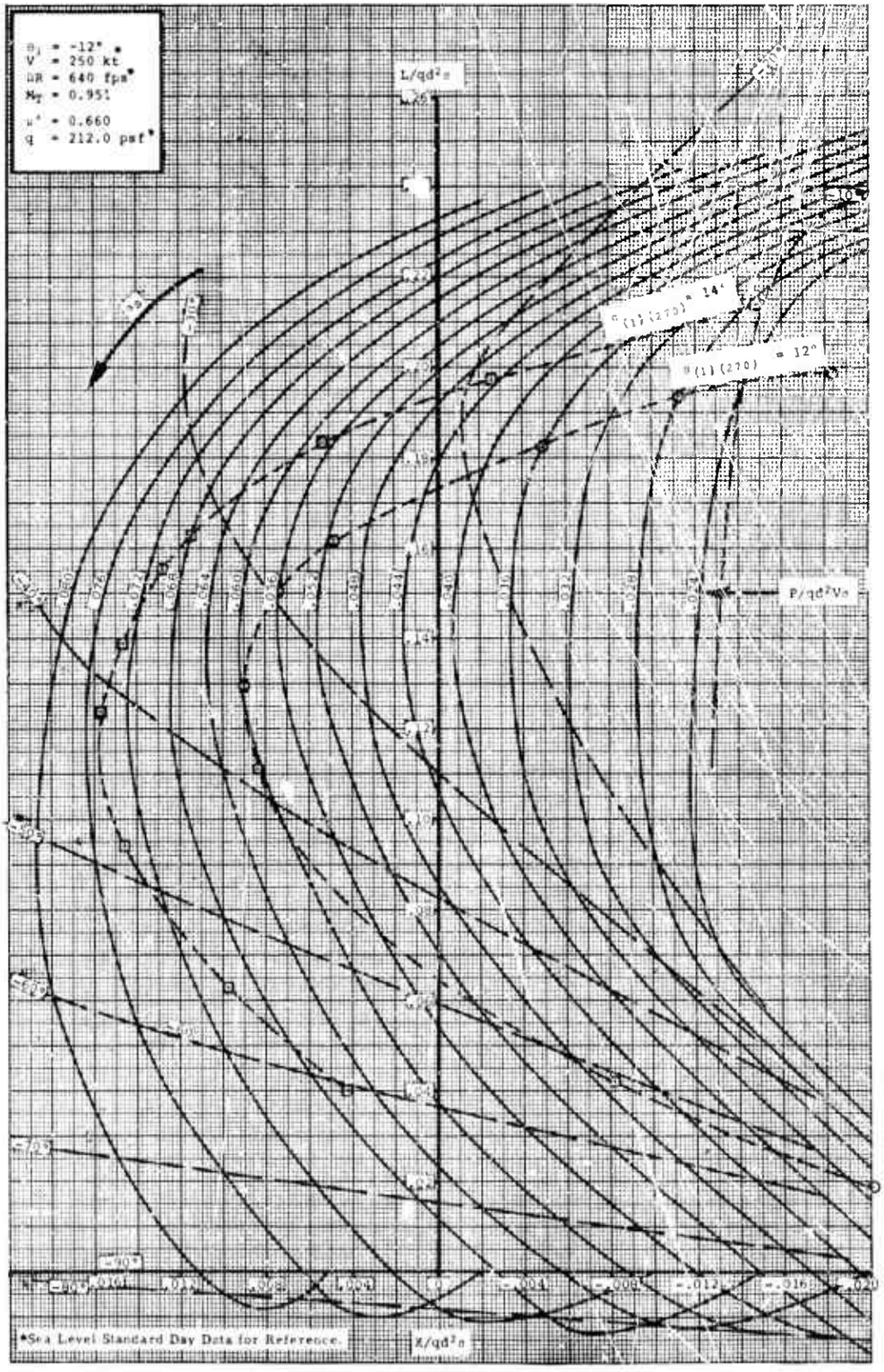
β_1 = -12°
V = 250 kt
ΔR = 640 fps*
M_T = 0.95
μ^* = 0.660
q = 212.0 psf*
L/qd²n
P/qd²Vn
$\beta_{(1)(270)}$ = 14°
$\beta_{(1)(270)}$ = 12°
*Sea Level Standard Day Data for Reference.
X/qd²n

Figure 84.

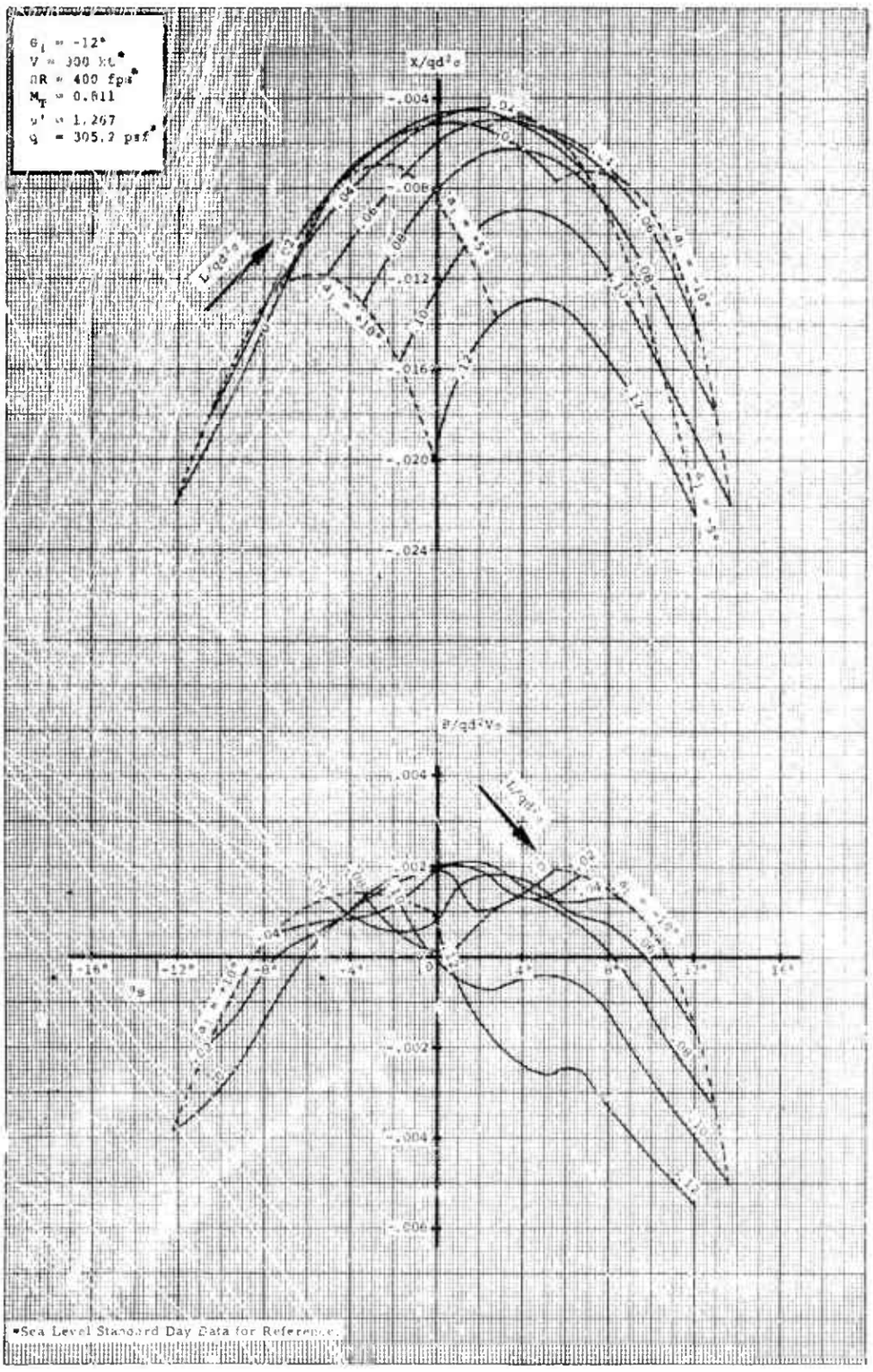
θ_i = -12°
V = 300 kt*
ΩR = 400 fps*
M_T = 0.811
μ' = 1.267
q = 305.2 psf*
X/qd²e
L/qd²e
P/qd²Vo
α
-16°
-12°
-8°
-4°
0
4°
8°
12°
16°
*Sea Level Standard Day Data for Reference

Figure 85.

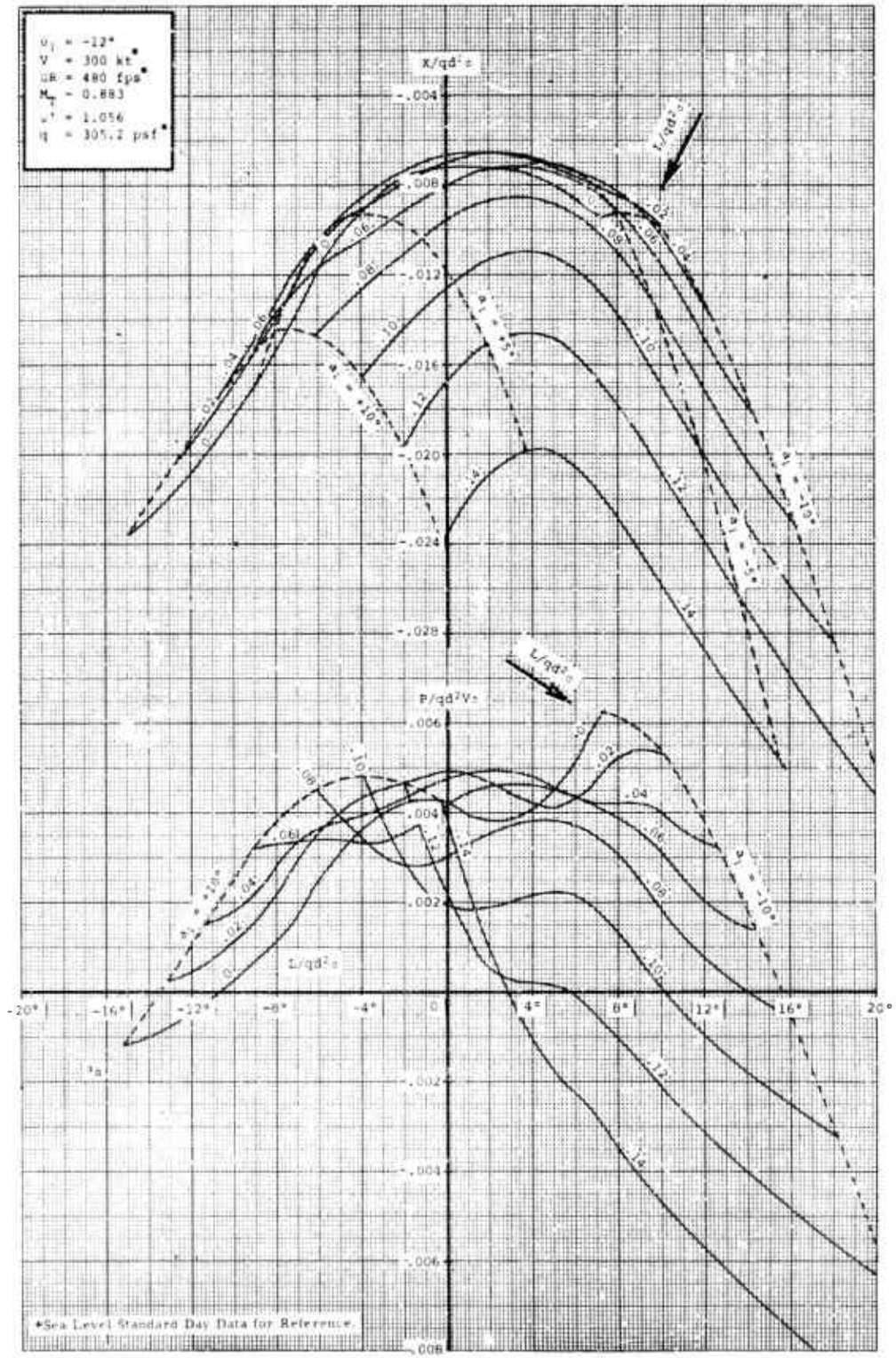
i_T = -12°
V = 300 kt*
aR = 480 fps*
M_T = 0.883
ω^* = 1.056
q = 305.2 psf*
X/qd²
-.004
-.008
-.012
-.016
-.020
-.024
-.028
L/qd²
P/qd²V
.006
.004
.002
-.002
-.004
-.006
-.008
-20°
-16°
-12°
-8°
-4°
0
4°
8°
12°
16°
20°
*Sea Level Standard Day Data for Reference.

Figure 86.

Unclassified

Security Classification

DOCUMENT CONTROL DATA - R&D

(Security classification of title, body of abstract and indexing annotation must be entered when the overall report is classified)

1. ORIGINATING ACTIVITY (Corporate author)	2a. REPORT SECURITY CLASSIFICATION
Vertol Division, The Boeing Company Morton, Pa.	Unclassified
	2b. GROUP NA

3. REPORT TITLE

GENERALIZED ROTOR PERFORMANCE

4. DESCRIPTIVE NOTES *(Type of report and inclusive dates)*

Summary report

5. AUTHOR(S) *(Last name, first name, initial)*

E. Kisielowski, R. Bumstead, P. Fissel, and I. Chinsky

6. REPORT DATE	7a. TOTAL NO. OF PAGES	7b. NO. OF REFS
February 1967	126	

8a. CONTRACT OR GRANT NO.	9a. ORIGINATOR'S REPORT NUMBER(S)
DA 44-177-AMC-142(T) b. PROJECT NO. 1P121401A14309 c. d	USAAVLABS Technical Report 66-83
	9b. OTHER REPORT NO(S) *(Any other numbers that may be assigned this report)* R-390

10. AVAILABILITY/LIMITATION NOTICES

Distribution of this document is unlimited.

11. SUPPLEMENTARY NOTES	12. SPONSORING MILITARY ACTIVITY
	US Army Aviation Materiel Laboratories Fort Eustis, Virginia

13. ABSTRACT

This report presents a summary of generalized rotor performance charts suitable for preliminary design in the rotary-wing field. Generality is achieved by nondimensional presentation of power requirements over the complete range of rotor lift and propulsive requirements for a wide spectrum of speed conditions. Lines of constant power are shown on a lift-drag coordinate system for each speed condition, providing a useful tool in the development of rotored aircraft configurations. Techniques are presented for employing the charts in a variety of design problems, including the compound helicopter, where the optimum combination of rotors, wings, and auxiliary propulsion devices is desired.

DD FORM 1 JAN 64 1473

Unclassified

Security Classification

14. KEY WORDS	LINK A		LINK B		LINK C	
	ROLE	WT	ROLE	WT	ROLE	WT

INSTRUCTIONS

1. ORIGINATING ACTIVITY: Enter the name and address of the contractor, subcontractor, grantee, Department of Defense activity or other organization *(corporate author)* issuing the report.

2a. REPORT SECURITY CLASSIFICATION: Enter the overall security classification of the report. Indicate whether "Restricted Data" is included. Marking is to be in accordance with appropriate security regulations.

2b. GROUP: Automatic downgrading is specified in DoD Directive 5200.10 and Armed Forces Industrial Manual. Enter the group number. Also, when applicable, show that optional markings have been used for Group 3 and Group 4 as authorized.

3. REPORT TITLE: Enter the complete report title in all capital letters. Titles in all cases should be unclassified. If a meaningful title cannot be selected without classification, show title classification in all capitals in parenthesis immediately following the title.

4. DESCRIPTIVE NOTES: If appropriate, enter the type of report, e.g., interim, progress, summary, annual, or final. Give the inclusive dates when a specific reporting period is covered.

5. AUTHOR(S): Enter the name(s) of author(s) as shown on or in the report. Enter last name, first name, middle initial. If military, show rank and branch of service. The name of the principal author is an absolute minimum requirement.

6. REPORT DATE: Enter the date of the report as day, month, year, or month, year. If more than one date appears on the report, use date of publication.

7a. TOTAL NUMBER OF PAGES: The total page count should follow normal pagination procedures, i.e., enter the number of pages containing information.

7b. NUMBER OF REFERENCES: Enter the total number of references cited in the report.

8a. CONTRACT OR GRANT NUMBER: If appropriate, enter the applicable number of the contract or grant under which the report was written.

8b, 8c, & 8d. PROJECT NUMBER: Enter the appropriate military department identification, such as project number, subproject number, system numbers, task number, etc.

9a. ORIGINATOR'S REPORT NUMBER(S): Enter the official report number by which the document will be identified and controlled by the originating activity. This number must be unique to this report.

9b. OTHER REPORT NUMBER(S): If the report has been assigned any other report numbers *(either by the originator or by the sponsor)*, also enter this number(s).

10. AVAILABILITY/LIMITATION NOTICES: Enter any limitations on further dissemination of the report, other than those imposed by security classification, using standard statements such as:

(1) "Qualified requesters may obtain copies of this report from DDC."

(2) "Foreign announcement and dissemination of this report by DDC is not authorized."

(3) "U. S. Government agencies may obtain copies of this report directly from DDC. Other qualified DDC users shall request through _____."

(4) "U. S. military agencies may obtain copies of this report directly from DDC. Other qualified users shall request through _____."

(5) "All distribution of this report is controlled. Qualified DDC users shall request through _____."

If the report has been furnished to the Office of Technical Services, Department of Commerce, for sale to the public, indicate this fact and enter the price, if known.

11. SUPPLEMENTARY NOTES: Use for additional explanatory notes.

12. SPONSORING MILITARY ACTIVITY: Enter the name of the departmental project office or laboratory sponsoring *(paying for)* the research and development. Include address.

13. ABSTRACT: Enter an abstract giving a brief and factual summary of the document indicative of the report, even though it may also appear elsewhere in the body of the technical report. If additional space is required, a continuation sheet shall be attached.

It is highly desirable that the abstract of classified reports be unclassified. Each paragraph of the abstract shall end with an indication of the military security classification of the information in the paragraph, represented as *(TS)*, *(S)*, *(C)*, or *(U)*.

There is no limitation on the length of the abstract. However, the suggested length is from 150 to 225 words.

14. KEY WORDS: Key words are technically meaningful terms or short phrases that characterize a report and may be used as index entries for cataloging the report. Key words must be selected so that no security classification is required. Identifiers, such as equipment model designation, trade name, military project code name, geographic location, may be used as key words but will be followed by an indication of technical context. The assignment of links, rules, and weights is optional.